Mechanical testing procedure for local building materials : rammed earth and laterite building stones

Abhilash Holur Narayanaswamy

N°d'ordre NNT : 2016LYSET015

THESE de DOCTORAT DE L'UNIVERSITE DE LYON

opérée au sein de

(L'Ecole Nationale des Travaux Publics de l'Etat)

(LGCB-LTDS UMR 5513)

Ecole Doctorale 162

(Mécanique, Energétique, Génie Civil, Acoustique)

Spécialité / discipline de doctorat : **Génie Civil**

Soutenue publiquement le 19/12/2016, par :

(Abhilash HOLUR NARAYANASWAMY)

Mechanical Testing Procedure for Local Building Materials: Rammed Earth and Laterite Building Stones

Devant le jury composé de :

AUBERT, Jean-Emmanuel	Professor, université Toulouse III	Président
REDDY, B V Venkatarama	Professor, Indian Institute of Science, Bangalore	Rapporteur
GALLIPOLI, Domenico	Professor, Université de Pau et des Pays de L'Adour	Rapporteur
FABBRI, Antonin	Chargé de Recherche, ENTPE	Examinateur
COLAS, Anne-Sophie	Chargé de Recherche, IFSTTAR	Examinateur
LAMARQUE, Claude-Henri	HDR, ENTPE	Directeur
MOREL, Jean-Claude,	Professor, Coventry University	Co-directeur

Acknowledgment

List of publications

Peer-review journal

1. H.N. Abhilash, F. McGregor , Y. Millogo, A. Fabbri, A.D. Séré, J.E. Aubert, J.C. Morel. "Physical, mechanical and hygrothermal properties of lateritic building stones (LBS) from Burkina Faso". Construction and Building Materials, Volume 125, 30 October 2016, Pages 731–741 - http://dx.doi.org/10.1016/j.conbuildmat.2016.08.082

Conference

2. Abhilash .H.N, J.C. Morel, A. Fabbri (in press). "Shear Test Procedure for Rammed Earth". In XIIth World Congress on Earthen Architecture, TERRA 2016, Lyon, France, 11th -14th July 2016.

3. Abhilash. H.N, J.C. Morel, A. Fabbri, "Shear Strength Parameters of Unstabilised Rammed Earth Interface". In Constructions en terre crue: avancées scientifiques, LOCIE, Université Savoie mont blanc, Chambéry, 17th-18th March 2016.

Table of contents

Abstract

Locally available building materials are proven energy efficient and eco-friendly, making them a sustainable building material. In the last two decades, use of raw earth as building material is augmented, owing to the environmental concerns construction industry is also reconsidering the use of raw earth, researchers on the other hand are working to understand the mechanical and dynamic behaviour of earthen buildings, yet the study of mechanical parameters possess multiple challenges due to material inert properties exposing the need of new experimental approaches to extract accurate mechanical parameters. Building techniques such as adobe, compressed earth blocks, rammed earth, and laterite building stones are on a verge of reclaiming elite position in construction industry.

In this study, experimental investigation on two naturally available building materials, unstabilised rammed earth (USRE) and laterite building stones (LBS) are carried out. The work focuses on the parameters that need to be considered in the experimental procedures, which influences the mechanical properties of USRE and LBS are seen. The locally available soils in the region of Rhone-alps, France and laterite building stones from Burkina Faso are used in this experimental campaign.

Rammed earth walls are constructed by compacting moist soil in layers, due to manufacturing technique there is a density gradient within the layer that leads to heterogeneity. On the other hand, the manufacturing parameters of the USRE such as compaction energy and manufacturing water content have a direct influence on the dry density of the material and therefore the strength. The manufacturing parameters and specimens replicating the in-situ condition are very important to understand the behaviour of USRE wall. Hence an experimental procedure to study the unconfined compressive strength, considering the influence of manufacturing parameters and specimens replicating in-situ conditions are performed along with the cyclic loading and unloading to study the elasto-plastic property of the USRE. The test procedure is performed on two different soils that are used to build USRE structures. Along with the compressive strength of USRE, the tensile strength and flexural strength are also presented by subjecting specimens under split tensile test and four point bending test.

Another important parameter is the mechanical strength properties of USRE layer interface under lateral loads. A novel experimental procedure to study the interface strength properties are discussed in this study. The experimental procedure is simple and

compact that can be performed using a simple uniaxial press using inclined metallic wedges that allows rectangular prism to undergo bi-axial loading. With the help of inclined metallic wedges, shear stress and normal stress can be induced on the specimen interface allowing to obtain coulomb's failure criteria and hence the strength properties of the interface.

Laterite building stones (LBS) which are mainly used in tropical countries are porous in nature. The moisture retention capacity of porous building material will bring indoor comfort, but the presence of water molecules within the material and their variation to the outdoor environment is responsible for complex mechanical behaviour. Hence an experimental investigation to analyse the moisture ingress of LBS and their influence on mechanical strength is designed. The moisture ingress is studied by subjecting LBS for moisture sorption and desorption test and moisture buffering test. Then the influence of moisture ingress on mechanical strength (flexure and compression) are investigated using three point bending test and unconfined compression test with loading and unloading cycles. This experimental investigation allows studying the moisture ingress and their influence on strength along with elasto-plastic behaviour of LBS.

1. Introduction

1.1. Locally available building material

Naturally available materials such as earth, stones, wood etc., are the earliest materials mankind has used for dwellings. The soil and stone suitable for building constructions are abundantly available around human habitation. These locally available materials in its natural state can be used as an effective building material. Raw earth in moist state can be compacted in a wooden mould and dried under sun can be used as an earthen block. Due to its simpler technique, locally available skills can be easily employed resulting in local empowerment and low cost.

Historical evidences proves that the utilisation of raw earth (adobe) as a building material can be dated back to 10,000years (Pacheco-Torgal & Jalali, 2012). Over a period of time different techniques of using raw earth were evolved (Gallipoli, Bruno, Perlot, & Salmon, 2014). Some of the most used techniques are adobe, compressed earth blocks, rammed earth. The main constituents of the earth used in earthen buildings are clay, silt, sand and gravel, where clay acts as a binder. The mechanical parameters are largely influenced by the presence of these four constituents. Soil suitable for earth building is found in great quantities, though some soils might need additional binder due to low clay content. (Houben & Guillaud, 1994) has provided an outline of soil suitable around the world for earth building construction as shown in Figure 1-1.

With modernisation and evolution of new technologies, the birth of new building materials evolved. The new building materials such as bricks, concrete, steel, etc., requires lot of energy to transform naturally available materials into a different state. It is unquestionable that these materials have higher mechanical strength in comparison to raw earth construction. But the impact on environment and cost of construction has raised lot of concerns over a period of time. Considering huge impact of modern construction practice on the environment, from the last two decades researchers are revisiting the use of ancient practice and its importance in application with modern construction trend.

Figure 1-1 Location of soil suitable for earthen buildings. Source: (Houben & Guillaud, 1994)

The rapid growth seen in the construction industry and its related activities in developed and developing countries has raised the concern of environmental pollution and depletion of natural resources (Spence & Mulligan, 1995). With increase in population and technological development, requirement for additional buildings and related activities are absolute necessary. But with conventional or modern construction practice (i.,e usage of industrial building materials), the treat for environment is high, and the embodied energy of buildings are considered to be high. In order to reduce and restore the modern construction impact, the usage of sustainable building materials is vital. The advantage of using locally available sustainable material is, it reduces transportation energy, extraction energy, and has better hygrothermal properties which reduces operational energy requirement.

The main parameters as specified by (B. V. Venkatarama Reddy, 2004) that requires attention in today's building materials are:

- Energy consumed in the manufacturing process,
- Transportation of materials from quarries or industrial location to in situ,
- Recycling and safe disposal,
- Impact on environmental,
- Long term sustainability

1.2. Energy performance of building material

(B. V. Venkatarama Reddy, 2004) shows the historical development of building materials as shown in Table 1-1. In today's construction industry, the most commonly used

materials in construction are bricks, cement, steel, aluminium, plastic products, polished stone, etc. These materials are proven to be energy intensive and contribute heavily to the global pollution. The contribution of building industry to global pollution is under scanner, the energy consumed due to extraction, manufacturing and transportation is under scrutiny. Policies on environmental issues such as reduction in CO2 emission, arresting sanctions of new quarries, obligations to rehabilitate quarry workings, and prohibition of material extraction from river beds are taken forefront (J.-C. Morel, Mesbah, Oggero, & Walker, 2001). Especially in developing countries where the construction activities are under immense development, high alert level control on exploitation of quarries, river sand, and polluting environment on a whole is given due importance.

Table 1-1 Historical development in building materials, Source: (B. V. Venkatarama Reddy, 2004)

Materials	**Period**
Mud, stones, wood/thatch	Prior 8000 BC
Sun dried bricks	6000 BC
Pottery products	4000 – 8000 BC
Burnt bricks	4000 BC
Lime	3000 BC
Glass	1300 BC
Iron products	1350 BC
Lime-pozzolana cement	300 BC – 476 AD
Aluminium	1808 AD
Portland cement	1824 AD
Plastics	1862

Energy consumption in buildings can be divided into two parts: (i) energy consumed due to production and transportation (embodied energy), (ii) energy consumed (required) for maintaining/servicing during the lifecycle of building. The second parameter varies from location to location depending on the climatic condition (B. V. Venkatarama Reddy, 2004).

Approximately 50% of total embodied energy of the typical house comes from the contribution of two main parameters: manufacturing of walls and floors, and transportation of building materials to site (Harris, 1999; B. V. Venkatarama Reddy, 2004). The embodied energy in various walls, floors and roofing systems as stated by (Reddy, 2009) is given in Table 1-2. As seen in the study of (Thormark, 2006), the choice of building

material will have significant influence on the embodied energy. (Cabeza et al., 2013) speaks about non stabilised rammed earth having nearly zero carbon options, which can be seen from the study of venkatarama reddy (Table 1-2). In comparison with the building constructed with modern building material and rammed earth using locally available soil or stone masonry using locally available stones, a gain of more than 250% of embodied energy was observed (J.-C. Morel et al., 2001). Hence, it can be said that the raw earth without any transformation has lowest embodied energy.

Table 1-2 embodied energy in various wall, floor and roofing systems. Source: (Reddy, 2009)

Type of building element	Energy per unit (GJ)
Burnt clay brick masonry (m^3)	2.00 – 3.40
SMB masonry (m^3)	0.50 – 0.60
Fly ash block masonry (m^3)	1.00 – 1.35
Stabilised rammed earth wall (m^3)	0.45 – 0.60
Non stabilised rammed earth wall (m^3)	0.00 – 0.18
Reinforced concrete slab (m^3)	0.80 – 0.85
Composite SMB masonry jack-arch (m^3)	0.45 – 0.55
SMB filler slab (m^3)	0.60 – 0.70
Non-reinforced masonry vault roof (m^3)	0.45 – 0.60

The concept of energy efficient buildings means buildings build with low embodied energy and also with less energy requirement during life cycle of the building. Buildings built with raw earth has better thermal conductivity, moisture buffering and hygrothermal properties (Chabriac, 2014; Chabriac, Fabbri, Morel, Laurent, & Blanc-Gonnet, 2014; Champiré, Fabbri, Morel, Wong, & McGregor, 2016; Gallipoli et al., 2014; Ionescu, Baracu, Vlad, Necula, & Badea, 2015; Pacheco-Torgal & Jalali, 2012). Besides the energy consumption, another important parameter is recycling potential (Cabeza et al., 2013). Raw earth used in its most natural state can be recycled with no or less energy (Gallipoli et al., 2014). Considering all the above points, raw earth suits as the most efficient energy performer with high recycling potential.

1.3. Sustainable practice

Sustainable building practice as defined in (John, Clements-Croome, & Jeronimidis, 2005) are the building practices which strives for integral quality (including economics, soil and environmental performance) in a broad way. Thus the rational use of

natural resources and appropriate management of the building stock will contribute to saving scarce resources, reducing energy consumption, and improving environmental quality.

Considering the rapid growth in construction industry and its future prospects, the demand for construction materials will increase exponentially. To meet the demands of present and future trend in construction activities, and to ensure the sustainable practice is involved to reduce environmental impact, following parameters need to be addressed (B. V. Venkatarama Reddy, 2004):

- Use of energy efficient alternative building technologies
- Effective utilisation of naturally available resources
- Optimal use of construction materials
- Recycling building materials and its usage
- Utilisation of industrial or mine wastes for manufacturing building materials
- Adopting energy efficient methods in manufacturing process of building materials
- Use of renewable energy and technologies to the maximum

In simple terms, the choice of building material as per OECD (as cited in(John et al., 2005) should be based on:

- Resource efficiency
- Energy efficiency
- Pollution prevention
- Harmonisation with environment
- Integrated and systematic approaches

Considering the increasing demand for housing, sustainable alternative building materials available locally are taking prime importance. But the confidence in using locally available building materials has its own limitations; this is mainly due to the lack of scientific information on the mechanical and dynamic properties of the material (J.-C. Morel et al., 2001). Raw earth being a recyclable material, with reduced embodied energy, excellent hygroscopic behaviour, acoustic characteristic, when manufactured with a proper skill and technique can have a reasonable strength, all these are achieved at a low cost as well (Gallipoli et al., 2014).

1.4. Raw earth as a building material

Unlike processed earth building materials like burnt bricks, in raw earth buildings, soil is used in its most natural state (Gallipoli et al., 2014). Simplest way of converting raw earth into building block is by compacting raw earth mixed with water in a mould, as the block dries it achieves mechanical strength. The earthen construction encompasses different manufacturing techniques, some of the commonly used techniques are called as adobe, CEB and rammed earth (Pacheco-Torgal & Jalali, 2012).

- Adobe is known as the most ancient earthen construction technique, the manufacturing process of adobe is relatively simple. The adobe is manufactured by pouring moist soil (at saturation state) in a wooden mould and allowed to dry under sun; hence it is also called as sun dried bricks.
- Compressed earth blocks (CEB) are the soil blocks which are compressed manually or mechanically in a metallic mould and dried in natural conditions to achieve strength. With the evolution of hydraulic machineries by adjusting water content and compaction energy, high strength compressed earth blocks are manufactured.
- Rammed earth means compacting moist soil in continuous layers within a wooden or metallic formwork, the compaction process can be manual or mechanical.

Another type of soil that is abundant in tropical countries is laterite; depending on the quarry laterite can be available as a loose soil or self-compacted blocks. The term laterite was coined by Buchanan in 1807 (M. D. Gidigasu, 1976). Laterites are rich in aluminium, silica, and iron oxides, its mineral and chemical composition varies based on the formation (Tardy, Kobilsek, & Paquet, 1991). It was first used as a replacement for bricks in Malabar region, India (M. D. Gidigasu, 1976). Due to its inherent properties, laterite is neither categorised as soil nor rock, hence it can be called as soft rock. In Burkina Faso, the laterite blocks used for construction of public building such as schools, churches, temples, etc., are cut from the locally available laterite deposits. Though, there no embodied energy study conducted on the laterite, considering its formation and extraction process, laterite can be categorised as the low embodied building material. Since it is naturally available and used without any transformation it can be called as a locally available raw earth building material.

1.5. Mechanical properties of earthen building material

At present, knowing importance of sustainable construction practice, countries such as Australia, USA, New Zealand, France, United Kingdom, Germany, Mexico have

produced guidelines for earthen construction (Pacheco-Torgal & Jalali, 2012). But they are not specific enough for modern construction practice. With growing concern regarding eco-friendly construction and evolution of the concept of sustainable construction practice, there is large community of researchers showing inclination towards studying sustainable building materials. In the last two decades, there is a tremendous growth in study of earthen building materials, research work on the study of mechanical parameters, dynamic parameters, hygrothermal parameters, durability characteristics, etc., of the soil are conducted. These studies are not limited to new construction practices, it also focuses on the conservation of ancient structures. Different experimental procedures are established to study the mechanical parameters of the earthen materials, yet there is lack of scientific information and precise procedure for manufacturing and testing specimens. Some of the mechanical parameters of adobe, CEB, rammed earth and laterite are discussed below.

In the laboratory, the mechanical characteristics such as compressive strength, tensile strength, flexural strength and shear strength of the materials is calculated by subjecting the specimens in unconfined compression test, split tensile (Brazilian) test, three point bending test and shear box or tri-axial test. The mechanical characteristics calculated in the laboratory are largely influenced based on the specimen size and shape (J. E. Aubert, Maillard, Morel, & Al Rafii, 2015). The specimen's aspect ratio of 2 or greater than 2 is considered to be more reliable information (J.E. Aubert, Fabbri, Morel, & Maillard, 2013). Specimen preparation is a very important part of the testing procedure, specimen tested should replicate the in-situ characteristics of the material.

The dry density of the adobe, CEB and rammed earth generally varies between 1.5-2.2g/cm^3. Broadly compressive strength of the material is considered as the basic parameter on which the suitability of material is decided. The compressive strength of adobe is in the range of 0.6MPa – 2MPa (Adorni, Coïsson, & Ferretti, 2013; Illampas, Ioannou, & Charmpis, 2014; Silveira, Varum, & Costa, 2013). The compressive strength of CEB was found to be in the range of 1MPa – 4 MPa depending on the density, moisture and soil composition. From the earlier studies, the compressive strength of unstabilised rammed earth (USRE) was found to be in the range of 0.7MPa – 3MPa (Araki, Koseki, & Sato, 2011; Q.-B. Bui & Morel, 2009; T.-T. Bui, Bui, Limam, & Maximilien, 2014; Champiré et al., 2016; Gomes, Gonçalves, & Faria, 2014; Hall & Djerbib, 2004; Maniatidis & Walker, 2003, 2008), some of the work indicated that the compressive strength of USRE can be as high as 7MPa (Gerard, Mahdad, Robert McCormack, & François, 2015).

In unstabilised earth, clay acts as a binder and suction plays a vital role in inducing the strength (Gerard et al., 2015; P. A. Jaquin, Augarde, Gallipoli, & Toll, 2009). From the studies clay content of 14-16% is said to be optimum, which results in maximum compressive strength of the materials (Reddy, Lal, & Rao, 2007; B. V. Venkatarama Reddy & Prasanna Kumar, 2011a), but in general clay content of 10-30% is said to be acceptable (Peter Walker, Keable, Martin, & Maniatidis, 2005). If the clay content is less or to improve the mechanical characteristics of the earthen materials, cement or lime stabilisation is carried out (Gallipoli et al., 2014). Stabilisation of soil is more common in manufacturing of CEB and rammed earth. The embodied energy of the stabilised earth is higher than the unstabilised earth, but it is still lower than the other building materials (B. V. Venkatarama Reddy, Leuzinger, & Sreeram, 2014; B. V. Venkatarama Reddy, 2004). The compressive strength of cement stabilised CEB is reported as 1MPa - 2MPa (J. Morel, Pkla, & Walker, 2007; Muntohar, 2011; Reddy et al., 2007; B. V. Venkatarama Reddy & Gupta, 2006; P Walker & Stace, 1997) and that of cement stabilised rammed earth (CSRE) is 2MPa - 12MPa (Daniela Ciancio & Gibbings, 2012; Jayasinghe & Kamaladasa, 2007; Reddy & Kumar, 2009), depending on the amount of cement and clay present. The tensile strength of the earthen building material is not studied as widely as compressive strength. But from the limited research work, tensile strength of the CEB and rammed earth is reported as nearly 10% of compressive strength (T.-T. Bui et al., 2014; Gerard et al., 2015).

1.6. Unstabilised rammed earth (USRE)

The scope of this study is restricted to USRE for the soils obtained from Rhone-Alps region France and LBS obtained from Houet province in Burkina Faso.

1.6.1. History of Rammed Earth

Rammed earth construction practice is also one of the very old techniques used in building construction practice. An examples of historical rammed earth building constructed in 2000 BC can be found in yellow river valley, china and early usage of rammed earth building can also be seen in Japan (Araki et al., 2011). Rammed earth construction technique was well known in counties such as France, Germany, U.K, northern India, Nepal, China, Japan, etc., (Beckett, 2011; Maniatidis & Walker, 2008), from the last few decades countries such as Australia, USA are showing immense interest in this technique (P. Jaquin, 2011). As discussed above, earthen construction can be manufactured using raw earth or with some stabilisation to improve mechanical strength. Therefore rammed earth construction can be broadly classified as unstabilised rammed

earth (USRE) and stabilised rammed earth (SRE). Stabilisation can be done using lime or cement, depending on the need. Stabilised rammed earth construction practice is commonly seen in countries like India, Australia, (P. A. Jaquin, 2008) considering the climatic condition. Stabilisation of rammed earth in European countries was common in late 19th century (after industrialisation) (Daniela Ciancio, Jaquin, & Walker, 2013).

There are certain questions regarding the durability aspect of USRE, but from the recent studies, the deterioration of the rammed earth wallets exposed to natural climatic condition for 20years was found to be within the reasonable limits (Q. B. Bui et al., 2009). In Europe, there are certain examples of rammed earth buildings built in late 19th century and early 20th century, which are in good serviceable condition with need of some renovation (Rendell & Jauberthie, 2009). These are the classical examples of earthen building, with proper protection and care the service life of more than 100years is easily achievable.

1.6.2. Manufacturing rammed earth

Any soil with sufficient clay, silt, sand and gravel content is mixed with water and poured in a wooden or metallic formwork and compacted manually or mechanically using metallic or hydraulic rammer. The moist soil is compacted in layers forming a monolithic structure. The compacted soil is allowed to dry in natural condition; upon drying the rammed earth attains certain mechanical strength.

1.6.3. Mechanical Performance

Mechanical properties of the USRE depend on the parameters such as compaction energy, manufacturing water content, moisture within the wall (suction), soil composition. Therefore arriving at a unique mechanical property of USRE is impossible considering the variability of above mentioned parameters.

Many studies in the recent times indicated that the compressive strength of the USRE is around 0.7MPa – 3MPa, but it is also important to understand how these parameters are established. Most of the studies report the mechanical parameters based on the test results of unconfined compression test or tri-axial test. But the importance of specimen manufacturing procedure is pointed out by only few researchers. Some researchers urged the need to replicate in-situ condition in the laboratory, which led to the manufacturing of wallets (small walls). Though wallets provided much better result interpretation of the wall, but its testing process needs huge space and the time consumed in manufacturing and testing wallets is very long. Some of the earlier work identified the variation of mechanical strength with change in specimen size and shape. Hence manufacturing specimens that are

easy to handle and also resembles in-situ condition, which provides better insight of material characteristics that replicates USRE wall is important.

The main parameters that need to considered while manufacturing specimens are: soil composition, Compaction energy, and Manufacturing water content. Considering the anisotropic behaviour of rammed earth, it is also important to manufacture specimens with similar effect (i.e. ramming on the top of the layer, which leads to higher density at the top of the layer and lower density at the bottom of the layer).

Since the rammed earth structure is compacted in layers, the interface behaviour of the rammed earth plays a major role in determining the structural stability of the building under seismic condition. Hence the need to understand the behaviour of layer interfaces.

This work was influence due to the lack of experimental procedure that can recommend to study compressive, tensile, flexural and shear strengths of USRE by manufacturing specimens that replicates in-situ condition. In this study an experimental protocol to study the interface strength parameter of USRE is also proposed.

1.7. Laterite building stones (LBS)

Laterite building stones (LBS) which are available in tropical countries are a sustainable alternative material that can be easily used as a masonry construction. Though it is naturally available and poses a good mechanical strength, its scientific application as a building material was found in 1800's (M. D. Gidigasu, 1976). The usage of LBS can be seen in developing tropical countries, but due to lack of scientific investigation on this material, its wide range application as a building material is restricted (Abdou Lawane, Pantet, Vinai, & Hugues, 2011; Unnikrishnan, Narasimhan, & Venkataramana, 2010). There are very limited research works on the LBS, some of the research works were carried out in India and Burkina Faso reported that the compressive strength of the LBS is around 1.5MPa – 4.0 MPa(A. K. Kasthurba, Santhanam, & Achyuthan, 2007; A Lawane, Vinai, Pantet, & Thomassin, 2011; Unnikrishnan et al., 2010).

In tropical countries, owing to seasonal climatic condition, the change in relative humidity and temperature will have an influence on moisture ingress within the LBS used for building construction. As it is known that the moisture content within the earthen material has a strong impact on the mechanical strength, it is important to study the influence of moisture change on the mechanical strength of LBS. Hence in this study an experimental procedure to study, the mechanical parameters of LBS with respect to change in the moisture condition of the specimens due to variation in relative humidity are proposed.

2. Material

2.1. Selection of soil

Any inorganic sub-soil, with limited clay content could be selected for rammed earth wall construction. Density of the rammed soil is one of the main parameter that can be controlled during manufacturing process, which has significant influence on durability and strength of the structure. Particle size distribution of any selected soil influences the density of the compacted material. The composition of unstabilised rammed earth consists of gravel & sand (45-80%), silt (10-30%) and clay (5-20%) (Daniela Ciancio et al., 2013; Delgado & Guerrero, 2007), gravels and sand forms the matrix, while clay acts as the binding material. At ideal conditions, well graded soil or any soil which satisfies fuller's requirement of grading will have fewer voids, hence higher density when compacted at optimum condition. Excess quantity of clay increases the possibility of shrinkage damage in structure. However influence of variation in grading on physical characteristics of rammed earth is yet to be studied in detail (Maniatidis & Walker, 2003). In this chapter, location and preliminary test details of the soils used for the studying mechanical characteristics are discussed.

2.1.1. Cras Sur Reyssouze (CRA)

Cras Sur Reyssouze (CRA), is the name of the village located in [46.3092° N, 5.1664° E] Rhone-Alpes region, south east of France, as shown in Figure 2-1. In this region, there are lots of ancient rammed earth buildings in need of renovation and few new rammed earth buildings being constructed. The soil used in this study is extracted from an ancient building wall which was demolished during renovation.

2.1.2. Dagneux

Dagneux is another soil used in this study, which is also located [45.8508° N, 5.0753° E] in the Rhone-Alps Region, south-east of France, as shown in Figure 2-1. As said earlier in this village too there is lot of ancient rammed earth construction. The soil samples fabricated in this study are extracted from the ancient rammed earth building, not in use anymore.

The main purpose of choosing these soils as raw material in this study is due to its immense usage in earth buildings. Since in this region there are many existing earth buildings, studying their physical and mechanical parameters are vital for renovation works

and also useful for new construction activities. The other advantage of using this soil in our study is its maximum granular size is less than 10mm, which will be easy to standardize the laboratory results for actual field conditions.

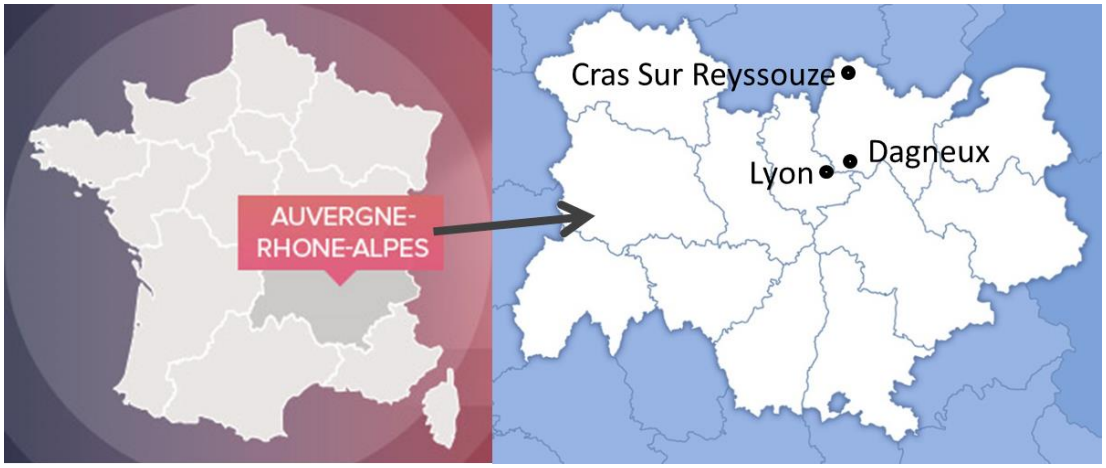

Figure 2-1 Location of the soils used in this study

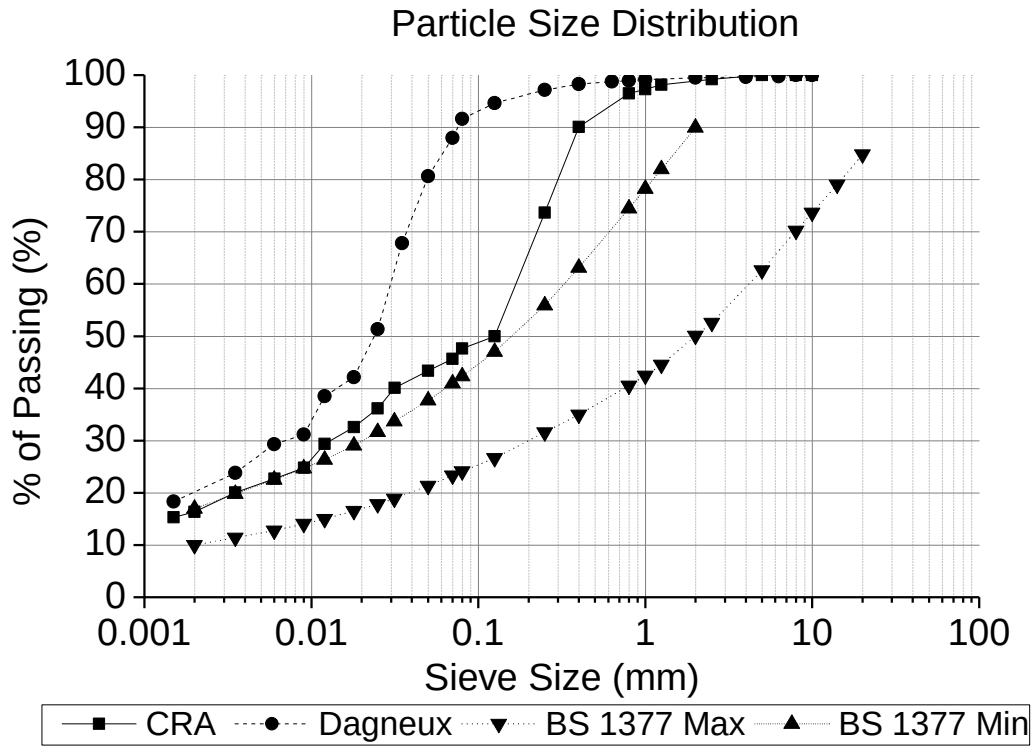

Figure 2-2 Particle Size Distribution of soil and maximum and minimum grain size distribution of soil for civil engineering purpose recommended by (BS 1377-2, 1990)

2.2. Soil particle Size Distribution

Particle size distribution of both soils (CRA and Dagneux) are carried out in accordance to British standard (BS 1377-2, 1990). Wet sieve method is adopted for removing clay and silt fraction from gravel and sand, later using various sieves, gravel and sand quantities is calculated. While clay and silt fractions are obtained through sedimentation test using hydrometer. By combining both sieve results and sedimentation results, particle size distribution of the soil is plotted in Figure 2-2. Both soils are out of the range given by (BS 1377-2, 1990), whereas this soils enabled to build safe houses lasting for more than 70 years with low maintenance. It is worth rejecting recommended maximum and minimum grain size distribution of soil, because they don't take into account the great variability of possible soils and techniques. Moreover these limits are against sustainability because they may discard a local suitable local soil which is favourable to decrease the impact on environment (Morel et al. 2001).

2.2.1. Discussion of soil selection based on Grain Size Distribution

Some guideline and technical document recommends the selection of soil with respect to grain size distribution and on the percentage of clay content present in the soil. In Table 2-1, from (Daniela Ciancio et al., 2013; Delgado & Guerrero, 2007; Gomes et al., 2014; Maniatidis & Walker, 2003; Peter Walker et al., 2005) studies, the recommendations of lower and upper limit of grains distributed in a soil for earth buildings are given. From earlier study and recommendations, in general it could be seen that soil with clay content varying from as low as 5% to as high as 30% is acceptable. Except (Alley, 1948 as cited in, Maniatidis & Walker, 2003) who proposed higher silt content (50-80%) and lower sand and gravel content (10-20%), other works commonly agree with minimum and maximum silt content of 10% and 30% respectively, along with the minimum and maximum sand and gravel content of 40% and 80% respectively. Studies which does not recommend silt content in the soil, proposes high quantity of sand and gravel content with lower and upper limit as 65% and 80% respectively, it should also be noted that when silt is not present an increased clay content is advised with minimum being 20% and 35% as maximum. Some of the works recommends sand and gravel quantities separately, though not all the earlier studies points out the maximum gravel size considered, in general it could be seen most of the authors consider 20mm down as the maximum gravel size.

In this study, the percentage of grain distribution of both CRA and Dagneux is given in the Table 2-2. The amount of clay present in both the soils satisfies the general

quota of clay required for obtaining a good mix. CRA satisfies the silt, sand and gravel content recommended by many normative and technical standards. But Dagneux, is high with silt presence (65%), and low with sand and gravel content, it represents the limits presented by (Alley, 1948; as cited in Maniatidis & Walker, 2003) in his work. Both the soils chosen for this study does not obey the limits stated by British standards (BS 1377-2, 1990) for earth constructions, but still they are actively used for earth wall construction from a very long period.

In this study, cautious decision is taken not to engineer the soil by mixing with sand, as there are many rammed earth structures built with the same particle size distribution. Hence it is very important to understand the behaviour of the soil as used in the construction. Another important reason to choose these soils under this study is its small maximum grain size which enable to use the whole soil (without sieving) to manufacture laboratory samples. The influence of variation in particle size distribution and amount of clay present on the strength and durability still remains unclear (Maniatidis & Walker, 2003). All the recommendations (given in Table 2-1) on grain size quantities seems to be correct, and it again proves the difficulty level to converge on a generalized selection criteria of the soil used for earth building construction.

Table 2-1 Particle size limits proposed by various study

Author/ Name	Clay	Silt	Sand & Gravel
(Peter Walker et al., 2005)	5-20%	10-30%	45-80%
(Alley, 1948) [1]	25-30%	50-80%	10-20%
(Schrader, 1981)[1]	20-30%	-	70-80%
(McHenry, 1984)[1]	30-35%	-	65-70%
(Norton, 1986)[1]	10-25%	15-30%	45-75%
(Houben & Guillaud, 1994)[1]	0-20%	10-30%	45-75%
(Radanovic, 1996)[1]	30-35%	-	65-75%
(SAZS 724:2001, n.d.)[1]	5-15%	15-30%	50-70%
(Bolton, 2001)	5-15%	15-30%	40-70%
British standard[2]	N.A*	N.A*	N.A*
HB-195, (Peter Walker & Standards Australia, 2002)[2]	5-20%	10-30%	45-75%
Bulletin 5[2]	N.A*	N.A*	N.A*
NZ standard for earthen construction	N.A*	N.A*	N.A*
MOPT (1992)[3], spain	5-26%	NA*	NA*
IETcc (1971)[3]	10-40%	20-40%	10-20%
(McHenry, 1984)[3]	15%	32%	30% (Sand) + 23% (Gravel)
Smith and Austin (1996)[3], New Mexico	4-15%	40%	60-80%
Gomes & Folque (1953)[4]	15-31%	7-17%	28-51% (Sand) + 0-33% (Gravel)
Doat, et al. (1979)[4], CraTerre	15-25%	20-35%	40-50% (Sand) + 0-15% (Gravel)
Keable (1996)[4]	5-15%	15-30%	50-70%
Keefe (2005)[4]	7-15%	10-18%	45% (Sand) + 30% (Gravel)
CRA	17%	28%	55%
Dagneux	20%	65%	15%

*Note: N.A – Not Available

Table 2-2 Grain Size of soils considered in this project

[1] As cited in (Maniatidis & Walker, 2003)
[2] As cited in (Daniela Ciancio et al., 2013)
[3] As cited in ((Delgado & Guerrero, 2007)
[4] As cited in (Gomes et al., 2014)

Grain's		CRA [%]		Dagneux [%]	
Gravel (60-2mm)	Coarse (60-20mm)	0	55%	0	15%
	Medium (20-6mm)	0		0	
	Fine (6-2mm)	1		0,5	
Sand (2-0,06mm)	Coarse (2-0,6mm)	4		1	
	Medium (0,6-0,2mm)	30		2,5	
	Fine (0,2-0,06mm)	20		11	
Silt (60µm-2µm)	Coarse (60-20µm)	11	28%	42	65%
	Medium (20-6µm)	11		13,7	
	Fine (6-2µm)	6		9,3	
Clay (<2µm)	<2µm	17%		20%	

2.3. Manufacture water content and Dry Density

Density of the construction material is an indicative factor of material durability and strength. Density of the oven dry (at 100-110°C) material is termed as Dry density and in general it is measured in g/cc or kg/m^3. For a given soil at known compaction energy, dry density of the soil varies with increase in the water content. It may reach a point where the soil is no more compressible as water completely occupies voids. During the compaction process if soil achieves its maximum dry density (MDD) this water content is called as ‘optimum moisture content’ (OMC) or optimum water content (OWC) for a given compaction energy. For the case of rammed earth, the Proctor test is commonly adopted (Maniatidis & Walker, 2003) to measure the maximum dry density and optimum moisture content for a given compaction energy.

From earlier studies, it is understood that dry density of rammed earth varies from 1.7 to 2.2g/cc (Araki et al., 2011; Q. Bui, Morel, Hans, & Walker, 2014; Cheah, Walker, Heath, & Morgan, 2012; Maniatidis & Walker, 2003). It is widely known that the material strength increases with increase in dry density (A W Bruno, Gallipoli, Perlot, Mendes, & Salmon, n.d.; B. V. Venkatarama Reddy & Prasanna Kumar, 2011b), but owing to lack of more reliable scientific studies on USRE, there is a need to understand the influence of dry density on the USRE wall.

Dry density and optimum moisture content of a compacted soil depends on the compaction effort adopted to manufacturing structure. Hence any comparison between the

compaction effort adopted at site and proctor test is always difficult, however Proctor compaction method still serves as the reliable scientifically proven procedure to investigate compaction energy and manufacturing water content of the USRE.

It goes without saying density of compacted soil varies from soil to soil with change in particle size distribution. It is absolutely necessary to know the target dry density to be achieved for the rammed earth wall in construction.

2.3.1. Proctor Test

The term proctor is coined after R R Proctor, who in 1933 showed that the dry density of a soil for a given compactive effort depends on the amount of moisture present in the soil at the time of compaction.

General practice involves proctor test on soil with standard (600kN.m/m^3) and modified (2733kN.m/m^3) compaction energy. Proctor test on the soils studied in this work is carried out in accordance to (ASTM D1557-12, 2012; ASTM D698-12e2, 2012).

In this study, both pneumatic and hand compaction are used to determine the OPM and maximum dry density of the soil. Pneumatic mechanical compactor as shown in Figure 2-3(A) has multiple options to generate standard and modified compaction energy by changing drop hammer. On the other hand two manual compactors as shown in Figure 2-3(B) are used to generate standard and modified energy. In both pneumatic and manual compaction, weight of standard hammer was 2.5kg and modified hammer was 4.54kg. By knowing the volume of the mould, weigh of the hammer, drop height of the hammer and number hammer blows on the soil, compacting energy of the soil is calculated or in other words by changing the number of hammer blows and volume of the soil compacted, compaction energy can be altered. The compaction mould (Figure 2-3(C&D)) used for both standard and modified was same with dimension of 152.4mm in diameter and 116.6mm in height without collar.

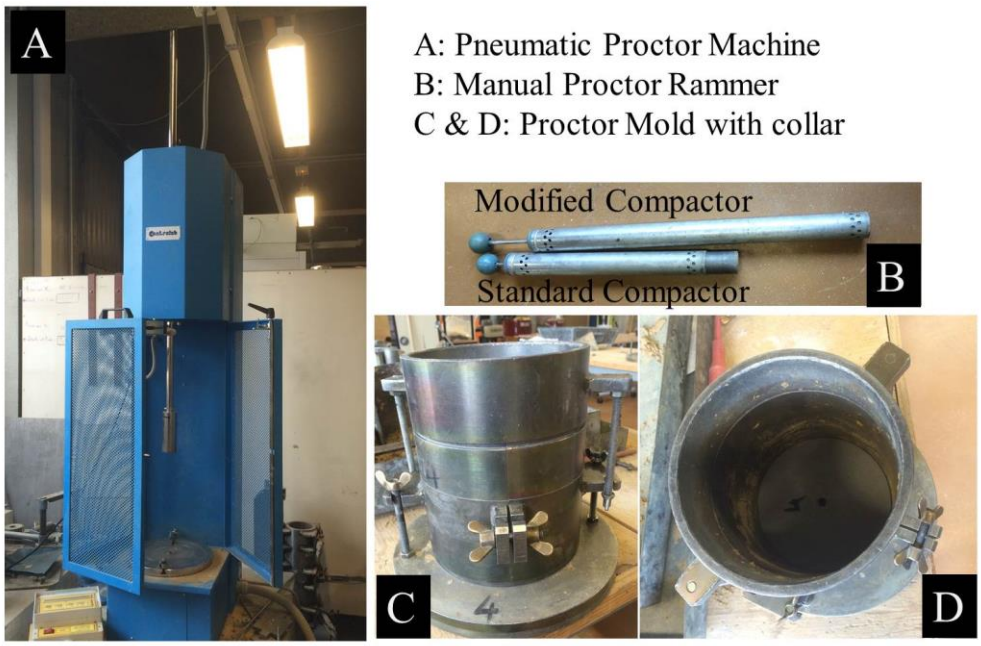

Figure 2-3 Proctor Testing Instruments

2.3.1.1. Test procedure

The procedure involves compacting the soil in question at different water contents until soil is no more compressible or saturated. Approximately 6kg of dry soil is mixed with 6% of water content by weight of the soil as a first trial. The soil is mixed by hand until homogeneous mix of moist soil is achieved. The moist soil is then poured into the standard compaction mould in three layers for normal compaction and five layers for modified compaction. Table 2-3 gives the compaction details of the proctor test used in this work. Each layer is subjected to 56 number of ramming with the hammer, when the final layer is rammed, the weight of the compacted soil is taken and the bulk density of the soil is calculated. Moisture content of the compacted moist soil is then calculated by measuring the difference in weight of moist soil sample and over dry sample in oven at 100-105°c for 48 hours as per (ASTM-D-2216-98, 1998). The compaction procedure is continued by adding additional water content at an increment of 2% until decrease in bulk density is noticed, same procedure is repeated for different compaction energies.

Table 2-3 Compaction Details of Proctor Test

	Standard (E-S)	Modified (E-M)	E3
Weight of Hammer	2.5kg	4.54kg	4.54kg
Height of fall	305	457	457
N° of Blows	56	56	56
N° of Layers	3	5	3
Compaction Energy	600kN.m/m^3	2731kN.m/m^3	1639kN.m/m^3

Dry density [γ_d] of the soil is calculated by using the relation, $\gamma_d = \frac{\gamma}{1+\omega}$, where [$\gamma$] is bulk density and [$\omega$] is moisture content of the soil. The variation of dry density with respect to increase in moisture content of the soil at compaction is given in Figure 2-4, in which both the soils (CRA & Dagneux) are represented. As said earlier it can be seen that the optimum moisture content of the soil decreases and maximum dry density increases with increase in compaction energy, the optimum moisture content and dry density for both the soils at different energies is given in the Table 2-4.

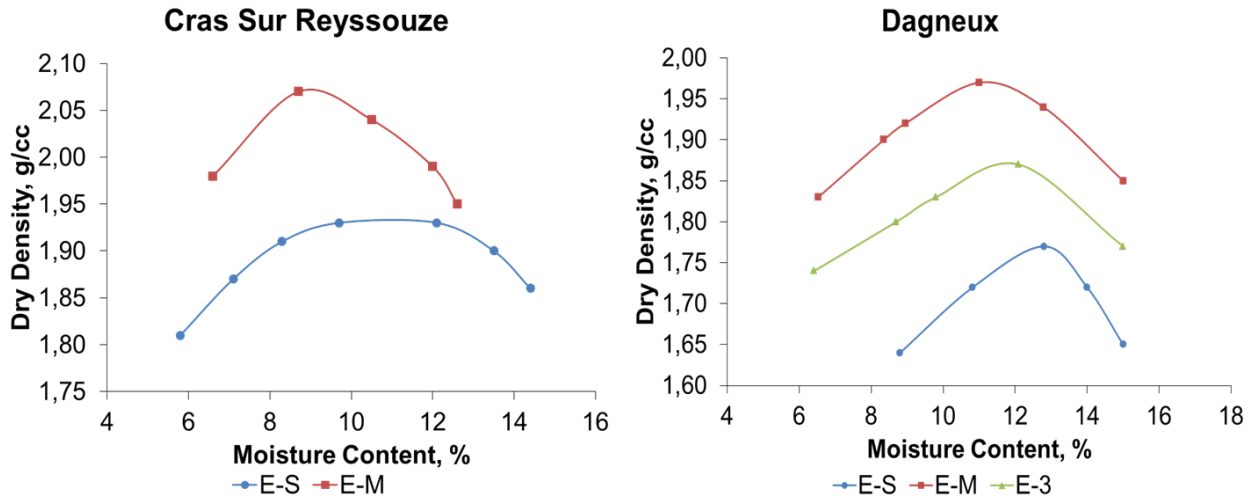

Figure 2-4 Optimum Moisture Content - Maximum Dry Density (Proctor)

Table 2-4 Optimum moisture content and maximum dry density of soils

Soil	CRA			Dagneux		
Compaction Energy, kN.m/m^3	600	-	2731	600	1639	2731
Optimum Moisture Content [ω], %	10.5	-	9.0	13.5	11.5	11.0
Maximum Dry Density [γ_d], g/cc	1.93	-	2.07	1.75	1.87	1.97

2.3.2. Importance of dry density and manufacturing moisture content

As said earlier, density of the material defines the strength and durability of the material, material with a high density will have better mechanical characteristics, but the influence of density on mechanical parameter of unstabilised rammed earth is not yet studied in detail. From proctor results, it can be seen that with different energies the density achieved is different, however it also depends on the manufacturing water content, defining the parameters such as manufacturing water content and compaction energy for a soil is very difficult, moreover in the field, measuring water content and compaction energy is difficult too. With different practitioners and depending the method they adopt to construct a rammed earth, density achieved will vary, (Quoc-Bao, 2008) in this work identifies masons using pneumatic rammers compact rammed earth with an energy of 1900kN.m/m^3.

2.3.2.1. Influence of manufacturing water content on density

In Figure 2-5, density variation with manufacturing water content and compaction energy is shown. On the left side of optimum moisture content, dry density for any compaction energy increasing until it reaches optimum moisture, which is also called as the 'dry side of OMC'. On the right side of optimum moisture content, density of the material decreases with increase in moisture, this portion is also called as 'wet side of OMC'. From the Figure 2-5, it can be seen that point a and a' have same density [γ_a] for a given compaction effort but have different manufacturing water content. Similarly b and b' exhibits same tendency, this is true for all the compaction curves. Hence there exists same density for two different moistures, one in dry side of OMC and other in the wet side of OMC. Practically it is very difficult to accurately add OMC to the soil for compaction, hence if there is a tolerance limit which side is better, dry side of OMC or wet side of OMC?. And also material can have same density at two different manufacturing water contents, what is its influence on material strength?. These two questions need to be answered: in the work of (Hall & Djerbib, 2004) the manufacturing water content with in ±5% of OMC is said to be acceptable, there is lack of information on the influence of manufacturing water content on USRE compressive strength. The work (B. V. Venkatarama Reddy & Prasanna Kumar, 2011a) reported that the compressive strength of CSRE specimens manufactured at wet-side of OMC is higher than the dry side, but the presence of cement and its influence will make the comparison with USRE difficult. Though this is not in the scope of this work, experimental investigation to study the influence of manufacturing water content on mechanical strength will be interesting.

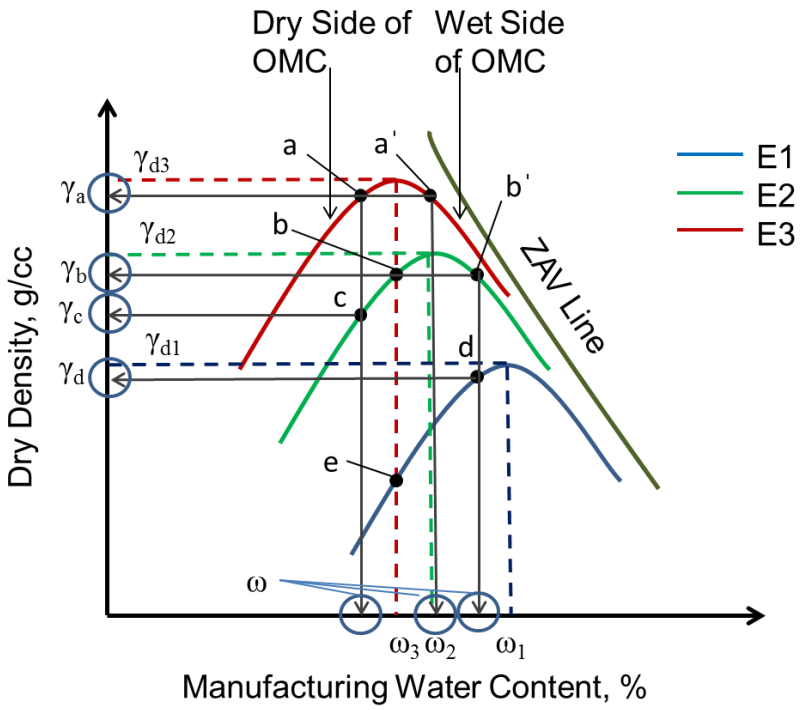

Figure 2-5 Concept of Manufacturing water content and achieved dry density

2.3.2.2. Influence of compaction energy on density

In Figure 2-5, it can also be seen that, points a and c, b and e, b' and d, share same manufacturing water content, but has different dry densities, it is due to difference in the compaction effort. It is to say if there is change in compaction energy for given water content, there will be change in density achieved. Hence studying the influence of density and compaction energy on mechanical parameters of unstabilised rammed earth is important. Answering these questions is vital for better practice of unstabilised rammed earth construction. To analyse the impact of different compaction energy and density on the mechanical parameters, the cylindrical specimens at different compaction energies are manufactured and subjected to compression test. In the following chapters specimen manufacturing and mechanical strength of USRE will be discussed.

2.4. Suction

Total suction is a measure of the free energy of the pore water or tension stress exerted on the pore water by the soil matrix. Total suction consists of two components, matric suction and osmotic suction. The matric suction is defined as the difference between the pore air pressure and the pore water pressure, matric suction is also known as capillary suction in the unsaturated soils (Beckett, 2011). Suction plays an important role in developing strength of the unsaturated earth (Daniela Ciancio et al., 2013). It is well understood that the strength of dry USRE is related to the level of suction developed

between the soil particles (P. A. Jaquin et al., 2009), which increases apparent cohesion thereby contributing to strength (Nowamooz & Chazallon, 2011). Suction increases with decrease in moisture, similarly the strength and modulus of USRE increases with decrease in moisture (Araki et al., 2011; Q. Bui et al., 2014; Gerard et al., 2015).

2.4.1. Measurement of suction

Measurement of suction can be classified into two main categories;

(i) Direct method for measuring matric suction, and

(ii) Indirect method for measuring matric, osmotic and total suction

Direct suction measurement technique includes: axis- transition technique, tensiometer and suction probe methods. Indirect suction measurement technique (for matric suction) includes: time domain reflectometry (TDR), electrical conductivity sensors, thermal conductivity sensor (TCS) and in-contact filter paper technique methods (Pan, Qing, & Pei-yong, 2010).

Filter paper technique is considered to be easily affordable and has wide range of suction measurement possibility (Bulut, 1996; Pan et al., 2010). Using filter paper method, both total suction and matric suction can be studied. The total suction of the soil can be studied by suspending the filter paper (without physical contact) with the specimen in a sealed contained. The matric suction of the soil can be calculated by bringing filter paper in contact with the specimen surface, thereby allowing direct contact for liquid phase and solutes to exchange freely. In this study, only matric suction is studied by using in-contact filter paper.

The in-contact filter paper technique works on the principal that, a dry filter paper in-contact with the soil specimen having specific suction attains moisture equilibrium state, with which suction can be correlated. Hence a good direct contact between filter paper and the soil specimen surface is essential. The moisture content of the filer paper relates to the soil suction value based on the calibration established for that filter paper. The most commonly used in-contact filter papers are ‘Whatman 42’ and ‘Sleicher & Schuell 59’, in this study ‘Whatman 42 filter paper’ is used. The calibration chart for Whatman 42 filter paper proposed by (ASTM D5298-03, 2003) is given in Figure 2-6, the calibration chart given in (ASTM D5298-03, 2003) corresponds to both total and matric suction. In addition to (ASTM D5298-03, 2003), additional suction calibration charts for Whatman 42 filter paper are presented and discussed in (Bicalho, Correia, Ferreira, Fleureau, & Marinho,

2007) depending on the type of suction and method used. The calibration curves widely accepted is presented in Table 2-5 (source (Bicalho et al., 2007)). It is recommended to establish a calibration curve for the Whatman 42 filter paper available in each lab. At ENTPE, Lyon, the calibration curve for Whatman 42 filter paper using salt solutions in accordance with the (ASTM D5298-03, 2003) was established by (SOUDANI, 2016) (Figure 9-1 - annexure). The suction value for Whatman 42 filter paper can be calculated from the equation $S = 5.2473 - 0.1241\, w$, which is obtained through calibration chart established by (SOUDANI, 2016) in ENTPE lab. Where S is suction in log kPa, w is the filter paper water content.

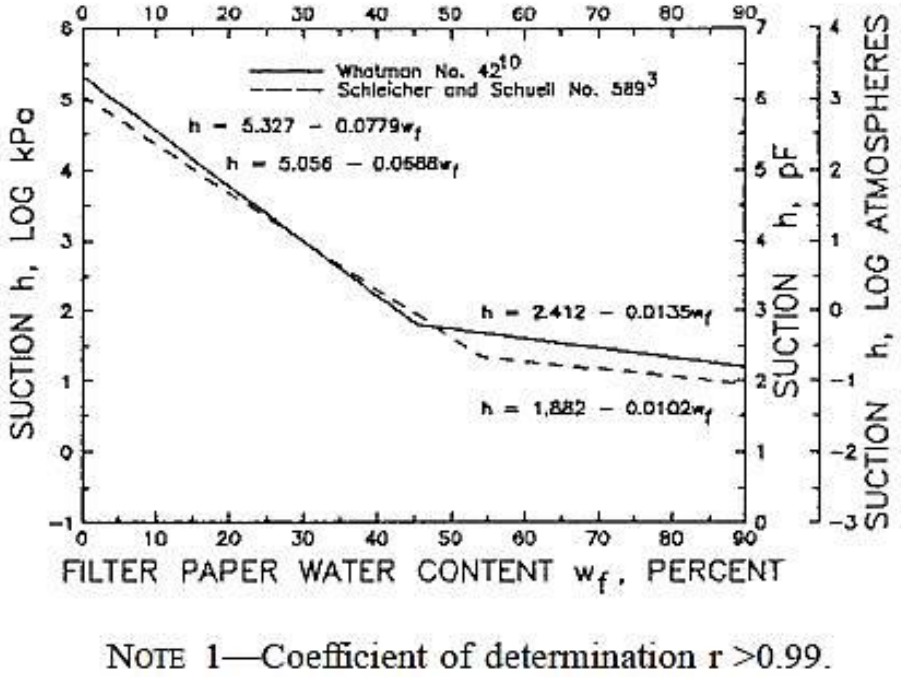

Figure 2-6 Calibration suction-water content curves for wetting of filter paper (source: (ASTM D5298-03, 2003)**)**

Table 2-5 Calibrations curves for Whatman 42 filter paper (source: (Bicalho et al., 2007) **)**

Reference	Suction	W (%) range	Log_{10} (suction), kPa
ASTM D5298	Total & Matric	W < 45.3	5.327 - 0.0779 w
ASTM D5298	Total & Matric	W > 45.3	2.412 – 0.0135 w
Chandler & Gutierrez (1986)	Matric	(*)	2.85 – 0.0622 w
Chandler et al. (1992)	Matric	W < 47	4.842 – 0.0622 w
Chandler et al. (1992)	Matric	W > 47	6.050 – 2.48 log w
Oliveira & Marinho (2006)	Total & Matric	W < 33	4.83 – 0.0839 w
Oliveira & Marinho (2006)	Total & Matric	W > 33	2.57 – 0.0154 w
(SOUDANI, 2016)	Total & Matric	W < 20	5.247 – 0.124 w

Note: w = Gravimetric water content and (*) suction range (80-6000kPa)

2.4.2. Procedure for suction test

In this study, the experimental procedure in accordance with (ASTM D5298-03, 2003) was followed. Cylindrical specimens of dimensions 100mm in diameter and 60mm in height were used. In order to speed up the experiment, cylindrical specimens with 4%, 6% and 8% water contents were manufactured, thereby reducing time taken in drying process. Each set of moisture content had 4 cylindrical specimens. The diameter of the Whatman 42 filter paper to be placed in-contact with the soil surface is curtailed and sandwiched in-between two filter paper of same make as shown in Figure 2-7. Before commencing the experiment, the air dry weight of the curtailed Whatman 42 filter paper is weighed to the precision of 0.001g, and the weight of the moist soil specimen is weighed with precision 0.01g.

The filter papers prepared are placed in between two cylindrical specimens one above the other as shown in Figure 2-7. So for every set of soil water, there are minimum of three filter paper positioned in contact with soil specimens. The stack of soil specimens are then wrapped air tight and stored in a climate controlled room at 23° C and 50% RH. As per (ASTM D5298-03, 2003) to attain moisture equilibrium between filter paper and soil specimens, a minimum of 7 days is required. Hence the specimens with filter paper is stored undisturbed for 8 days. Immediately after removing soil specimens from air tight contained, the weight of moist filter paper is measured with precision 0.001g and transferred into oven at 100-105° C for measuring oven dry weight. Similarly the weight of moist soil is measured and transferred into oven to measure oven dry weight. The oven dry weight of filer paper and soil specimen is measured after 48 hrs. From the difference in weights, the filter paper water content and soil water content are calculated. The oven dry

soil specimens are reused to measure suction values at less than 4% soil water content. The oven dry soil specimens are categorised into three groups, one group of specimens are placed in climatic controlled room at 23° C and 50% RH, the second group of specimens are placed in air tight box with salt solution to maintain a RH of 23% at 23° C, and finally the third group of specimens are used as over dry state. These three groups of specimens had a soil moisture content of around 2% and 1% and 0% (oven dry state).

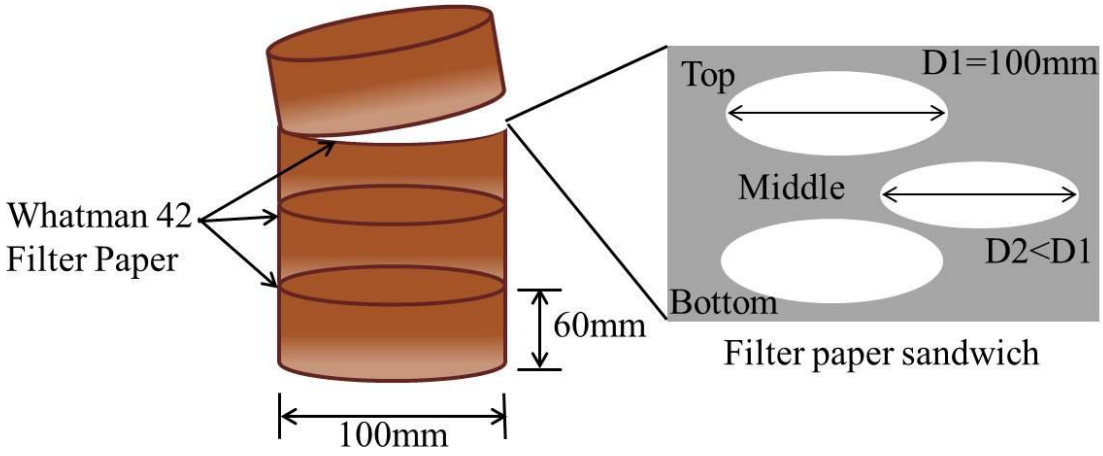

Figure 2-7 Filter paper arrangement

2.4.3. Result

The calculated soil water content and filter paper water content for both the soils are plotted in the Figure 9-2 (annexure). The maximum filter paper water content is found to be around 33%, hence (ASTM D5298-03, 2003) proposed calibration for filter paper water content less than 47% is used to calculate soil suction. To observe the difference in soil suction from different calibrations proposed by researchers as suggested in (Bicalho et al., 2007), the calibration of Chandler et al. (1992) and Oliveira & Marinho (2006) as cited in (Bicalho et al., 2007) are used. To have more accurate suction values the calibration curve established by (SOUDANI, 2016) for the Whatman 42 batch used in ENTPE is also used. The suction values for the examined soils are calculated based in the following calibration equations (Table 2-6). The suction values of CRA and Dagneux soils with respect to soil water content are plotted in the Figure 9-3 (annexure) and Figure 9-4 (annexure). As explained in (Bicalho et al., 2007; Pan et al., 2010), the difference in suction values from different calibrations are higher at higher water content and reduces with reduction in water content.

Table 2-6 suction calibration equations used for CRA and Dagneux soil

Reference	Suction	W (%) range	Log_{10} (suction), kPa
ASTM D5298	Total & Matric	W < 45.3	5.327 – 0.0779 w
Chandler et al. (1992)	Matric	W < 47	4.842 – 0.0622 w
Oliveira & Marinho (2006)	Total & Matric	W < 33	4.83 – 0.0839 w
Lucile (ENTPE, Lab)	Matric	-	5.2473 - 0.1241 w

Note: 'w' is the filter paper water content

The suction values are calculated with respect to the filter paper water content, but in the analysis gain of suction is expressed with respect to change in soil water content. The suction values of CRA and Dagneux soil specimens with respect to the calibration of (SOUDANI, 2016), ENTPE is presented in Figure 2-8. The soil suction increases with decrease in soil water content for both the soils examined, this is in agreement with (Q. Bui et al., 2014; Daniela Ciancio et al., 2013; Gerard et al., 2015; P. A. Jaquin et al., 2009; Nowamooz & Chazallon, 2011). Hence suction contributes to the gain in strength of USRE with decrease in moisture content. Considering the significant difference in suction calibration values, to obtain a good correlation, it is recommended to establish a calibration chart for the batch of filter paper used in the lab.

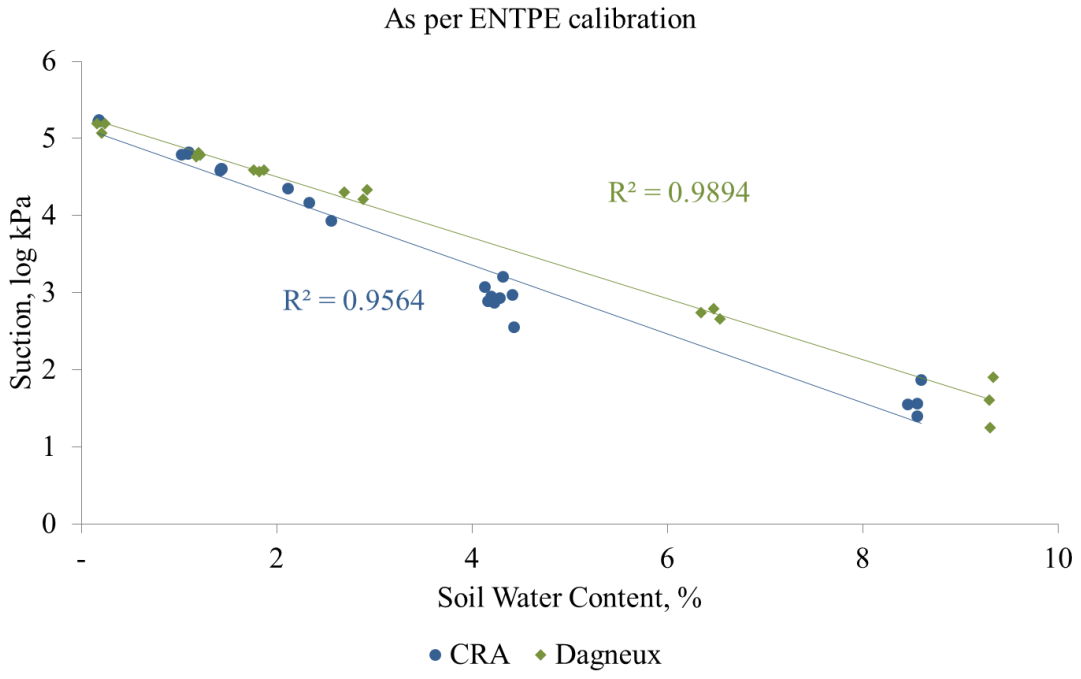

Figure 2-8 suction values of CRA and Dagneux soil specimens with respect to ENTPE calibration values

3. Sample Preparation and Conditioning

In this section, different soil specimens manufactured for studying suction, compressive strength, tensile strength, shear strength, and flexural strength of the material will be elaborated.

3.1. Preparation of USRE cylindrical specimens

3.1.1. For Compressive Characteristics

Cras-sur-Reyssouze and Dagneux soils are extracted from an ancient building which was demolished during renovation work. These were unstabilised walls, and large cubes were transported to laboratory. As a preliminary work, soils are manually crushed using hammer, to obtain maximum grain size of 10mm, crushed soils grain size were roughly estimated and passed in a mechanical crusher with maximum size of 10mm.

Soil is air dried before estimating the initial moisture content present in the lot. Designed water content is calculated and added to the soil and mixed well until the homogeneous mix is achieved, depending on the quantity of soil mixed, manual or mechanical stirrer is used, if the quantity of soil mixed is less than 50kg then hand mixing is preferred. Homogeneous wet soil is then transferred to air tight plastic bags and preserved for 24hrs before using them to manufacture specimens; this will ensure that the water equilibrium is achieved within the soil mix.

3.1.1.1. Large Size cylinders

For studying the characteristics of the unstabilised rammed earth in compressive loading, cylindrical specimens of dimension 320mm (height) × 160mm (diameter) as shown in Figure 3-1, are manufactured at different energies. All the specimens of Crass-Sur-Reyssouze soil were compacted using the electromagnetic rammer. The prepared moist soil is poured into the metallic compaction mould (160mm (diameter) and 320mm (height)) in 3 or 5 layers as per the required density to be achieved. Moist weight of soil required per layer is calculated and the same quantity is poured for compaction process, so that similar layer thickness is achieved and a more homogeneous specimen is manufactured. It has to be noted that all the rammed earth specimens manufactured will have higher density at the top of the layer and lower density at the bottom of the layer; this is due to higher compaction effort at the top like in situ materials.

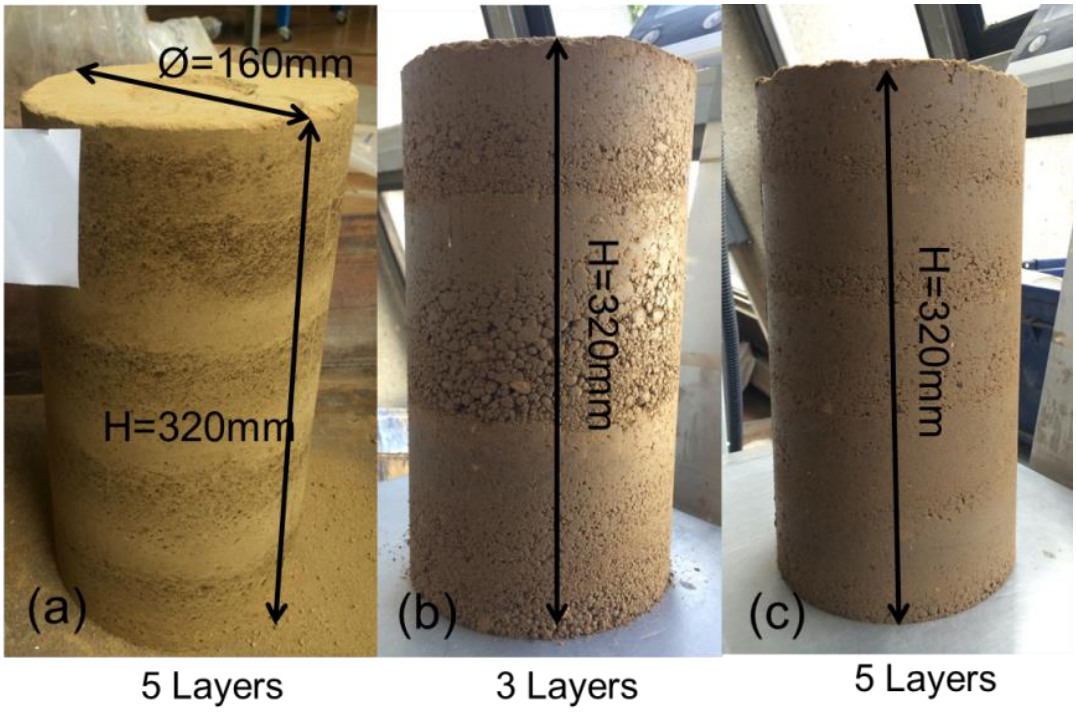

Figure 3-1 Cras-Sur Reyssouze Cylindrical Specimens: (a) E3 compaction energy, (b) Standard Energy & (c) Modified Energy

To obtain different dry densities [Υ_d] of the rammed earth soil specimens, soil was mixed with different water contents referring to OMC obtained from the proctor test, which can be classified as dry side of OMC and wet side of OMC. Specimens C3 and C5 are manufactured at different water contents, but the dry densities achieved are same for compaction energy of 2730kN.m/m^3, and also C6 and C8 are manufactured on similar lines for compaction energy of 990kN.m/m^3, specimen details are given in the Table 3-1.

Also another important criterion considered is to manufacture specimens by varying compaction energy for same manufacturing water content. C2 and C8 are manufacture at 9.5% manufacturing water content for 600kN.m/m^3 and 990kN.m/m^3 compaction energy respectively. C4 and C5 are manufactured at 10.2% manufacturing water content for 600kN.m/m^3 and 2730kN.m/m^3 compaction energy respectively.

To obtain the required compaction energy, number of blows used for ramming the soil specimen is altered along with the hammer weight and height of fall.

Table 3-1 Manufactured Specimen Details of CRA soil

Compaction Energy, [kN.m/m^3]	Specimen	N° Of Layers	Manufacturing Water Content	Dry Density, [g/cc]	OMC
600	C2 C4	3 3	9.6% 10.2%	1.89 1.87	10.5%
956	C1	3	5.7%	1.86	-
990	C6 C8	5 5	10.8% 9.4%	1.95 1.95	10%
2730	C3 C5	5 5	11.1% 10.2%	2.02 2.02	9%

Manufacturing water content of the soil specimens are calculated in accordance with (ASTM-D-2216-98, 1998), a portion of soil used for compaction layers is taken for determining water content. Water content is calculated by calculating the weight difference of the moist soil and oven dried soil at 100-105°c after 48hrs.

The metallic cylindrical mould used for manufacturing specimens were released as soon as the final layer is compacted, precautions were taken not to damage the specimen during release of compaction mould.

3.1.1.2. Small Size Cylinders

In this study, cylindrical specimens of dimension 110mm in diameter and 220mm in height are defined as small size cylindrical specimens. Small size cylindrical specimens with aspect ratio of 2 are manufactured using Dagneux soil passing through 10mm sieve. Manual compaction process was adopted for manufacturing small cylindrical specimens, knowing the manufacturing water content and density to be achieved, number of blows required for each layer in hand compacting proctor rammer was calculated and adopted for three different energies as detailed in Table 3-2. Specimens (as shown in Figure 3-2 (b)) were manufactured in a cardboard cylindrical tube (as shown in Figure 3-2(a)) of dimension similar to specimens. The cardboard cylindrical tubes are positioned in a rectangular wooden box. The gap between the cardboard tubes and wooden formwork is

then filled with sand, such that the cardboard is not displaced or broken due to the energy generated during ramming process.

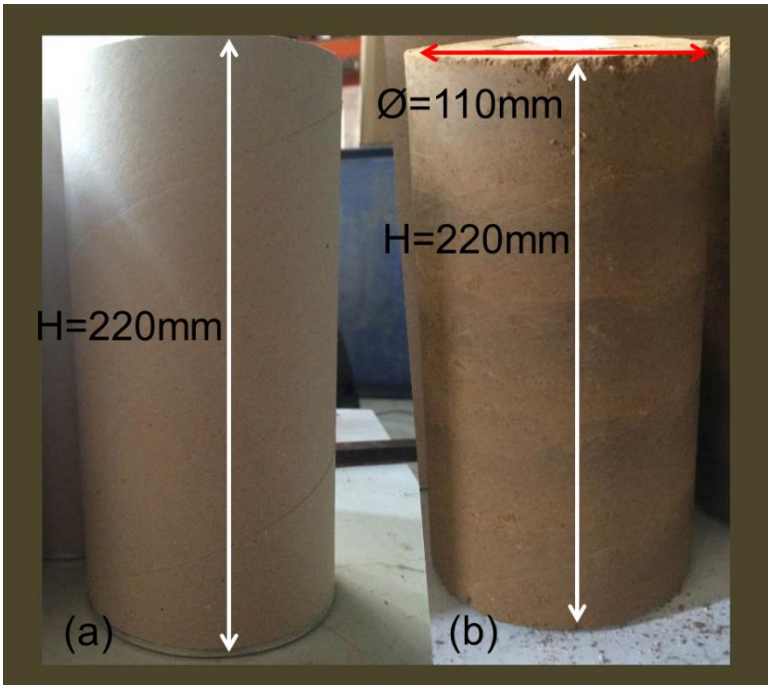

Figure 3-2 Small Cylinders of dimension 110mm (diameter) and 220mm (height), (a) Cylindrical cardboard tube (formwork), (b) Manufactured specimen

Table 3-2 Small Cylindrical Specimens - Manufacturing Conditions

Compaction Energy, [kN.m/m^3]	Specimen's	Manufacturing Water Content, [%]	Dry Density, [g/cc]	N° of Specimens
600	D1	10.6%	1.77	1
970	D2	9.9%	1.82	4
2580	D3	11.2%	1.96	3

3.1.1.3. Specimen Conditioning/ Curing

The manufactured large size cylindrical specimens are exposed to ambient atmosphere in the laboratory for a period of 7-10 days before shifting them in to the climate controlled room at 25°c and 60% relative humidity. Specimens were stored in the climate controlled room until they were tested. Small size cylinders were also stored in similar climate chamber at 25°c and 60% relative humidity. Controlled storing was adopted to ensure that all the specimens are exposed to similar environmental condition

during drying process, so that the moisture state of all the specimens are identical. Specimens were subjected to test, when the weight difference of two consecutive readings (24hours) was constant (± 0.01g).

3.1.2. For Tensile characteristics

Cylindrical specimens similar to large size cylinders are manufactured to study the tensile strength of both CRA and Dagneux soils. Specimens are manufactured in a cylindrical cardboard tube of dimension 160mm in diameter and 320mm in height, specimens were rammed by placing the cardboard tube in a wooden box filled with sand such that the external surface of the tube is covered by the sand. Weighed quantity of moist soil for each layer is poured into the cardboard tube and manual compacted using a metallic rammer (as shown in Figure 3-3) until the desired layer thickness of 60mm (± 2mm) is achieved. Three specimens for each soil was manufactured and stored in the climate camber at 25°C and 60% relative humidity.

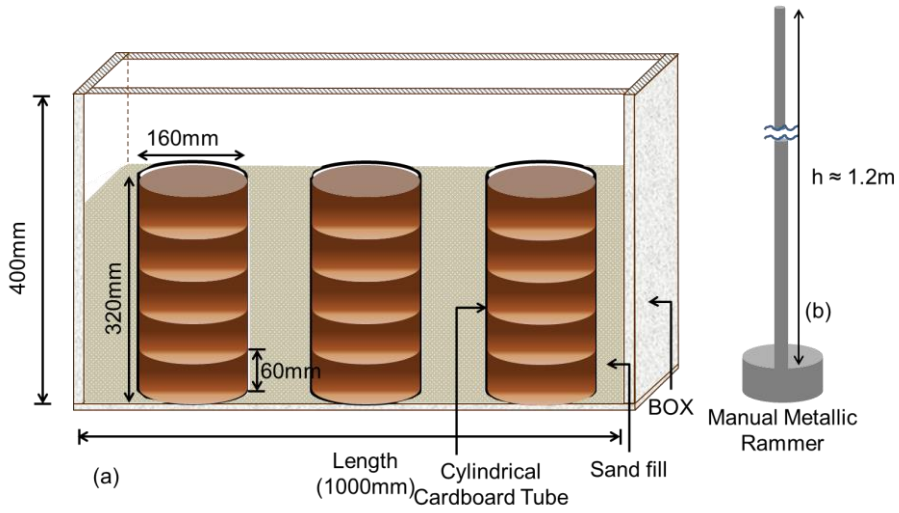

Figure 3-3 Manual Compaction of Cylindrical (Large) Specimens (a) Manufacturing Set up, (b) Rammer

3.2. Preparation of USRE Prisms

Rectangular prism samples are manufactured and tested to study the interface behaviour of rammed earth walls under biaxial loading (shear test). To obtain the shearing parameters of the interface, samples are tested at different vertical angles such that, resolved failure stress are different for each inclination. Length of the rectangular prism specimens tested at different inclinations is altered, so that the vertical symmetry of the test samples at different inclinations is attained, dimensions of the specimens tested are shown in Figure 3-5. The width and thickness of the all the prism specimens is 120mm. In this

study, only two layered rectangular specimens were manufactured and tested, with layer thickness of 60mm (+/-2mm) each.

All the rectangular prisms are manually compacted in a wooden box fabricated in the laboratory as shown in the Figure 3-4 (a). Using a metallic rammer as shown in the Figure 3-4 (b), weighed moist mass of soil for each layer is rammed until the desired layer thickness of 60mm is achieved. In order to improve the cohesion force of the layer interface, for some of the specimens, forced indentation (as shown in Figure 3-6) was made on the layer interface surface before ramming the top layer, this layer indentation or surface scratching was done only for Dagneux soil. For CRA and remaining Dagneux specimens, no surface indentation was made; hence it has a smooth layer interface surface.

Since manual compaction was adopted, the compaction energy was not monitored, but the manufacturing water content of the soil was controlled while mixing. The moisture content of the moist soil is measured for each specimen manufactured. Moist soil is prepared similar to as explained in the above section. Weighed moist soil rammed for each layer was calculated according to the desired dry density to be achieved. The manufacturing details of the rectangular prism specimens manufactured for studying interface shear properties are given in the Table 3-3.

Failure of prism specimens tested for interface shear strength test are due to delamination of interface, thereby two layers of rammed earth prism are obtained after the test. Care has been taken to select specimen layers without damage. Specimens without damage are later used to study the compressive strength and flexural strength of the prisms. Prism specimens (layer) with dimension of 210×120×60 mm (obtained from 30°inclination) are used for compression test, and 330×120×60 mm (obtained from 20° inclination) is used for flexural test.

To study the flexural strength of the rammed earth within the layer, i.e. at the top and the bottom of the layer, additional specimens of dimension 330(L) × 120(b) × 60(t) mm are manufactured and tested in flexural (bending) test.

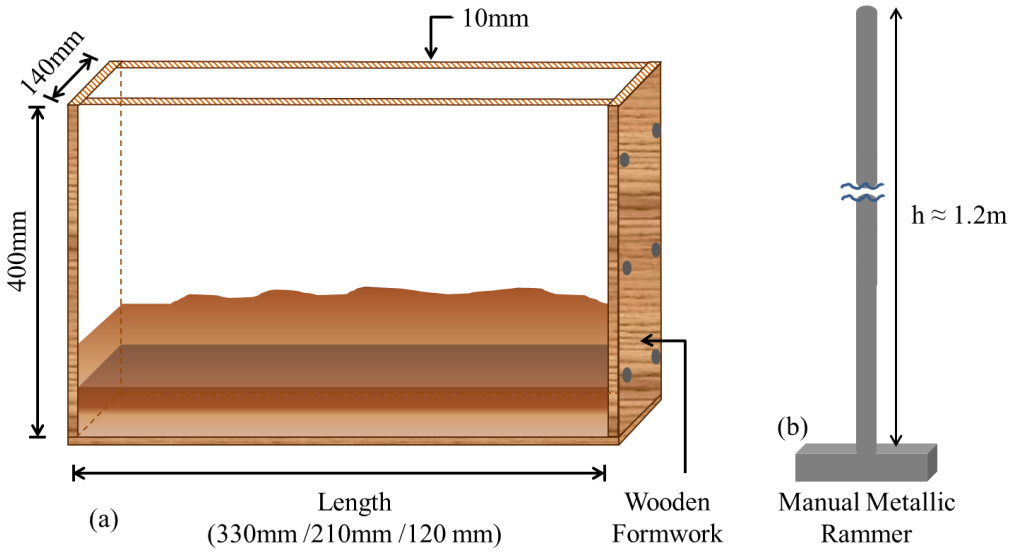

Figure 3-4 (a) Wooden Formwork used for Ramming Prism Specimens, (b) Manual Metallic Rammer

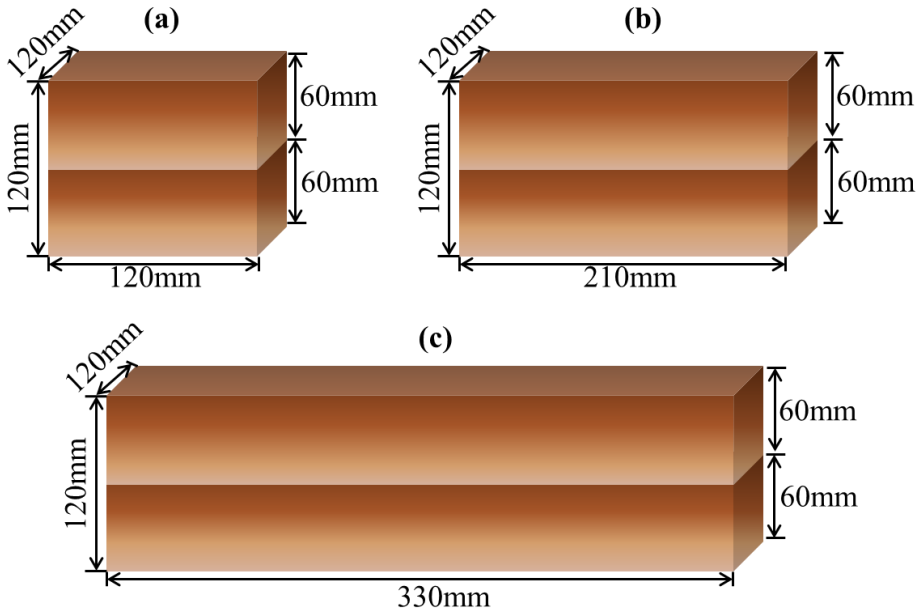

Figure 3-5 Specimens used for Shear Test (a) for 45° Inclination, (b) for 30° Inclination, (c) for 20° Inclination

Figure 3-6 Layer Surface Indentation

Table 3-3 Rectangular Prism Specimen Manufacturing Details

Soil	Angle of inclination tested	N° of Specimens	Manufactured water content	Dry Density, g/cc
CRA	20°	3	9.20	1.70
	30°	3	9.80	1.88
	45°	3	9.20	1.94
Dagneux	20°	3	10.63	1.72
	30°	5	9.52	1.84
	30°(Indentation)	7	10.95	1.81
	45°	6	10.70	1.85
	45°(Indentation)	4	10.65	1.82

3.3. Density profile

Due to the manufacturing technique of rammed earth wall, the density within the layer is not uniform. As the compaction energy at the top of the layer is maximum and the energy is distributed linearly within the layer, the density of the rammed earth at the top of the layer should be higher than the bottom of the layer (Figure 3-7). It is assumed that the density within the layer is varying linearly. The work of (Q.-B. Bui & Morel, 2009) identifies the heterogenetic property of rammed earth due to variation in density within the layer. In this work, an effort to analyse the variation of density within the layer due to change in compaction energy is carried out.

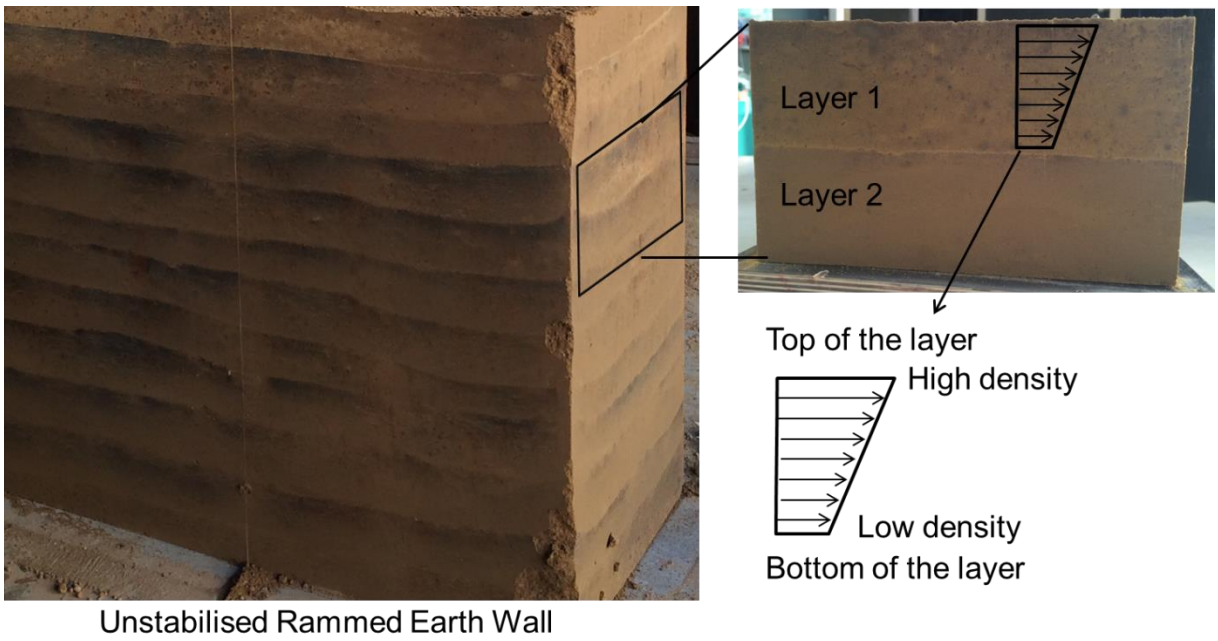

Figure 3-7 representation of variation of density within the layer

To analyse the variation of densities within the layers, cylindrical specimens manufactured at three different compaction energies are considered. Layers of the cylindrical specimens were delaminated and each layer is cut in the middle, such that top and bottom part of the layer is extracted as shown in Figure 3-8. As a next step, three samples from top and bottom part are taken for calculating the densities within the layer. The densities of the samples extracted within the layers are calculated based on the Archimedes principle.

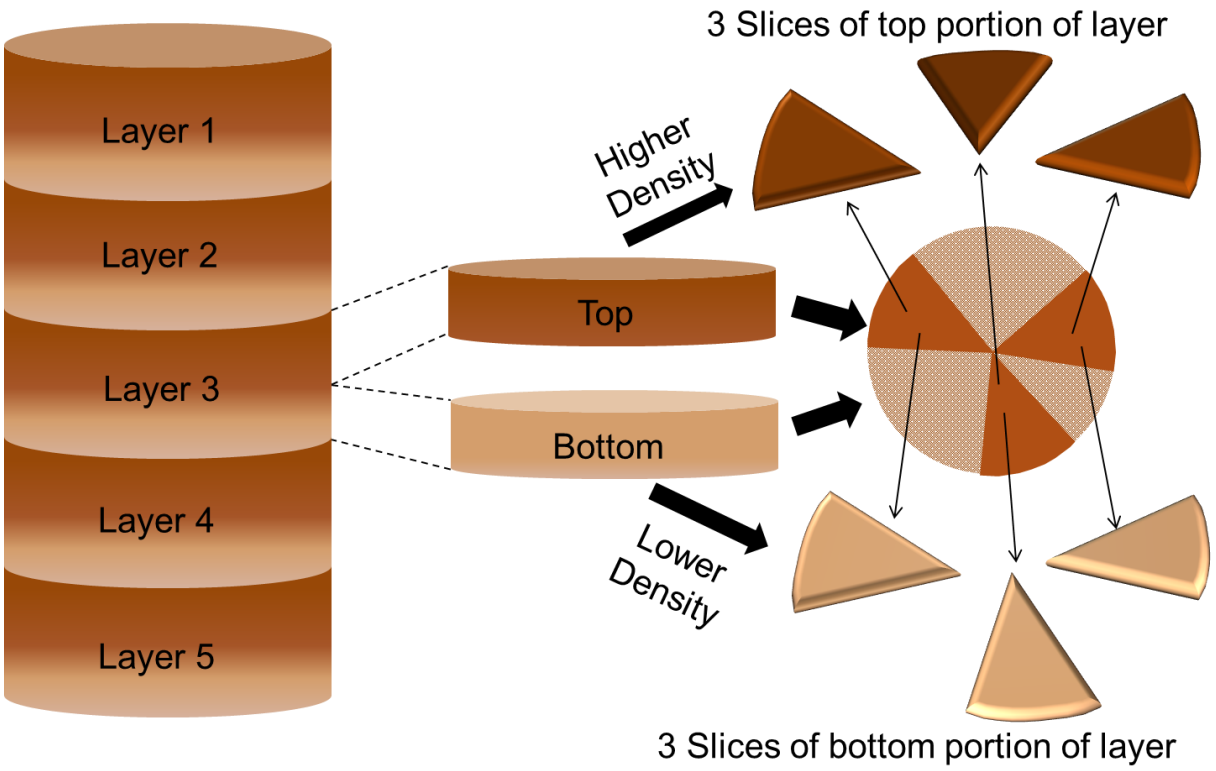

Figure 3-8 graphical explanation of specimen extraction for density calculation

The dry density of the top and bottom parts of the layer is calculated for all 5 layers, and the average dry density of top and bottom layer is taken for analysis. In case of CRA soil specimen manufactured at 600kN.m/m^3, only three layers are investigated. The variation of dry density for CRA and Dagneux specimens is given in Table 3-4. The difference in dry density within the layer decreases with increase in compaction effort, leading to more homogenised layer formation.

Table 3-4 Density variation of CRA and Dagneux soil specimens

Soil		CRA			Dagneux		
Compaction energy		600	990	2730	600	970	2580
Dry density, g/cc	Top	2.13	2.11	2.15	1.95	2	2.06
	Bottom	1.9	2.02	2.13	1.70	1.84	2.01
Difference in dry density, g/cc		0.23	0.09	0.02	0.25	0.16	0.05
% variation from top to bottom		11%	4%	1%	13%	8%	2%

4. Compression Testing of Unstabilised Rammed Earth (USRE)

4.1. Introduction

Compressive strength is one of the most important parameter considered in design guidelines; it serves as the basic mechanical parameters in selection of material for building construction (J. Morel et al., 2007; B. V. Venkatarama Reddy & Prasanna Kumar, 2011a). The compressive strength of USRE is considered to be in between 0.5MPa – 4 MPa (Daniela Ciancio & Jaquin, 2011; Maniatidis & Walker, 2003) and the other earthen building material such as CEB was reported to vary in between 2-15MPa depending on the stabilisation (Deboucha & Hashim, 2011; J. Morel et al., 2007; Muntohar, 2011; Reddy et al., 2007; B. V. Venkatarama Reddy & Gupta, 2006, 2008; P Walker & Stace, 1997). The study of (A W Bruno et al., n.d.), showed that the mechanical parameters of unstabilised CEB can be enhanced by increasing the compaction effort. The strength of the CEB's compacted at high pressures were found to be in between 4.2-10MPa, this kind of strength is similar to that of stabilised CEB's. Hence the influence of the compaction energy on the earthen building materials has a very important role in design. In case of CEB's, compaction on top and bottom surface of the block is adopted, whereas in rammed earth the ramming process is limited to top surface, thereby creating a varying density profile within the layer. It was also seen that the variation of density within the layer reduces with increase in compaction effort. As the compaction energy changes, the manufacturing water content should also change in order achieve maximum dry density(Beckett & Ciancio, 2014; Smith & Augarde, 2014; B. V. Venkatarama Reddy & Prasanna Kumar, 2011b), hence the influence of manufacturing parameters on the rammed earth is vital in understanding mechanical parameters. Unlike the standardised experimental procedure specified for concrete, there is no conclusive testing procedure to manufacture and test the rammed earth compressive strength (J. E. Aubert et al., 2015; Q.-B. Bui & Morel, 2009; D. Ciancio & Augarde, 2013; Maniatidis & Walker, 2008; J. Morel et al., 2007).

The compressive strength of USRE for a soil is dependent on various parameters (Beckett & Ciancio, 2014; Miccoli, Müller, & Fontana, 2014), some of the most important parameters are compaction energy, manufacturing water content, testing moisture content, dry density (Agostino Walter Bruno et al., 2015; Reddy & Kumar, 2009; Peter Walker et al., 2005). Some of the current practices (Beckett & Ciancio, 2014; Daniela Ciancio & Jaquin, 2011; Daniela Ciancio et al., 2013) recommend the use of proctor compaction energy as reference to manufacturing specimens. But the question is how to replicate the in-situ condition in the laboratory (Q.-B. Bui, Morel, Hans, & Meunier, 2008; J. Morel et

al., 2007). Proctor compaction energies are considered to be more suitable to geotechnical works and has very less relevance for earthen construction (Mesbah, Morel, & Olivier, 1999). To overcome this ambiguity and in the absence of suitable measurable compaction energy to manufacture specimens that can replicate in situ conditions, (Gerard et al., 2015; Hall & Djerbib, 2004; Peter Walker et al., 2005) proposed a technique which resemble in-situ compaction effort. This technique states that the moist soil poured into the formwork has to be compacted until ringing sound is heard upon the impact of hammer on the surface of the compacted soil layer. Similarly to identify the manufacturing water content of the soil, (Maniatidis & Walker, 2003) proposed the drop test to identify the required water content. Considering the above two methods to be very perspective and depended on the mason, many doubts were raised on the reliability and reproducibility (Smith & Augarde, 2014).

Since, it is difficult to replicate the specimens with the exact nature of in-situ walls, and also considering huge variable factors on manufacturing water content and compaction energy. In this study, the cylindrical specimens that are manufactured using Proctor method at three different compaction energies are experimentally investigated for their compressive behaviour. The experiment is focused on studying the reliability of Proctor method for manufacturing specimen. The compressive stress strain characteristic such as, initial tangent modulus and average cyclic modulus are studied by inducing loading and unloading cycles at different stress levels. The influence of dry density and compaction energy on compressive strength and modulus are also presented.

4.2. Experimental studies on rammed earth: a review

Considering that the mechanical testing principle and procedure for both USRE and SRE (cement and lime) to be similar. The literature review of most relevant works on USRE and SRE is discussed below.

To study the mechanical parameters of the soil used in ancient USRE construction, a detailed laboratorial experimental investigation was conducted by (Araki et al., 2011). In this experimental campaign, specimens are subjected to unconfined compression test, unconfined tensile test, and tri-axial compression test. To understand the elastic behaviour of the specimens, cyclic and monotonic loading were applied to specimens under unconfined compression and tensile test. The soil used is a blend of clayey sand and silty sand, an approximate of 16% of clay was present in the blended mix. The specimen tested were manufactured using modified compaction energy at OMC to achieve the dry density

of 1.95g/cc to 1.99g/cc. For compression test, cylindrical specimens with dimension of 50mm in diameter and 100mm in height were used, whereas to accommodate necking effect in tensile test at the mid height, specimen length was increased to 140mm high with trimmed diameter at mid height. For cyclic loading, two stress points were predefined one at 40-50% of peak stress and the other at 80% of the peak stress, peak stress was found in monotonic loading. Unconfined compression test was carried out at an axial strain rate of 1%/mm, while unconfined tensile test was carried out at 0.01%/mm for monotonic loading, and 0.05%/mm for cyclic loading. From this experimental investigation initial tangent modulus, secant modulus, peak stress (compressive strength), influence of drying period on compressive strength, relation between tensile strength and compressive strength were studied. The average peak strength of the soil for different series depending on type of curing varied from 2.8MPa to 4.2MPa, with average initial and average secant modulus of 2500MPa and 1000MPa (data extracted from graph - approximate values). The tensile strength was found to be 10% of compressive strength, but the initial tangent modulus in tensile test was similar to compressive test. It was also noticed that the strength and modulus of the material increases with decrease in strength, which is attributed to suction effect. It is interesting to note that the secant modulus is less than initial tangent modulus.

The effect of moisture content on the mechanical strength of the rammed earth was studied by (Q. Bui et al., 2014). In this study, compressive strength, suction effect, elastic modulus of 5 different soils was studied. Cylindrical specimens with aspect ratio of 2 were used to study compressive strength characteristics of the specimens. To study the elastic property of the material, specimens were subjected to cyclic loading pattern. The initial modulus and secant modulus of the specimens were also calculated. From the compressive stress train characteristics, author describes that the material has a linear elastic region up to 15% of the peak stress. From the interpretation of the experimental results, the compressive strength of the specimens increased with the decrease in moisture content, but the rate of increase in strength varied with change in soil. The compressive strength of USRE soil specimen's was in quasi static state for less than 4% moisture content. Using filter paper technique, suction strength of the USRE specimens were measured and a relation of suction with respect to compression strength was also established.

(T.-T. Bui et al., 2014) presents the experimental results of compressive strength, tensile strength, and also determines the shear strength with the help of Mohr's circle theory. This paper also presents compressive test on wallets (small walls) to validate the numerical simulation. The compressive strength of USRE soil specimens were calculated

by testing cylindrical specimens, prism specimens, and wallets under compressive loading. In case of prisms, compressive strength of the USRE specimens in the direction perpendicular to layers and parallel to layers were studied. The compressive strength of cylindrical specimens was found to be 1.9MPa with young's modulus of 500MPa and Poisson's ratio of 0.22. During testing of prism specimen in the direction parallel to layers, authors observed layer separation phenomena without any decrease in load carrying capacity of the specimen. This is an example of heterogeneity of the material and low cohesion of the layer interface. From the analysis, tensile strength of the rammed earth within the layers and between the layers was found to be same, and it was 11% of the compressive strength. From the compressive testing on the wallets, the compressive strength was found to be lower than the cylindrical representative specimens. This raises the discussion to reliability of strength produced by cylindrical specimens. From the Mohr's theory, the shear strength of the USRE was found to be 14% of compressive strength, the values were found to be in accordance with the earlier works (P. A. Jaquin, 2008). From the results, the author recommends to use 10% of compressive strength as the tensile strength and shear strength for the practical purpose.

(Champiré et al., 2016) has conducted experimental investigation to study the mechanical parameters of the compressed earth with respect to change in exposure environment of the specimen (relative humidity). In this study, non-contact sensors such as digital correlation tool are adopted to understand the stiffness parameters. Cylindrical specimens of aspect ratio 2.17 were subjected to cyclic loading and reloading phenomena to study elastic properties of the specimens. Author has made several analysis on the mechanical parameters such as variation of compressive strength, young's modulus, irreversible strain with respect to change in moisture content of the specimen due to change in relative humidity. For all the three different soils studied, relation between compressive strength and young's modulus is also established. From this analysis author concludes that the unstabilised earthen building materials faces reduction in strength parameters with increase in moisture content, but the percentage of variation is independent to soil itself. This study also quotes the importance of clay type in the contribution to mechanical parameters.

(Daniela Ciancio et al., 2013) studied 10 different engineered soils to access the suitability for rammed earth construction. From the experimental investigation, it was found that PSD is an indication of soil to achieve better density, and it cannot be taken as the sole indicator to select the soil for USRE construction. In the experimental campaign,

experiments such as unconfined compressive strength, accelerated erosion test, drying shrinkage test were conducted apart from the preliminary soil investigation such as PSD, Atterberg's limits and proctor tests. In this study, both USRE and CSRE were studied to compare the experimental results with existing guidelines. From the results, a correlation between dry density and compressive strength was figured out, but the results were scattered for USRE preventing to draw a conclusion. The accelerated erosion test procedure is not in synchronisation with the real climatic exposure as studied by (Q. B. Bui et al., 2009), hence more insight to this laboratorial procedure is required. From this analysis, the shot comings of the existing guidelines were exposed, calling for more experimental investigation on rammed earth structures.

In an another interesting work by (Gerard et al., 2015), a unified failure criterion which includes effect of suction due to change in relative humidity is established. The experimental program included the study of unconfined compressive strength, split tensile strength, suction strength of the material (Belgium soil). Author also believes that the normal proctor energy is a good referral but more suitable to geotechnical studies, for earthen structures, where the compaction energy is higher, an alternative method to find OMW and MDD is more appropriate. In this study, dynamic compaction process is adopted, where the compaction is carried out until the ringing sound is heard upon the impact of hammer (Peter Walker et al., 2005). OMC obtained from the above procedure is used for manufacturing the specimens. Filter paper method is adopted to extract the suction strength of the soil specimens. In this analysis to the author highlights the increase in compressive strength with decrease in moisture content of the specimens. The tensile strength is approximately 13% of the compressive strength for specimen with moisture content varying 8%-3.6%. The tensile strength reported for specimens with 1.8% moisture is close to 2% of compressive strength. To obtain the effective stress parameter for the constitutive model, cohesion (6.2kPa) and internal friction (36.5°) were found from the tri-axial test on saturated specimens.

In the study of (Hall & Djerbib, 2004), the sub soil is engineered to produce 10 different possible soil composition, which will fall within the recommended PSD as specified in (Houben & Guillaud, 1994). As the proctor compaction energy is not widely accepted to replicate the in-situ compaction energy, in this study compaction is carried out as specified in the NZS 4898:1998. In order to replicate the in situ practice, specimens are manufactured through manually compaction using a custom made metallic rammer. The manufacturing water content of 7-9% is taken in accordance to guidelines specified by

NZS4898:1998. 4 no's of 100mm cube consisting 3 layers were manufactured for each soil combination. Dry density of the specimens manufactured varied in between 2g/cc to 2.15g/cc. The cube specimens were tested in a load controlled (20kN/min) procedure. The correction factor of 0.7 (as per NZS4898:1998) is multiplied to the compressive strength obtained from the test. The compressive strength of the specimens varied between 0.7-1.5MPa. Author points out change in dry density have no impact on the compressive strength of the material and also notes that the binder aggregate ratio might have a contribution to strength parameter, though it needs more investigation. An observation from the graph brings up a very interesting topic, to study the impact of PSD on the strength of USRE. By interpreting the strength from the graphical data available, the compressive strength changes with respect to binder ratio within the PSD. The compressive strength remained low (0.7-1 MPa) When the binder (silt and clay) was 20%, whereas the strength was higher (1.4-1.5MPa), when the binder ratio was 30%, contrastingly, when the binder was 40%, the strength decreased (1-1.35MPa).

(Maniatidis & Walker, 2008), in this work to verify the validity of masonry design principle for the design of rammed earth structure, an experimental and analytical investigation on rammed earth was carried out. In the experimental campaign, small scale cylinders, large scale prisms and full scale columns were tested under compression loading, and for columns reduction factor based on eccentric loading and slenderness are also analysed. From the experimental results, the strength of the small scale cylindrical specimens are higher that the large scale cylindrical and prism specimens. The decrease in strength was attributed with the increase in gravel size and more moisture presence at the interior parts of large scale specimens. The full scale columns of varying heights were tested under concentric and eccentric loading. The strength of the specimen's decreases with increase in eccentric loading, for 30% eccentricity, there is a drop in 45% of strength. From the theoretical comparison, it was noticed that the masonry guidelines works for limited eccentricities, with increase in eccentricity due to change in material properties, masonry principle no longer is applicable. Author points out the need to include material tensile characteristics to improve the precision of analytical model.

(Miccoli, Müller, et al., 2014) in an attempt to compare the mechanical properties of adobe, rammed earth and cob, conducts an experimental campaign. In this experimental investigation, wallets are subjected to compression and diagonal compression test to study, compressive and shear properties of the rammed earth, adobe and cob. From the results it was seen that the mechanical strength of the rammed earth is higher compared to the other

two materials, it is mainly due to the higher dry density. The compressive strength and shear strength of the rammed earth was found to be 3.7MPa and 0.17MPa respectively along with young's modulus and shear modulus of 4143MPa and 2326MPa respectively.

In the work of (Q.-B. Bui & Morel, 2009), the anisotropic behaviour of rammed earth is experimentally studied. This study involves, experimental testing of rammed earth specimens (in different directions) and CEB specimens (with different densities), and correlate the same using homogenisation theory to find out the heterogeneity present within the rammed earth layers. The USRE representative specimens were subjected to compression loading in the directions perpendicular to the layers and parallel to the layers, to verify the strength characteristics in both the directions. With the help of cyclic loading, the modulus of elasticity at different preload points are calculated and compared for both the test procedures. At low loads a difference of 25% in modulus was found, but interestingly the difference in modulus was found to be insignificant at higher loads. The difference in compressive strength for both direction was also found to be very less (<10%). Author calculates the variation of densities at top and bottom of the layers and develops a novel homogenisation equation to calculate compressive strength. In the second experimental phase, CEB with two different densities matching with that of top and bottom densities of rammed earth layer is tested for compressive strength. The compressive strength, modulus and density obtained from the CEB specimens are used to calculate the representative strength parameters of rammed earth in both vertical and horizontal directions. The modulus calculated using the homogenization model and the experimental results were showing good correlation. The author also stresses upon the need to obtain more methods to investigate the variation of densities with the layer.

Knowing the importance of OWC (optimum water content), the study conducted by (Smith & Augarde, 2014) focuses on proposed practices to measure OWC in lab and in site. To compare the OWC of laboratory methods and in site practice, an experimental investigation on the specimens manufactured using three methods are penned. OWC's are calculated through: (1) on site compaction process (specimens manufactured using pneumatic rammer), (2) as per BS test verification, and (3) drop test as proposed in (Houben & Guillaud, 1994; Peter Walker et al., 2005). From the results, author concludes the drop test procedure lacks repeatability and suitable only to cross check the water content of the soil. The OWC calculated as per BS using vibrating hammer is in correlation with the in situ procedure. Hence to manufacture the specimens in laboratory, procedure proposed by British Standard-1377 (part-4) using vibrating hammer seems to be more

appropriate. The shortfall of this study is that the work mainly focuses on identifying the OWC, but in practice any change in water content or compaction energy, the dry density of the material changes impacting the strength. Hence suggesting the need to obtain a relation between dry densities, compaction energy with strength is important for each soil type.

The work of (Beckett & Ciancio, 2014) aimed at understanding the effect of manufacturing water content on the strength of rammed earth material stabilised with cement. In place of soil, crushed lime stone with 5% cement stabilisation is used. Material OWC was found to be 12.4% in modified proctor test. Hence specimens at water contents of 10.4%, 12.4% and 14.4% were manufactured and tested for compressive strength. The compressive strength of specimens in relation with manufacturing water content was found by subjecting specimens in uniaxial compression test at a controlled displacement rate of 0.3mm/min (5μm/s). From the results the compressive strength of the specimens manufactured at lower manufacturing water content than OWC were higher. The authors explained the reduction of strength with increase in manufacturing water content is due to the particle matrix structure.

In an experimental study carried out by (Daniela Ciancio & Gibbings, 2012) to propose recommendations, that could be used at site as a quality control procedures, experimental investigation on CSRE moulded and cored specimens were conducted. In this investigation, specimen with different aspect ratio and size effect were manufactured at site and also cored from the in-situ wall. From the moulded specimens the compressive strength variation with change is aspect ratio is plotted and a correction factor is proposed. Interestingly, the cylindrical specimens with varying diameters from 50mm to 160mm having aspect ratio of 2 yielded similar results, needing no correction factor. Though there is influence of size effect, it is not conclusive and also very minimalistic. There is a clear difference in strength obtained from moulded specimens and cored specimens, author's analysis the impact of drilling might have damaged the cored specimens, whereas the moulded specimens were manufactured in a controlled manner. From the results it was also noticed that for a small change in bulk density (5-8%) there is 52% increase in compressive strength of the specimens, to obtain a good relation more experimental work in needed. From the results, author recommends to use similar moisture and compaction effort to manufacture the specimens at laboratory.

To identify the potentiality of locally available laterite soil in Sri Lanka, (Jayasinghe & Kamaladasa, 2007) studied the mechanical properties of the cement

stabilised rammed earth using laterite soil. The wall panels manufactured with three different cement contents (%) for three different locally available soils were tested for compressive strength characteristics. The results were correlating with respect to the earlier works and indicated a lot of confidence to construct one storey buildings.

Considering the various parameters involved in the manufacturing process of CSRE, (B. V. Venkatarama Reddy & Prasanna Kumar, 2011a) studied the influence of moulding water content on the compressive strength of CSRE. The experimental program was planned such that specimens are manufactured at three moulding moisture content (dry of OMC, OMC and Wet of OMC) for three different cement contents. The results states that the compressive strength of CSRE is higher for the specimens manufactured with higher moulding water content (wet side of OMC). More water presence could possible means more water for hydration, which contributes to increase in strength. It was also observed that, with increase in dry density the compressive strength of the material increases linearly. In continuation of the above work, the experimental investigation on prism and wallet specimens, to study the stress strain characteristics under the influence of clay presence, moisture, density are detailed in (B. V. Venkatarama Reddy & Prasanna Kumar, 2011b). The compressive strength of the prisms increases with decrease in moisture at test. The wet strength to dry strength ratio decreases with increase in clay content for low cement presence, as the cement content increases wet to dry strength ratio remain constant even with increase in clay, indicating higher cement content reduces saturation of clay. From the relation of wet to dry strength of prism, wallets wet and dry strengths are calculated and compared with respect to clay content. The strength increases with increase in clay content upto a limit and later it reduces, hence it was found that the optimum clay content for CSRE is around 16%. It was also found that the dry compressive strength increases by 300% with increase in 20% of dry density. From stress strain relation, initial tangent modulus was also found to increase with increase in dry density and cement content.

4.3. Objective

The objective of this study is to find a testing methodology that enable to analyse the compressive stress strain characteristics of USRE, in relation with USRE manufacturing parameters. By establishing a relationship for compressive strength with

respect to compaction energy, it would be very convenient to interpret the compressive strength of the material for any required compaction energy. The dry density is interdependent on compaction energy and manufacturing water content, hence the influence of manufacturing water content is also analysed.

4.4. Experimental Protocol for USRE

The compressive stress strain characteristics of the USRE specimens were studied by subjecting the specimens to unconfined compression test. The loading is programed such that the stiffness property of the USRE can be studied with the help of extensometers and LVDTs. Specimen preparation, extensometer, LVDT and loading program is briefed below. From the results author highlights the importance of consideration of the compaction conditions when interpreting correlation of strength with respect to dry density.

4.4.1. Specimen setup

The cylindrical specimens stored in climate controlled room are constantly monitored for weight change, until the difference between consecutive measurements in a span of 48hrs are same (±0.01g). To establish a proper contact between the specimen and loading plates, the undulated top surface of the cylindrical specimens (Figure 4-1 (a)) are levelled and smoothened with the help of mortar screed. The mortar screed levelling paste (Ragréage fibre autolissant – DELTAPRA) is poured on the undulated surface (Figure 4-1 (b)) and allowed to dry for a period of 48hrs before subjecting to compression test. Finally loose particles and roughness on the specimen surface is removed using a sand paper (Figure 4-1 (c)).

The cylindrical specimens weights before and after application of mortar screed is measured and recorded. The surface prepared cylindrical specimens are positioned on the loading cell, such that the centroid of the loading plates and the specimen are in same vertical axis. As shown in the Figure 4-2, specimens are then mounted with three extensometers and three LVDT’s (Linear Variable Displacement Transducers), to measure axial deformation and lateral deformations respectively.

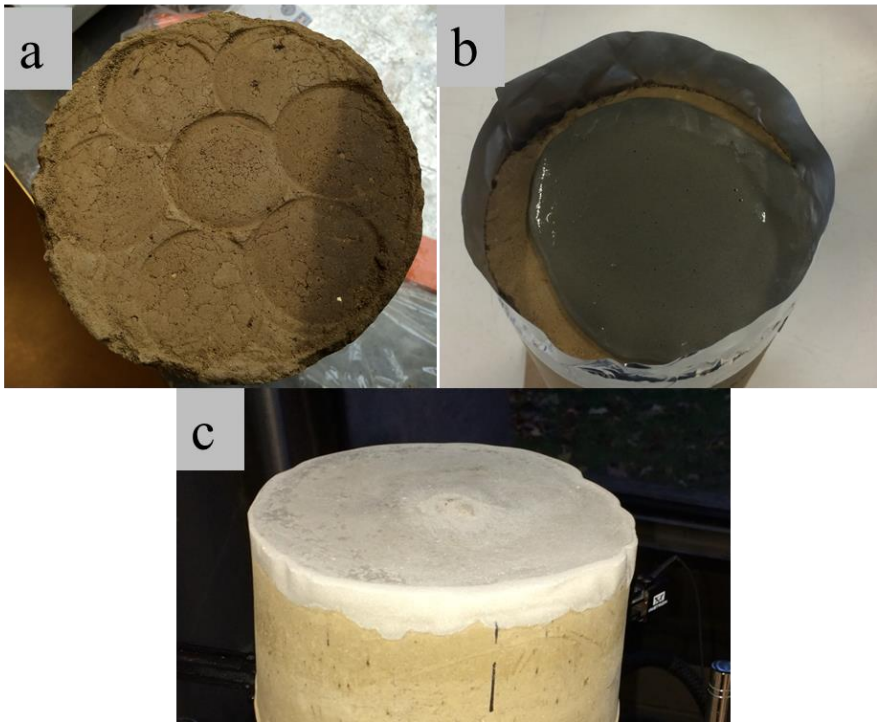

Figure 4-1 Cylindrical specimen capping: (a) undulated top surface, (b) pouring wet capping material, (c) levelled top surface with capping

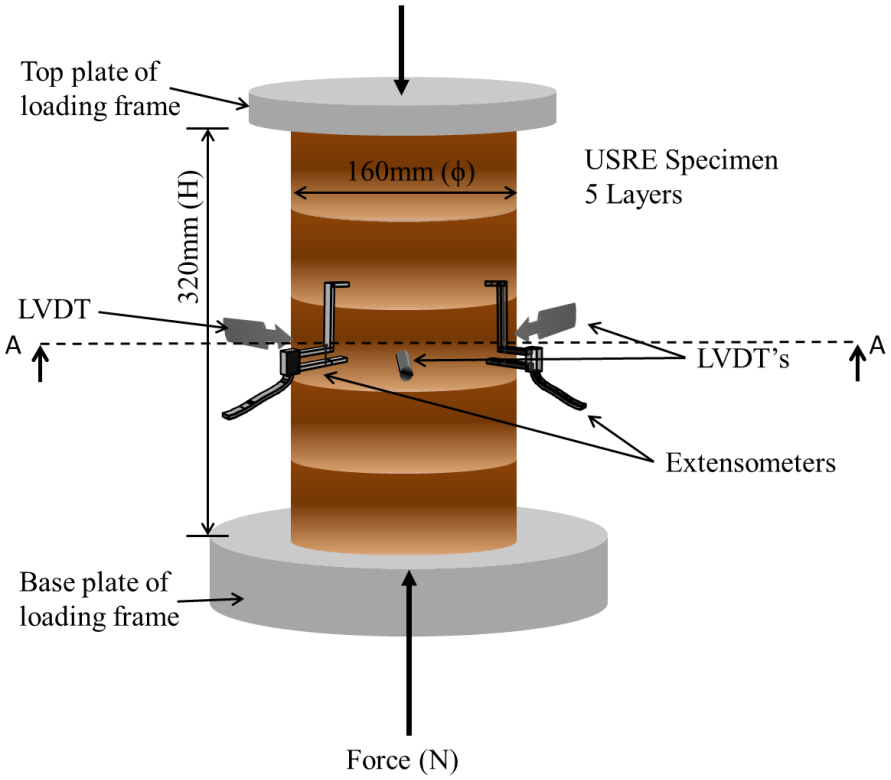

Figure 4-2 Experimental setup for cylindrical specimen in compression test

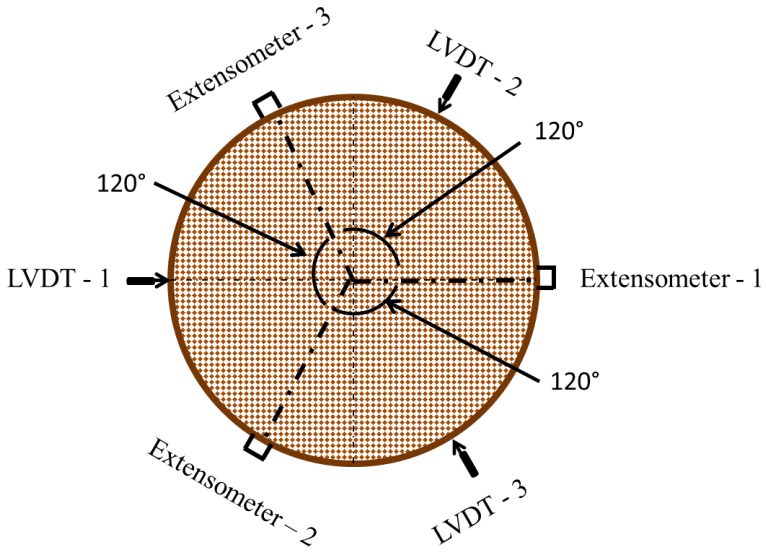

Figure 4-3 cross section A-A of cylindrical specimen

4.4.2. Extensometer

Surface contact Instron dynamic extensometers of gauge length 75mm long (shown in Figure 4-4) were used to measure the axial strain of the specimens. Three extensometers at a radial spacing of 120° between each other with respect to the centre of the specimens as shown in Figure 4-3 are positioned ate mid 1/3rd height of the specimen, such that the impact of platen restrain effect is negotiated. Use of three extensometers is most effective to measure the strain fields of the specimen. The average strain measured by three extensometers is taken as the axial strain of the specimen under compressive load. The extensometers are mounted on the specimen with the help of elastic bands. While positioning the specimens, care has been taken to avoid layer interface and also shrinkage cracks if any, so that the best position within the mid 1/3rd height is chosen. In order to understand the layered behaviour of rammed earth, extensometers are placed in between the layers, passing from centre on one layer to the other.

In this study, extensometers are used to measure the axial strain of the specimen in cyclic loading. Since the extensometers are very sensitive and the possibility of damage is high in case of sudden failure, the extensometers are demounted from the specimen after 70% of estimated failure load. The compressive stress strain presented in this study is restricted to less than 70% of the failure stress.

Figure 4-4 INSTRON extensometer 75mm (source: INSTRON website)

4.4.3. Linear variable displacement transducers (LVDT's)

Linear variable displacement transducer (LVDT) is an electrical transducer used to measure linear displacement. The LVDT used in this study was ±2.56mm long with precision of 0.001mm, which are calibrated in the LVDT calibration device before every use. LVDT's are then positioned at mid-height of the specimen. In order to obtain accurate measurement three LVDT's are used to measure the lateral (radial) displacement of the specimen. Three LVDT's are positioned at a radial distance of 120° with each other as shown in Figure 4-3. Considering the radial displacement of the specimen to be less and assuming that the specimen retains its circular shape even after deformation, the average radial displacement of the specimen is calculated as explained in annexure I. Considering the rough texture of specimen surface, a piece of aluminium scotch is glued to the specimen where LVDT comes in contact with the specimen.

Figure 4-5 Linear variable displacement transducer (LVDT)

4.4.4. Loading Program

The elastic property of USRE specimens are studied by subjecting specimens under cyclic loading (Q.-B. Bui & Morel, 2009; Kouakou & Morel, 2009). A test specimen without extensometers and LVDT's are subjected to unconfined compressive test until failure. The compressive strength of 2MPa was obtained for both CRA soil specimens and Dagneux soil specimens. Predefined load points for both soil specimens are established based on the compressive strength of the test specimen.

For CRA soil specimens, three predefined load points at 0.2MPa, 0.4MPa and 0.75MPa were chosen which represents 10%, 20% and 37.5% of estimated failure stress (2MPa). Whereas for Dagneux soil specimens, four predefined load points at 0.2MPa, 0.4MPa, 0.7MPa and 1.0MPa were chosen, which represents 10%, 20%, 35% and 50% of estimated failure stress (2MPa). CRA soil specimens were studied prior to Dagneux soil specimen, from the analysis of CRA soil specimen test data it was understood that the study of elastic behaviour at 50% of failure stress for Dagneux soil specimens would be interesting, hence 4^{th} cycle was added. The load cycles consists of loading and unloading parts as shown in Figure 4-6 and Figure 4-7.

The load cycles are programed such that, the reloading point is kept at 0.01MPa, that is the lowest unloading stress material has undergone is 0.01MPa. The reloading point of 0.01MPa is defined considering the practical difficulties in loosing contact between specimen and load plate at 0 stress, and also the minimum scale of loading press.

The specimen is loaded up to first predefined load point of 0.2MPa, which is called as cylcle-1 loading and then unloaded until 0.01MPa (100N) which is called as cycle-1 unloading. Similarly cycle-2 is loaded from the reloading point 0.01MPa; this process of reloading and unloading is programed for the said predefined load points for each cycle. The final cycle (cycle-4 loading for CRA and Cycle -5 for Dagneux) is loaded until the failure of the specimen. At close to 75% (say 75%-85%) of failure load, test is paused for a brief moment until the extensometers and LVDT's are demounted.

All the specimens are subjected to compressive loading and unloading at a rate of 10µm/s loading press displacement control mode.

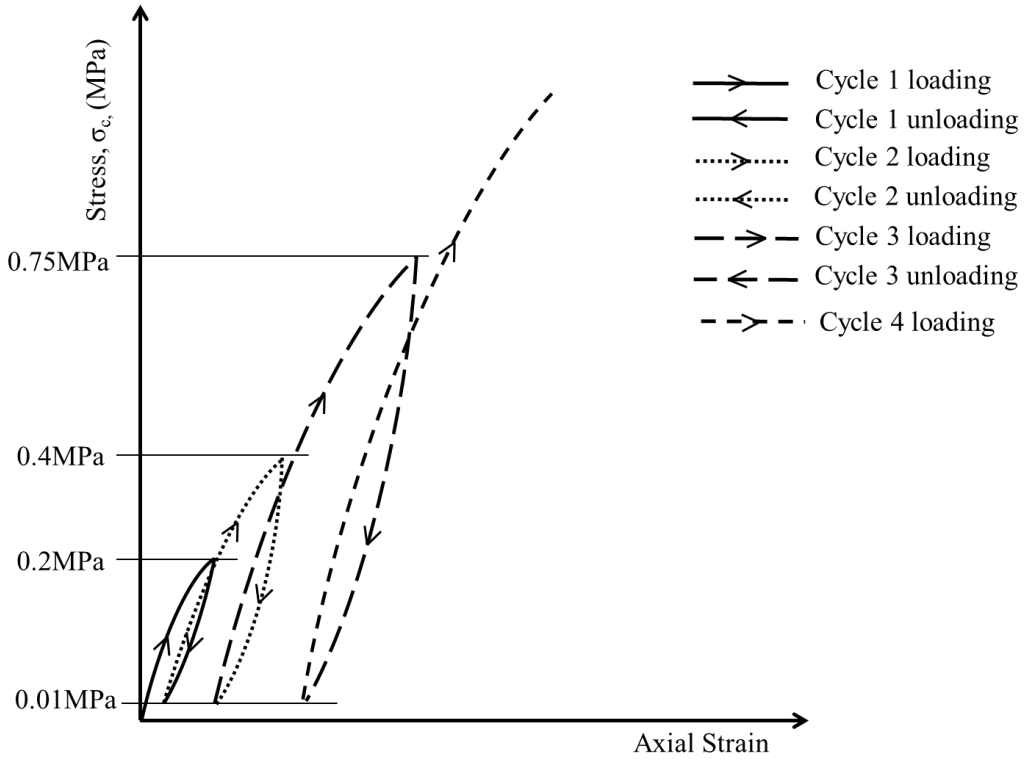

Figure 4-6 graphical explanation of cyclic loading adopted to study compressive behaviour of CRA soil specimens

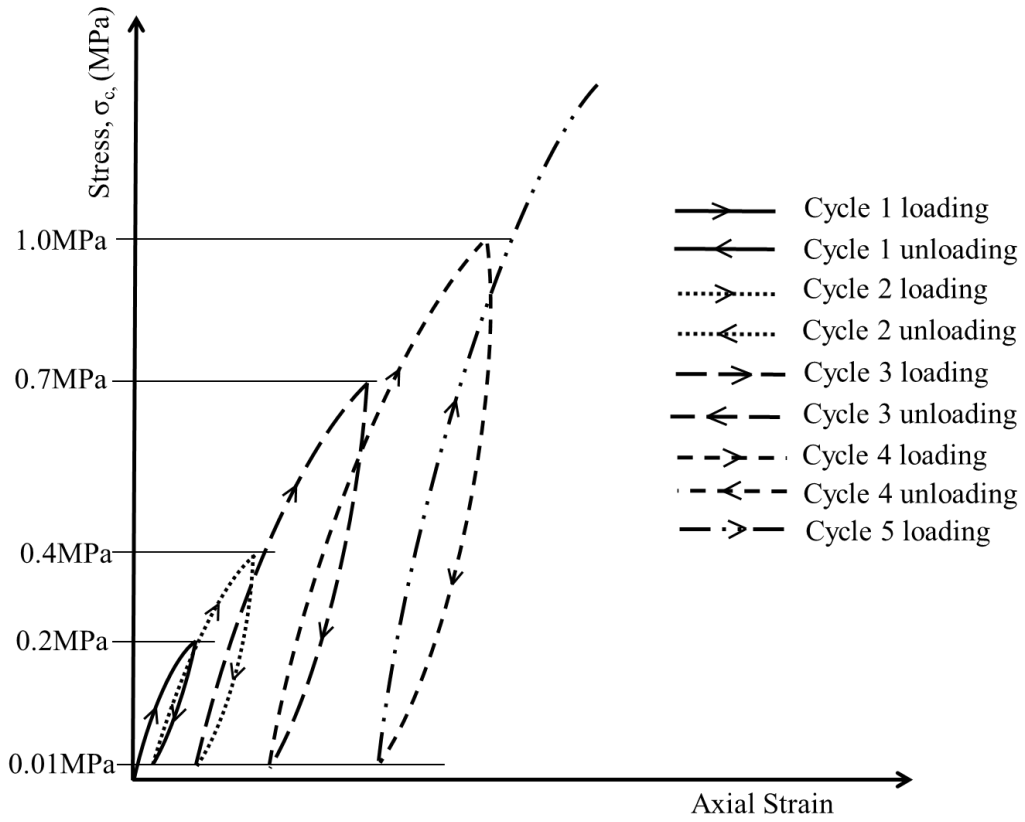

Figure 4-7 graphical representation of loading cycle program adopted for studying compressive behaviour of Dagneux soil specimens

4.4.5. Modulus of elasticity

Modulus of elasticity or elastic modulus is defined as the ratio of stress to strain, which is slope of stress strain graph in elastic strain region. Though the material tested in this study is not perfectly elastic material (Q.-B. Bui & Morel, 2009; Kouakou & Morel, 2009).

The stress strain curves of the materials tested in this study are not perfectly linear, so initial tangent modulus and cyclic modulus are calculated. As shown in Figure 4-8 (a), at very low stresses, i.e. for cycle-1 loading stress strain varies linearly, hence initial tangent modulus of the material is calculated as the slope of best fit linear interpolation of cycle-1 loading. Similarly, the slope of best fit linear interpolation of unloading and loading cycles is called as cyclic modulus, and then the average of all cyclic modulus is called as average cyclic modulus. Initial tangent modulus and cyclic modulus will be very helpful in designing numerical and analytical simulation of rammed earth structures.

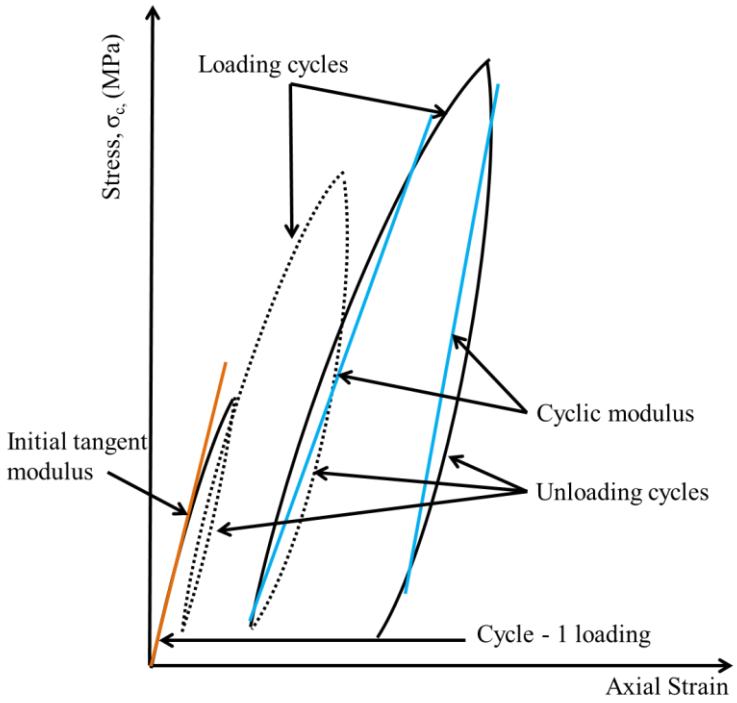

Figure 4-8 Graphical presentation of initial tangent modulus and cyclic modulus

4.4.6. Coefficient of Poisson

Poisson's ratio or coefficient of Poisson is defined as the ratio of lateral strain to axial strain of the material. In this analysis, coefficient of Poisson is calculated by fitting a secant line starting from the origin to end of cyclic loading as shown in Figure 4-9.

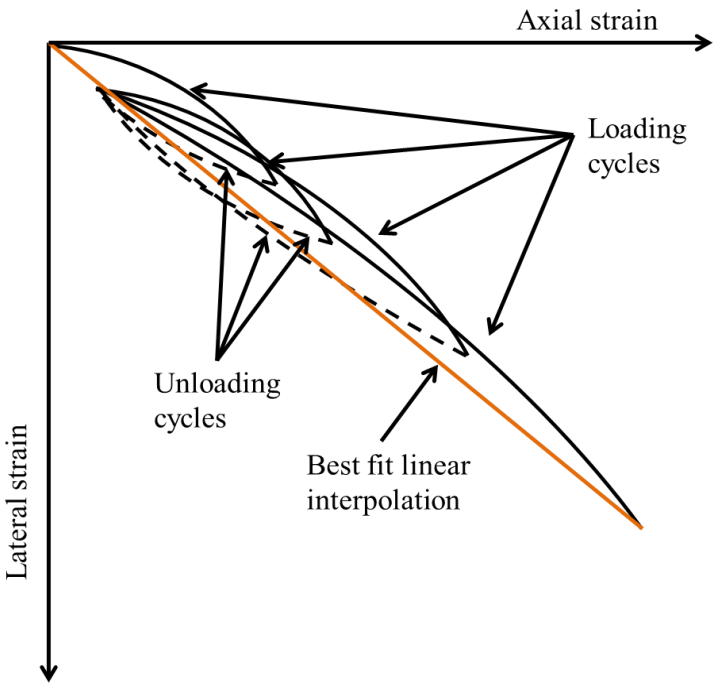

Figure 4-9 calculation of coefficient of Poisson

4.5. Result and Discussion

4.5.1. Compressive strength characteristics of CRA soil specimens

4.5.1.1. Stress strain characteristics

An example of compressive stress strain behaviour of CRA USRE soil specimen's at different compaction energies (series) are shown in Figure 4-10. The compressive stress stain presented in Figure 4-10 is restricted to 1MPa (<50% of compressive strength), where material behaviour under cyclic loading and unloading is shown. The compressive stress strain behaviour of C5 series (2730kJ.m/m^3) specimens are presented in Figure 4-11 as an example to show concerns of repeatability. It can be seen that none of specimens repeat similar straining, even though their compressive strengths are similar to each other. The similar phenomenon is observed in all the specimens under different compaction energies (series), thus the results of stiffness parameters have high deviation (shown in Table 4-1). It was noted that all the cylindrical specimens manufactured had shrinkage cracks prior to testing; this could be the major reason for non-repeatable performance of the material. From site visits and discussion with expert mason Mr. Nicolas Meunier, it was understood that the USRE walls build using CRA soil naturally exhibits shrinkage cracks. Therefore decision was made to test specimens with shrinkage cracks and understand its behaviour under loads, but due to non-repeatable performance accurate results were not achieved. It can be said that, for CRA proctor method of manufacturing specimens was not accurate

enough to produce similar specimens. At this point, it is difficult to conclude which is the best method to manufacture CRA soil specimens that can be consistent and reproduce in-situ behaviour.

Even though there is no repeatability, two specimens in each series behave quiet similar, but this is not sufficient to conclude the material characteristics. As an approximate analysis and to compare the experimental result of (Champiré et al., 2016), where same soil is used, the data obtained from this experiment is processed. In comparison with the stress strain curves presented in (Champiré et al., 2016) work (Figure 4-12), the stress strain presented in this work follows similar hysteresis under cyclic loading and unloading. But some of the specimens in each series gains more strain and undergoes more strain during unloading and reloading at very low stress. This phenomena is difficult to explain without knowing the matrix structure of particles, this behaviour could be due to closure of pores or closure of shrinkage cracks. Hence while calculating the cyclic modulus the best linear portion is considered.

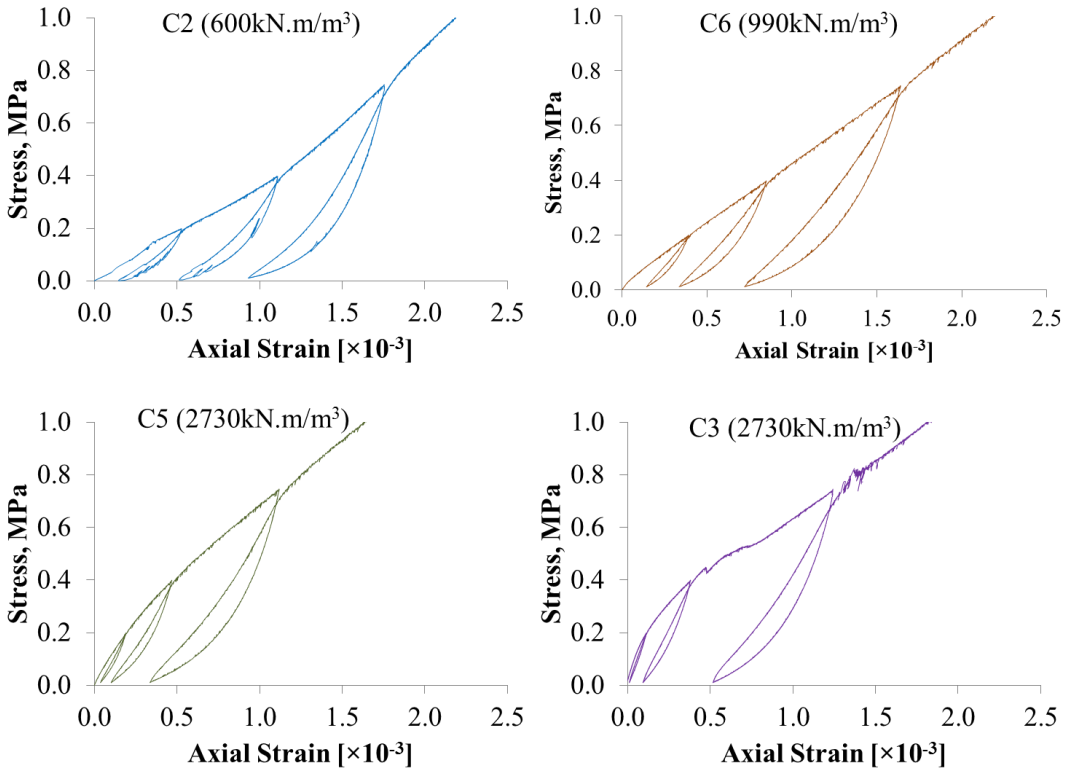

Figure 4-10 stress strain behaviour representation of CRA specimens at different compaction energies

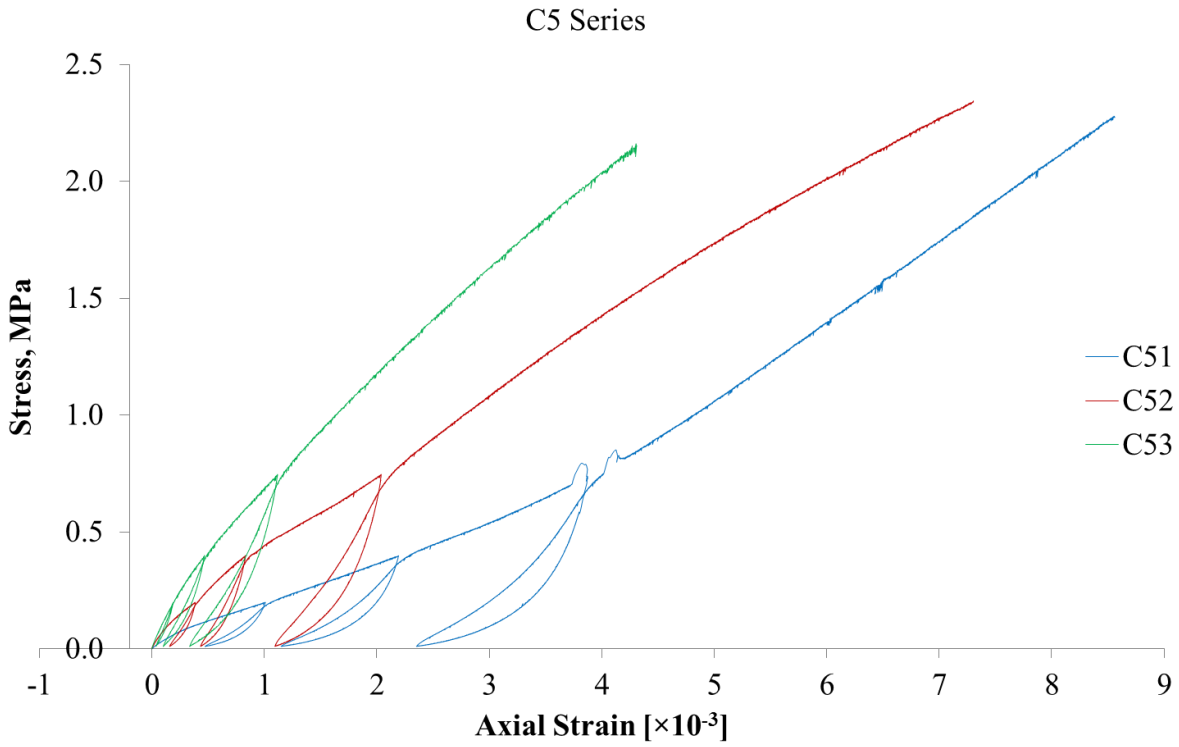

Figure 4-11 evolution of compressive stress-strain of C5 series (2730kJ/m^3)

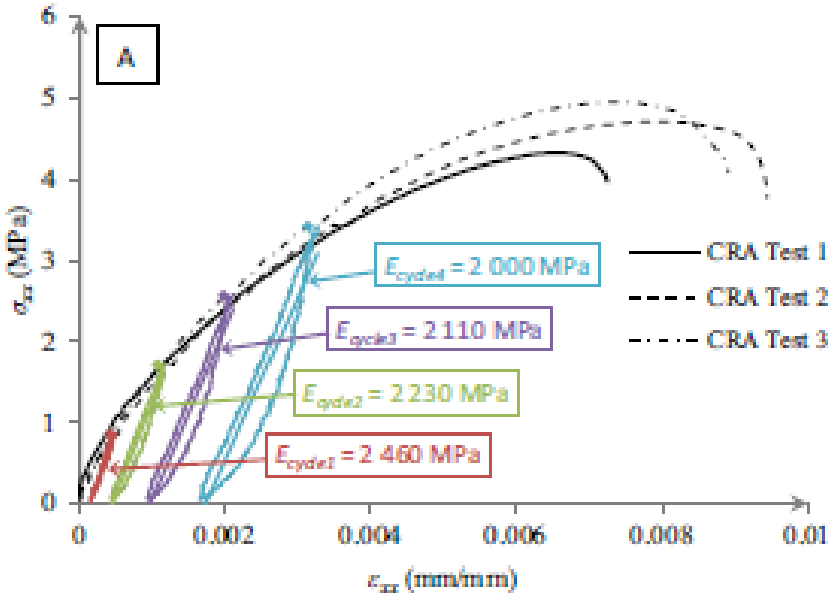

Figure 4-12 compressive stress strain of CRA soil specimens tested at 25% RH, source: (Champiré et al., 2016)

The stress strain characteristics of CRA demonstrated in the work of (Champiré et al., 2016) follows similar pattern as presented in this analysis. The dimension of the CRA specimens tested by (Champiré et al., 2016) were small and homogeneous, the

compressive strength and modulus of elasticity reported was varying in between 1MPa – 4.2MPa and 500MPa – 2200MPa depending on the specimen testing moisture content.

Table 4-1 compressive strength characteristics of CRA soil specimens

Specimen	C21	C22	C23	C61	C62	C63	C51	C52	C53	C31	C32	C33
Compaction Energy, KN.m/m3	600			990			2730			2730		
Manufacturing. Water Content, %	9.5	9.3	10.1	11.2	11.1	10.3	9.6	10.5	10.5	10.9	11.1	11.2
Dry Density, g/cc	1.91	1.87	1.88	1.95	1.93	1.98	2.05	2.00	2.05	2.04	2.01	2.03
Testing Water content, %	1.54	1.23	1.32	2.44	2.52	1.55	2.74	2.3	1.55	1.27	1.04	1.03
Compressive Strength, MPa	2.17	2.15	2.6	2.65	2.87	2.85	3.27	3.14	3.3	2.93	2.46	2.13
Avg. Comp St, MPa	2.3			2.8			3.2			2.5		
Std. Dev	0.3			0.1			0.1			0.4		
Initial Tangent modulus, MPa	1505	580	390	472	1759	495	245	624	1021	1720	1537	1550
Avg. initial tangent modulus, MPa	825			909			630			1602		
Std. Dev	597			737			388			102		
Cyclic modulus, MPa	1389	549	631	714	1489	632	314	733	850	1278	2036	1150
Avg. cyclic modulus, MPa	856			945			632			1488		
Std. Dev	463			473			282			479		
Poisson's ratio	0.31	0.22	0.17	0.14	0.31	-	0.11	0.11	0.19	0.12	0.22	-
Avg. Poisson's ratio	0.23			0.23			0.14			0.17		
Std. Dev Poisson’s ratio	0.07			-			0.05			-		

4.5.1.2. Influence of Compaction Energy on Compressive Strength

Thought there is a concern of repeatability of stress strain behaviour the compressive strength of the specimens shows less variance, therefore more reliable. The C5 and C3 series are compacted at the same compaction energy and has similar densities, the comparison between them seems to be more relevant. The average compressive strength of C5 and C3 series was found to be 3.2MPa and 2.5MPa respectively. The parameter which varies between C5 and C3 series is manufacturing water content; the later one has been manufactured with little bit more (approximately 1%) of water content compared to C5 series. The reduction is strength might be due to the manufacturing water content

4.5.1.3. Influence of Dry Density on Compressive Strength

The dry density is a symbolic way of expressing durability and strength of earthen material. Similarly for USRE dry density is an important mechanical parameter, which expresses the strength. In general higher the dry density of material better the strength (Daniela Ciancio et al., 2013; Kouakou & Morel, 2009). The dry density of rammed soil varies with change in compaction energy and manufacturing water content. In Figure 4-13, the variation of compressive strength is plotted with respect to dry density of the CRA soil specimen. Excluding C3 series specimens, all other specimens exhibit an increasing tendency of compressive strength with increase in dry density. Whereas, C3 series specimens with dry density of 2.02g/cc has relatively low compressive strength compared to specimens with dry density of above 2g/cc. Even though the manufacturing water content between C3 and C5 series are different, the dry densities are very similar for same compaction energy. The presence of shrinkage cracks in C3 and C5 specimens might have impacted the dry density calculation, providing mean dry densities including cracks volume. Considering C2, C6 and C5 series specimens, a linear correlation (R^2=0.80) of compressive strength with respect to dry density can also be seen in Figure 4-13.

It has to be noted that all the CRA soil specimens were stored in the climatic chamber at 23° C and 50% R.H, but due to technical faults in climatic chamber and non-availability of climatic chamber force specimens C51/C52/C61/C62, to be dried at atmospheric conditions for a period of 4 weeks. Therefore the testing water content of the above mentioned specimens are higher than the other specimens dried in controlled climatic chamber.

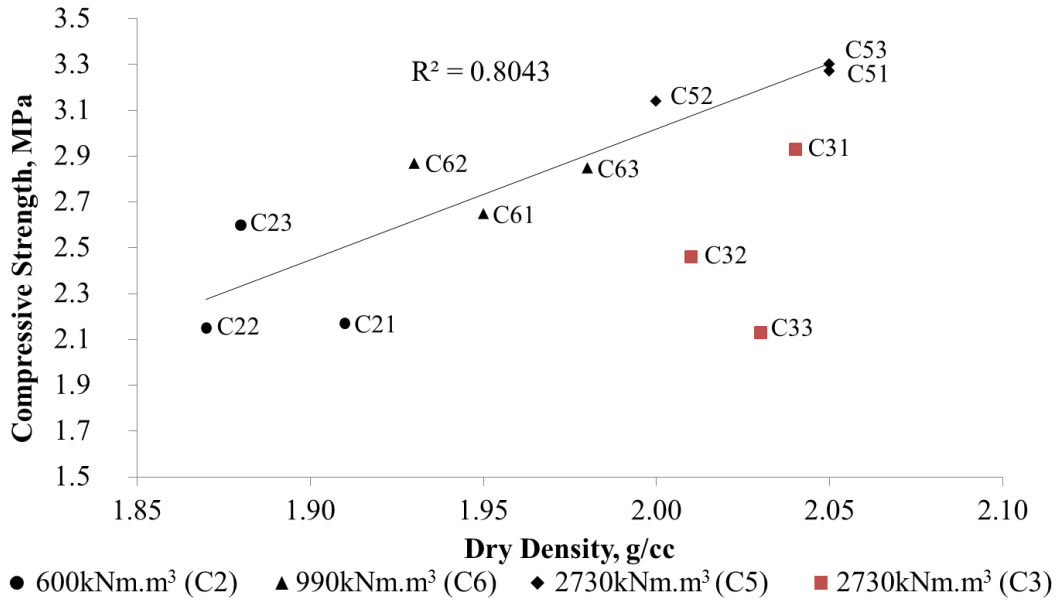

Figure 4-13 compressive strength vs dry density of CRA soil speicmens

4.5.1.4. Coefficient of Poisson

The coefficient of Poisson calculated for all the specimen of CRA soil series is given in Table 4-1. The average coefficient of Poisson for C2, C6, C5 and C3 series are 0.23, 0.23, 0.14 and 0.17. In general, coefficient of Poisson is assumed to vary in between 0.2-0.3 for USRE specimens (Q.-B. Bui et al., 2008; Q. Bui et al., 2014; T.-T. Bui et al., 2014; Champiré et al., 2016). The average coefficient of Poisson for CRA soil specimens was calculated to be 0.19.

4.5.1.5. Summary of CRA test

The experimental procedure conducted on CRA soil specimens in this work uses cylindrical specimens (large) manufactured using proctor process. The cylindrical specimens are not homogeneous and have shrinkage cracks, which is consistent with in-situ properties. Replicating specimens similar to in-situ leads to heterogeneous samples with cracks, therefore deteriorating the measure of stiffness which is made locally, the compressive strength is the mean of the specimen or global measurement and are more consistent. The large deviation in stiffness parameters means more accurate procedure to manufacture CRA soils specimens are needed. A comparison of CRA USRE specimen characteristic is given in Table 4-2, where the same soil is used by (Champiré et al., 2016) to study the material behaviour due to change in relative humidity. The specimens used in (Champiré et al., 2016) work are small size and more homogeneous as it is extracted from CEB. Author doesn't points anything related to shrinkage. The results of (Champiré et al.,

2016) show good repeatability, the specimens tested had different testing moisture contents, whereas the specimens tested in this work had different dry densities but moisture at test was similar. Though the results presented in this study is not accurate, the modulus, compressive strength and coefficient of Poisson falls within the results presented by (Champiré et al., 2016). This shows that the procedure presented in this method is a good progress, but needs more insight on specimen preparation.

Table 4-2 comparison of CRA USRE soil characteristics

Parameters	(Champiré et al., 2016)	**This work**
Modulus	1000MPa – 2200MPa	700MPa – 1700MPa
Compressive strength	2.2MPa – 4.2MPa	2.3MPa – 3.2MPa
Coefficient of Poisson	0.15 – 0.2	0.14 – 0.23
Testing water content	1.5% - 2.5% (25% RH – 75% RH)	1% - 2.7%
Density	1.97 g/cc (bulk)	1.87 g/cc – 2.05 g/cc (Dry)

4.5.2. Compressive strength characteristics of Dagneux soil specimens

4.5.2.1. Stress strain characteristics

The compressive stress strain characteristics of the Dagneux soil specimens are plotted in Figure 4-14, representing D1, D2 and D3 series respectively. D1, D2 and D3 series are grouped based on the compaction energy at which the specimens are manufactured. D1, D2 and D3 series specimens represents 600kN.m/m^3, 970kN.m/m^3 and 2580kN.m/m^3 respectively. In ‘D1’ series only one specimen test result is discussed, while 4 specimens in ‘D2’ and 3specimens in D3’series are discussed, summary of test results are given in Table 4-3. Similar to CRA compressive stress strain results, Dagneux soil specimens stress strain characteristics are limited to the 70% of its peak stress. The compressive stress strain of Dagneux specimens showed good repeatability as shown in Figure 4-15.

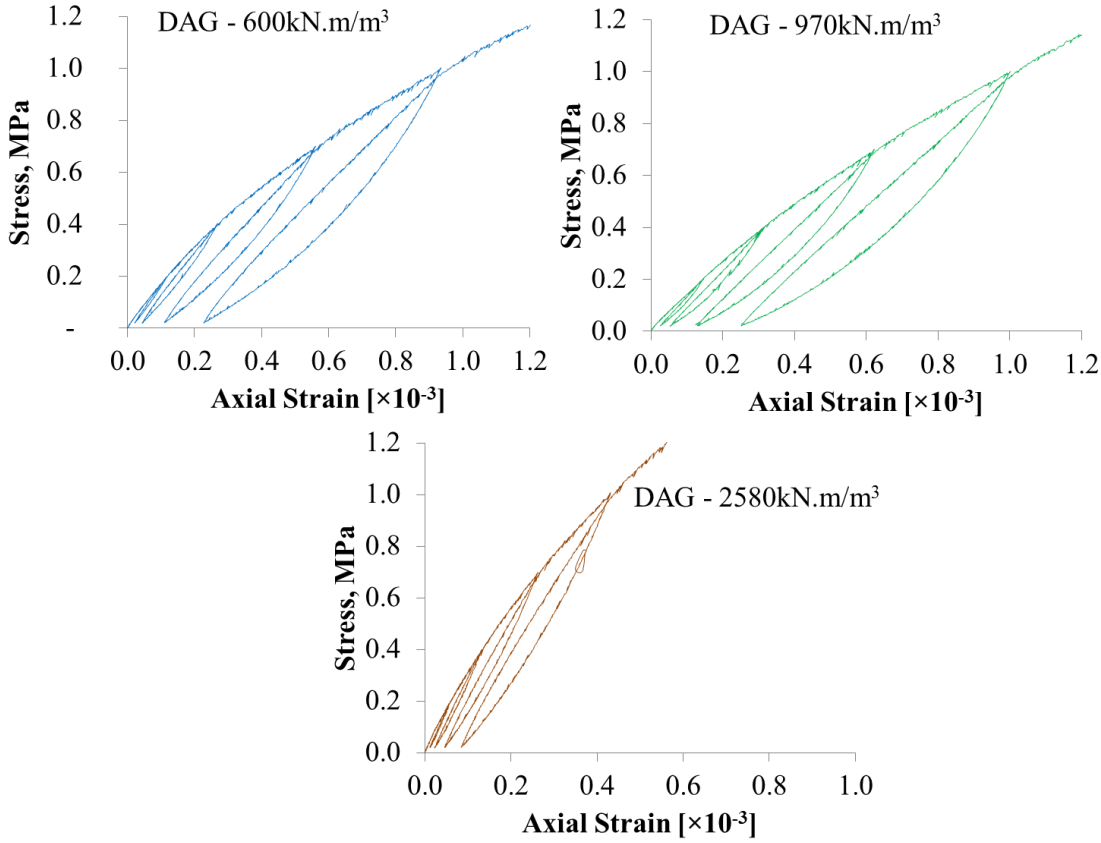

Figure 4-14 representation of compressive stress strain behaviour of Dagneux soil specimens

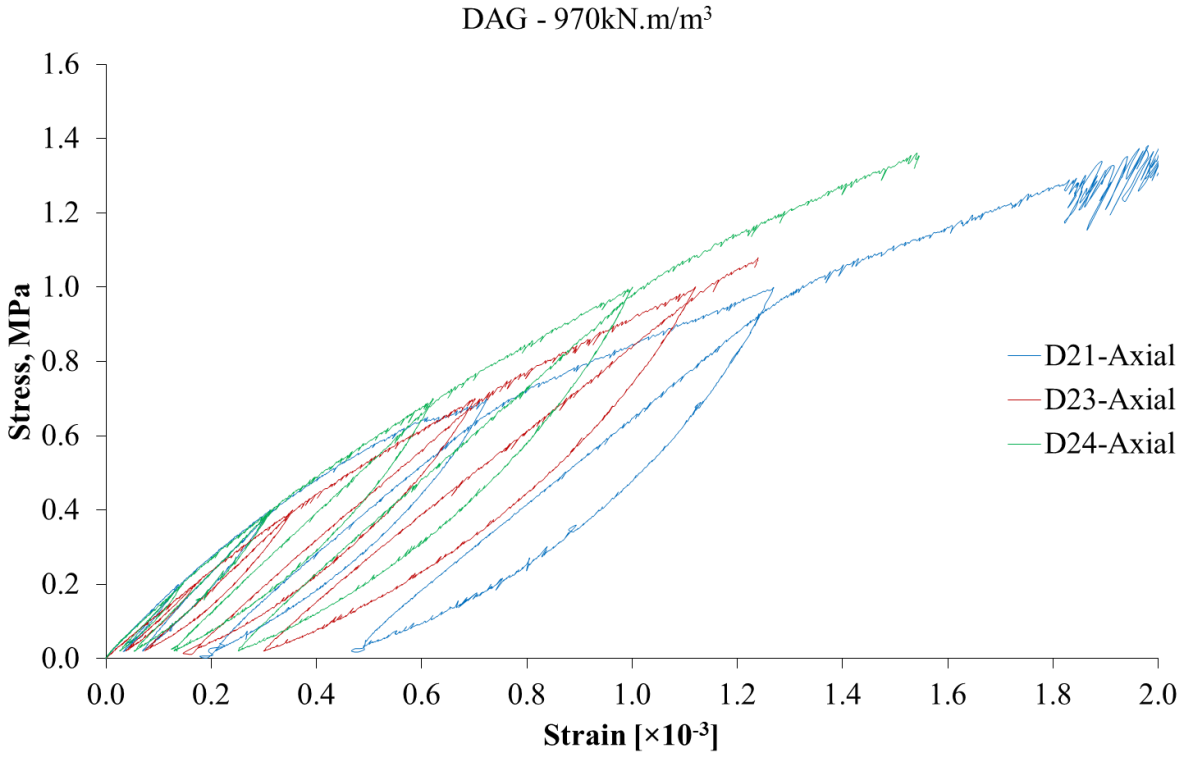

Figure 4-15 compressive stress strain characteristic Dagneux specimens (D2 series)

4.5.2.2. Influence of Compaction Energy on Compressive Strength

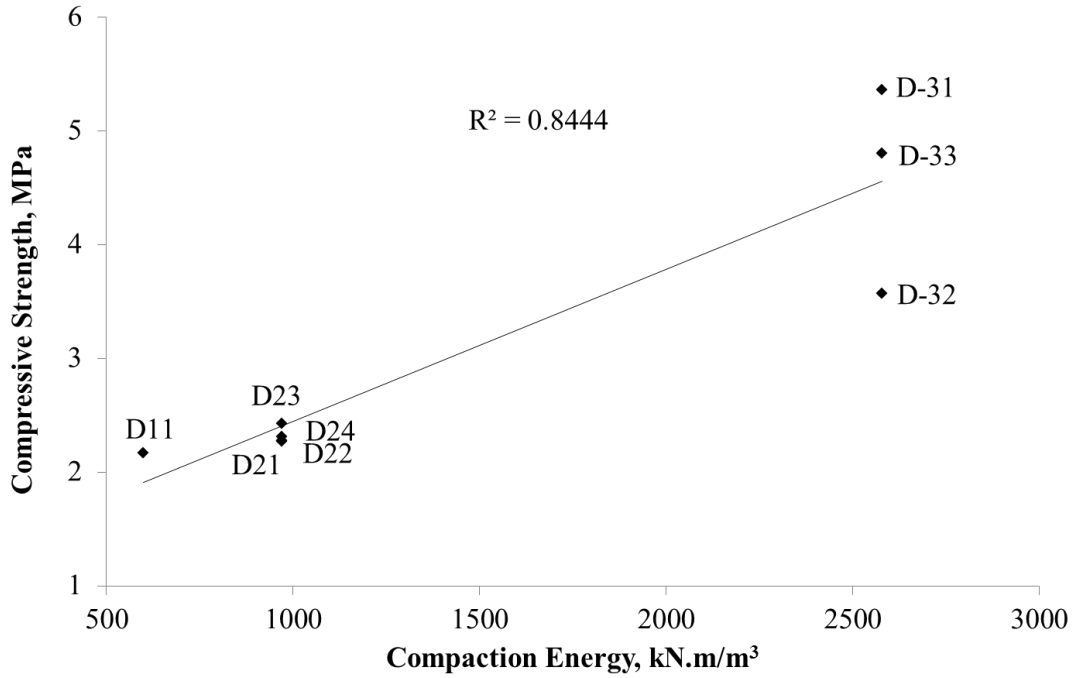

Figure 4-16 compressive strength vs compaction energy of Dagneux soil speicmens

The compressive strength of USRE increases with increase in compaction energy. To understand the rate of increase in compressive strength of Dagneux soil with change in compaction effort, compressive strength of all the Dagneux soil specimens are plotted against the compaction energy as shown in Figure 4-16.

4.5.2.3. Influence of Dry Density on Compressive Strength

As stated in many works, the compressive strength increases with increase in dry density, the compressive strength of Dagneux soil also increases with increase in dry density as shown in Figure 4-17.

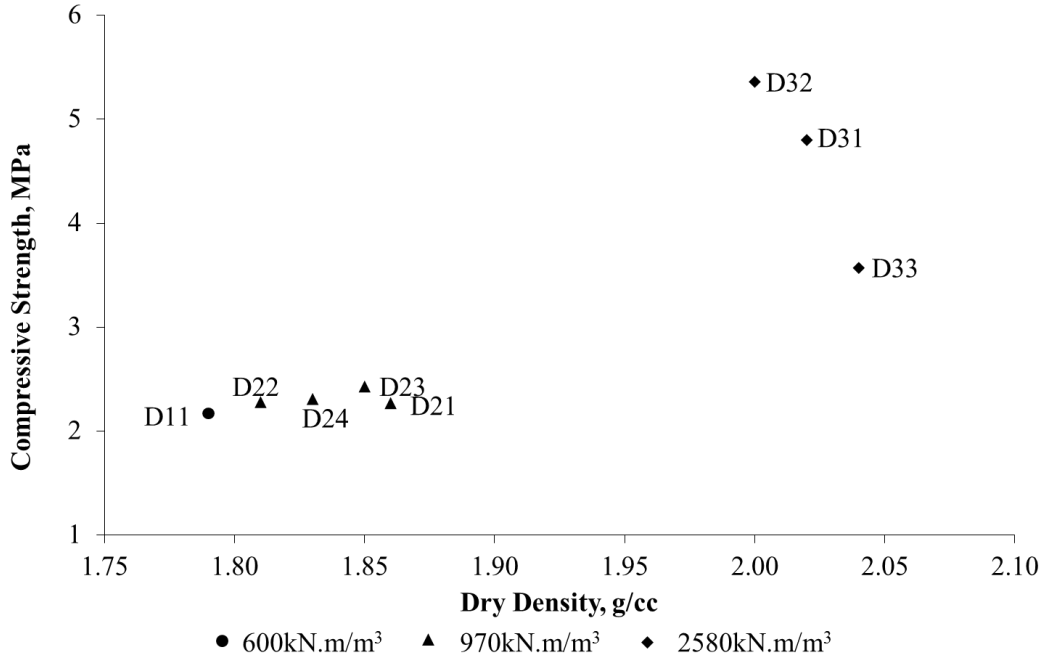

Figure 4-17 variation of compressive strength of Dagneux soil specimens with repsect to dry density

4.5.2.4. Initial tangent modulus and cyclic modulus

The stiffness parameters of Dagneux are divided into initial tangent modulus and average cyclic modulus. The average cyclic modulus is the average modulus of each cycle starting from cycle 1 unloading until cycle 5 loading. The stiffness parameters for all the Dagneux soil specimens subjected to compressive testing program are calculated and given in Table 4-3. The average values of initial tangent modulus and cyclic modulus of each series of specimens tested in compression test is plotted against the dry density as shown in Figure 4-18. Though the initial tangent modulus and average cyclic modulus varies with change in dry densities, at low dry densities (i.e. 1.80-1.86g/cc) the initial and average cyclic modulus seems to be similar. The initial and average cyclic modulus increases with increase in dry densities, and the difference between initial and average cyclic modulus is also increasing exhibiting more damage.

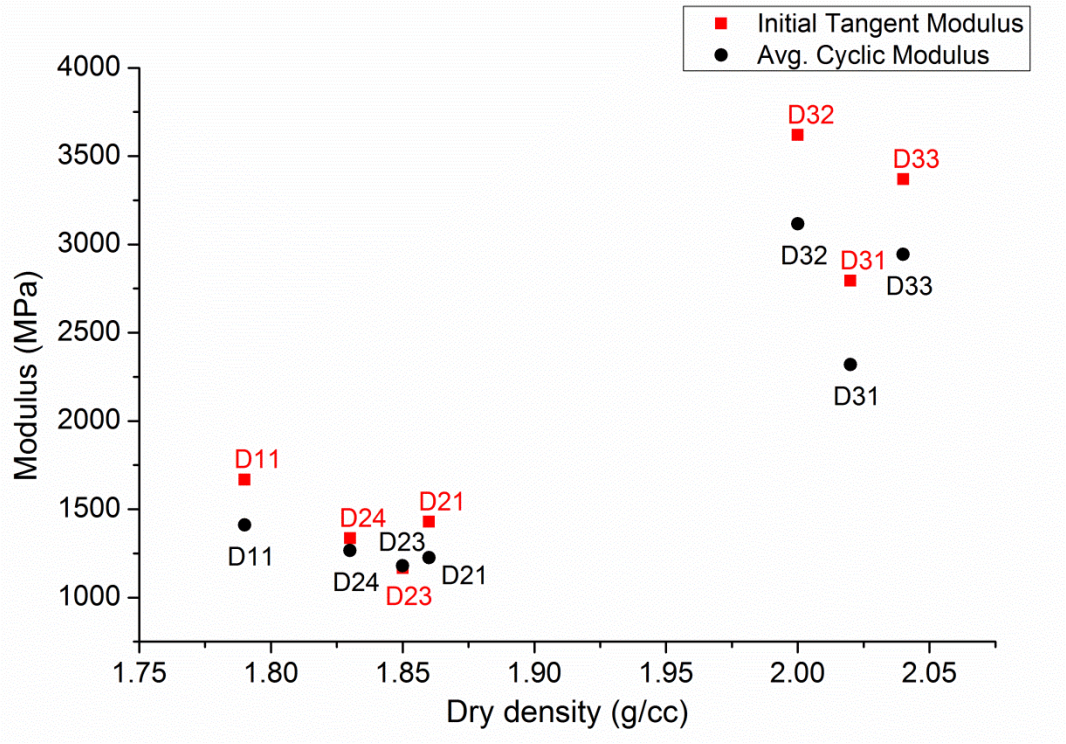

Figure 4-18 variation of initial tangent modulus and average cyclic modulus with respect to dry density for Dagneux soil specimens

By observing the variation of cyclic modulus at compressive stress levels as shown in Figure 4-19, the degradation in stiffness with increase in compressive stress can be seen. The cyclic modulus presented is the average cyclic modulus of loading and unloading part of each cycle at defined pre-stress levels (0.2MPa, 0.4MPa, 0.75MPa and 1MPa), finally the cyclic modulus corresponding to 1.5MPa represents the loading part of final cycle (cycle-5). The cyclic modulus of D2 and D3 presented in the Figure 4-19 corresponds to the average of 3 specimens in their respective series. As seen earlier, with increase in dry density the cyclic modulus of the Dagneux soil specimens also increases, but the rate of degradation is also higher. Note that, the compressive stress level of 1.5MPa corresponding to D1 and D2 series represents 70% (approximately) of their failure compressive stress, whereas it is approximately 30% for D3 series. The cyclic modulus of D3 series at 70% of failure compressive stress might be same as D1 & D2 series.

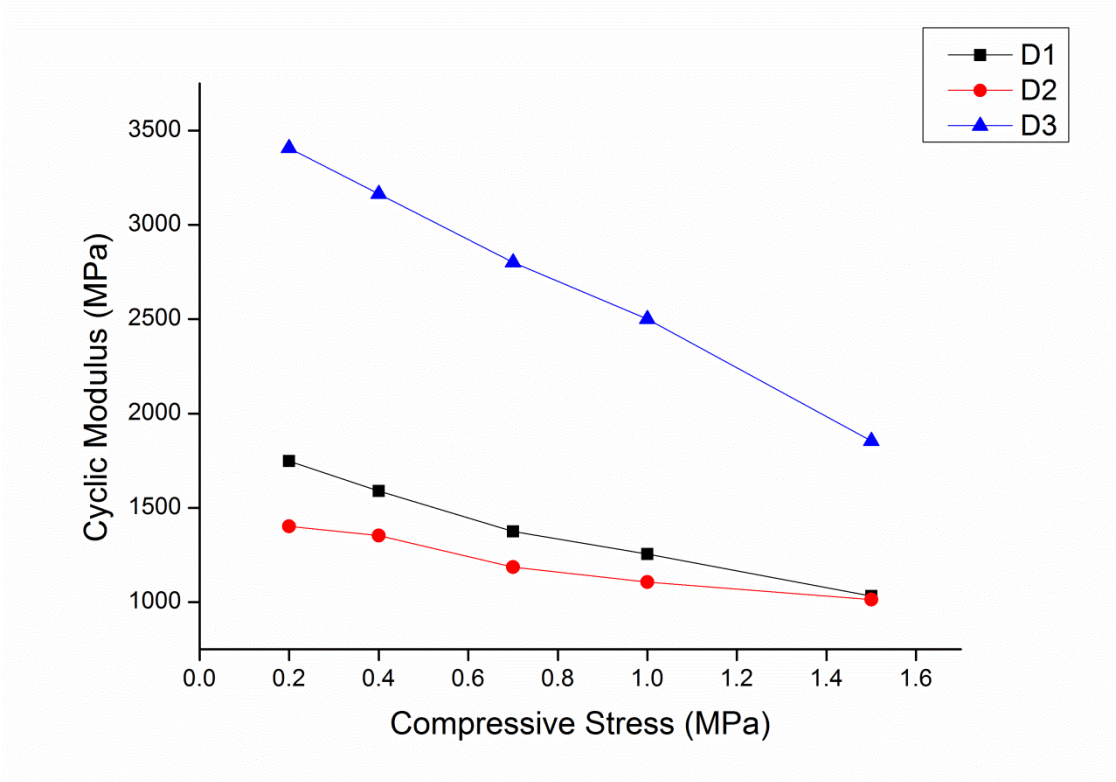

Figure 4-19 cyclic modulus with respect to compressive stress level - Dagneux

4.5.2.5. Coefficient of Poisson

The coefficient of Poisson calculated by plotting lateral strain vs axial strain for the specimens in D2 and D3 series are reported in Table 4-3. The average Poisson's ratio of Dagneux soil specimen was calculated to be 0.23. This shows that the assumption of coefficient of Poisson being in between 0.2-0.3 for USRE is valid from both the soils tested in this work.

Table 4-3 Compressive strength characteristics of Dagneux soil specimens

Series	D1	D2				D3		
Specimen	D11	D21	D22	D23	D24	D31	D32	D33
Compaction Energy, kN.m/m3	600	970				2580		
Manufacturing Water Content, %	10.6	9.6	9.6	10.2	10.2	11.2	11.2	11.2
Dry Density, g/cc	1.79	1.86	1.81	1.85	1.83	2.02	2.00	2.04
Avg. Dry density, g/cc	1.79	1.84				2.02		
Std. Dev	-	0.02				0.02		
Testing Water content, %	2.07	2.16	2.17	2.19	2.16	2.09	2.21	2.09
Compressive Strength, MPa	2.17	2.27	2.28	2.43	2.31	4.8	5.36	3.57
Avg. Comp St, MPa	2.17	2.32				4.58		
Std. Dev	-	0.1				0.9		
Initial Tangent modulus, MPa	1668	1429	-	1167	1336	2794	3620	3369
Avg. initial tangent modulus	1668	1311				3261		
Std. Dev	-	133				423		
Cyclic modulus, MPa	1411	1226	-	1180	1266	2319	3116	2943
Avg. cyclic modulus	1411	1224				2793		
Std. Dev	-	43				419		
Poisson's ratio	-	0.18	-	0.24	-	0.32	0.33	0.09
Avg. Poisson's ratio		0.21				0.25		
Std. Dev Poisson’s ratio	-	-				0.14		

4.6. Conclusion

An experimental procedure to study the compressive strength characteristics of USRE is discussed. In this experiment cylindrical specimens with aspect ratio of 2 that are manufactured using Proctor method are used for investigation. Specimens are allowed to dry in a climate controlled room that allows having similar moisture at test. Extensometers and LVDT's are used to capture local strains of the material. Loading and unloading cycles are performed at various stress levels to observe the elasto-plastic behaviour of specimens. This experimental investigation is carried out on two different locally available soils.

As it is difficult to identify the exact compaction energy used at site to manufacture USRE, specimens at laboratory are manufactured with three different compaction energies at near OMC as manufacturing water content. Thanks to different compaction energies, it helps in manufacturing specimens at different dry densities. The dry densities of CRA and Dagneux specimens varied between 1.87-2.05g/cc and 1.8-2.03g/cc respectively, the dry densities of the USRE walls built using these soils were within the above said limits.

To manufacture specimens, Proctor method was chosen as it shows close resemblance of ramming method adopted in situ, so that specimens can replicate in-situ characteristics. Similarly CRA exhibits in-situ characteristics including shrinkage cracks which are found to be consistent with in-situ walls. The presence of shrinkage cracks impede in the measurements made by extensometers, thereby causing non-repetitive performance. The stress strain characteristics of CRA were difficult to conclude, whereas the compressive strength measured was found to be consistent. On the other hand Dagneux specimens exhibit repeatable performance, which allows investigating stress strain characteristics and compressive strength. The Proctor method of manufacturing specimens is questionable for soil specimens that exhibit shrinkage cracks. But to measure compressive strength and extract stress strain characteristics of soil specimens without shrinkage cracks, Proctor method specimens seems to be acceptable.

The increasing tendency of compressive strength with respect to dry density and compaction energy was found for both soil specimens. Observing stress strain of loading and unloading cycles, irreversible strain can be witnessed for both the soils. For Dagneux specimens, the analysis of cyclic modulus at different stress levels shows the degradation of stiffness due to damage. From the lateral strain, the coefficient of Poisson for both soil specimen were found to be in between 0.21 and 0.3, which is in agreement with (Q. Bui et al., 2014; Champiré et al., 2016).

5. The splitting and flexural test for USRE

5.1. Introduction

Building material strength properties such as tensile, flexural and compressive strengths are important in design consideration. The compressive strength of USRE was discussed in the chapter 4, it was seen that the compressive strength is largely influenced by manufacturing parameters. The compressive strength of USRE is in between 2-4MPa depending on dry density and moisture at test. The tensile and flexural strength of earthen building materials are very low and in some cases it is recommended to consider as zero (Maniatidis & Walker, 2003). Some of the research work on rammed earth indicated the tensile strength of the rammed earth is close to 10-15% of its compressive strength (Araki et al., 2011; T.-T. Bui et al., 2014; Gerard et al., 2015).

(Araki et al., 2011) carried out direct tensile test on the USRE specimens stored and dried in the similar conditions. The tensile strength of USRE was found to be 10% of its compressive strength, but the dry densities of the compressive and tensile test specimens were slightly different. In another study (T.-T. Bui et al., 2014), rammed earth cylindrical specimens were subjected to split tensile test (Brazilian test) and a relationship of tensile strength in terms of compressive strength was established, it was found that tensile strength of rammed earth is 11% of its compressive strength. Similarly in the work of (Gerard et al., 2015), indirect tensile test (Brazilian test) on USRE at different moisture content was studied, from the results presented it can be seen that the tensile strength was in between 10-15% of respective compressive strength. Flexural strength is another important parameter on a building material, in earlier studies due importance to flexural strength of USRE is not given. (Jayasinghe & Mallawaarachchi, 2009) carried out bending test on cement stabilised rammed earth (CSRE) in the direction parallel and perpendicular to the compacted layers, the flexural strength of 0.46MPa (parallel) and 0.92MPa (perpendicular) was reported. In NZS 4297:1998 guidelines (as cited in (Maniatidis & Walker, 2003), the flexural strength equal to 10% of characteristic compressive strength is recommended in the absence of experimental investigation.

It was found that the tensile and flexural strength of USRE is also important parameter along with the compressive behaviour. Hence in this work, tensile and flexural strength of USRE are presented along with the compressive strength of rectangular prism specimens. The split tensile test and four point bending test are followed to study tensile and flexural strength of the specimens. The rectangular specimens used for studying

flexural behaviour are the layers recovered from the interface behaviour (shear) test. Due care has been taken to eliminate specimens which were damaged during the interface behaviour (shear) test.

5.2. Spilt tensile test

5.2.1. Experimental procedure

The split tensile test, which is also called as indirect tensile test is carried out in accordance to the (ASTM C496/ C496M, 2004). The rammed earth cylindrical specimens of dimension 160mm in diameter and 320mm in length that are compacted manually and stored in climatic chamber at 23° C and 50% RH, similar to cylindrical specimens that are used for compression test. The specimen is placed in between the two diametrically opposite bearing sticks within the split tensile test frame as shown in Figure 5-1(a). The split tensile frame along with the specimen is mounted on the axial compression testing press for applying diagonal compressive load on the cylindrical specimen. The diametrical compressive load induces tensile failure plane due to the ultimate tensile force perpendicular to the direction of compressive load as shown in Figure 5-1(b). The load is applied at a rate of 5µm/s press displacement control mode. The failure load of the specimen from the load sensor is recorded as the failure load (P), which is used in the Equation 5-1 to calculate tensile strength of the USRE specimen.

Equation 5-1

$$\sigma_t = \frac{2P}{\pi l d}$$

σ_t = Tensile strength, MPa; P = Failure load, N; l = Length of the specimen, mm; d = Diameter of the specimen, mm

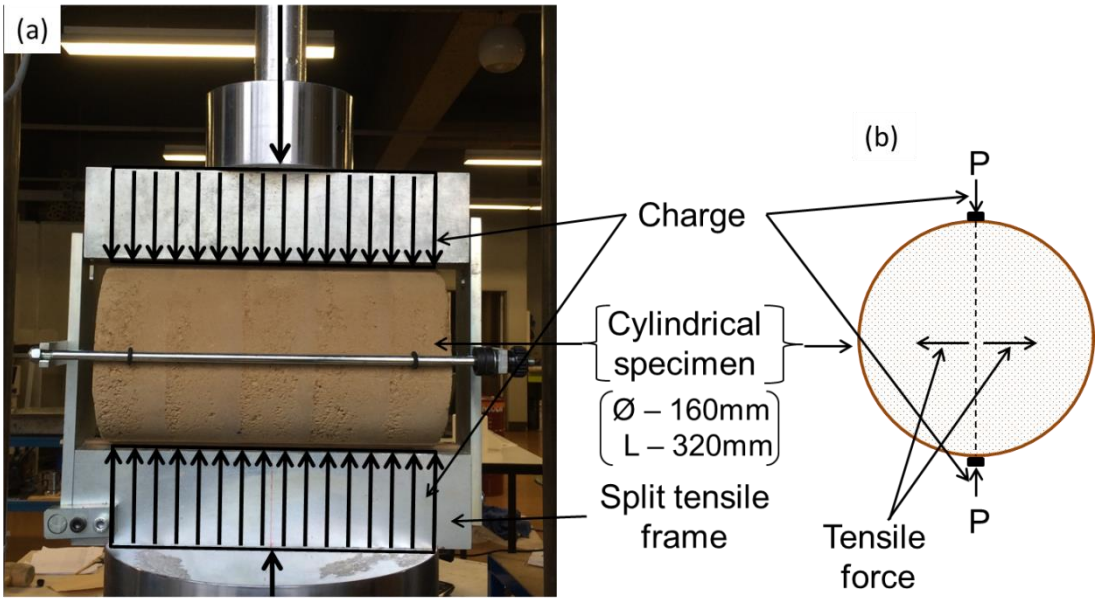

Figure 5-1 Specimen and apparatus for split tensile test

5.2.2. Result and discussion

From the Equation 5-1, the tensile strength of the CRA and Dagneux USRE specimens are calculated and plotted against the dry density of the specimens, given in Figure 5-2. All the specimens exhibited similar failure pattern as shown in the Figure 5-3, the failure tensile crack was initiated at the centre and propagated on either sides. The tensile strength of both the soils were increasing with increase in dry density, interesting observation would be the difference in tensile strength between the two soils. Though the dry density of CRA soil is higher than the Dagneux, the tensile strength of Dagneux is higher than the CRA. This phenomenon is also observed in the compression test, though this phenomenon is not analysed in detail, the change in mechanical strength can be attributed to the influence of particle size distribution and clay content of the soil (Reddy et al., 2007; B. V. Venkatarama Reddy & Prasanna Kumar, 2011b). The average tensile strength of CRA and Dagneux were found to be 0.14MPa and 0.16MPa respectively. The moisture at test was found to be around 2% for both the soil specimens, and the average dry density of CRA and Dagneux were 1.84g/cc and 1.79g/cc.

The average compressive strength of the CRA and Dagneux soil cylindrical specimens were found to be 2.31MPa and 2.29MPa at average dry densities of 1.89g/cc and 1.83 g/cc. The tensile strength of CRA and Dagneux were found to be 6% and 7% of their respective compressive strength. The relationship obtained between tensile strength and compressive strength does not agree with the results of earlier studies, where the tensile strength of USRE was proposed to be 10% of its compressive strength (Araki et al., 2011; T.-T. Bui et al., 2014). The reduction in tensile strength with respect to compressive

strength might be due to the low dry density of tensile specimens. The influence of dry densities on compressive strength was discussed in the chapter 4.

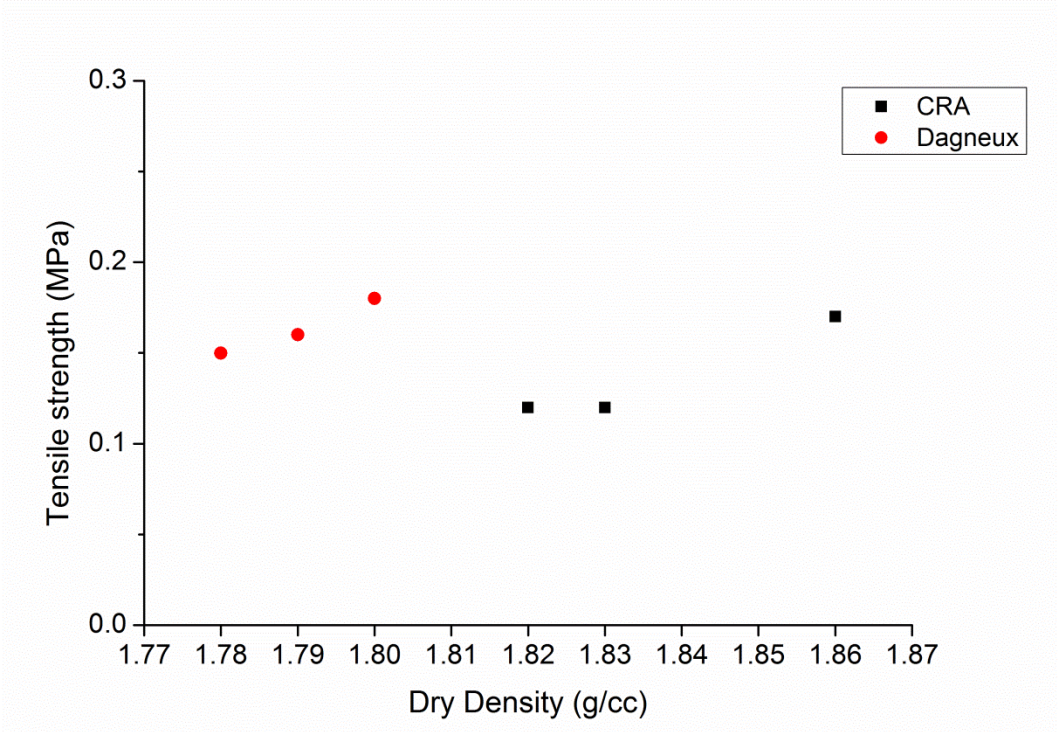

Figure 5-2 Tensile strength of CRA and Dagneux soil specimens with respect to dry density

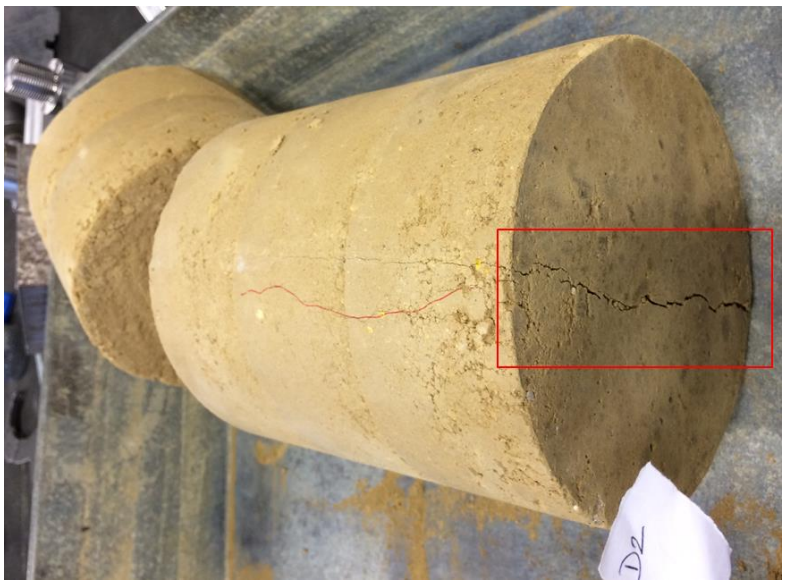

Figure 5-3 Failure of cylindrical specimens due to tensile stress

5.3. Bending test

The flexural strength or modulus of rupture of a material is studied by subjecting material under bending test. Generally three point or four point bending test is adopted depending on the material strength. The disadvantage of three point bending test is that the material is not in pure tension zone, this becomes difficult to access the cause of failure in the case of materials with less strength. Hence for USRE beam specimens four point bending test is adopted, in this case the mid central part of the specimen is under pure tension zone with zero shear force, hence the failure is due to excess tensile stress.

5.3.1. Experimental procedure

The four point bending test in accordance with the (ASTM D 1635, 2000) was carried out. The separated layers of specimens tested at 20° inclination during interface shear test are recovered and tested for flexural strength. These individual layers are called as USRE small beams specimens. The dimension of the USRE beam specimens are 330mm in length, 120mm in width and 60mm in depth. The USRE beam specimen is placed on the bottom supports having a span of 270mm as shown in the Figure 5-4, the distance between the upper load points is 90mm and is symmetrical with the vertical axis of the frame. The top frame of the four point apparatus is fixed to the press, and bottom plate is moved until the top layer of specimen is in contact with the upper load points. The specimens under bending test are loaded at a rate of 5µm/s press displacement controlled mode. The USRE specimens under four point bending test failed in the middle 1/3rd span; hence the flexural strength is calculated as per the Equation 5-2.

Equation 5-2

$$\sigma_f = \frac{Pl}{bd^2}$$

Where; σ_f = Flexural strength, MPa; P = Failure load, N; l = span, mm; b = width, mm; d = depth, mm

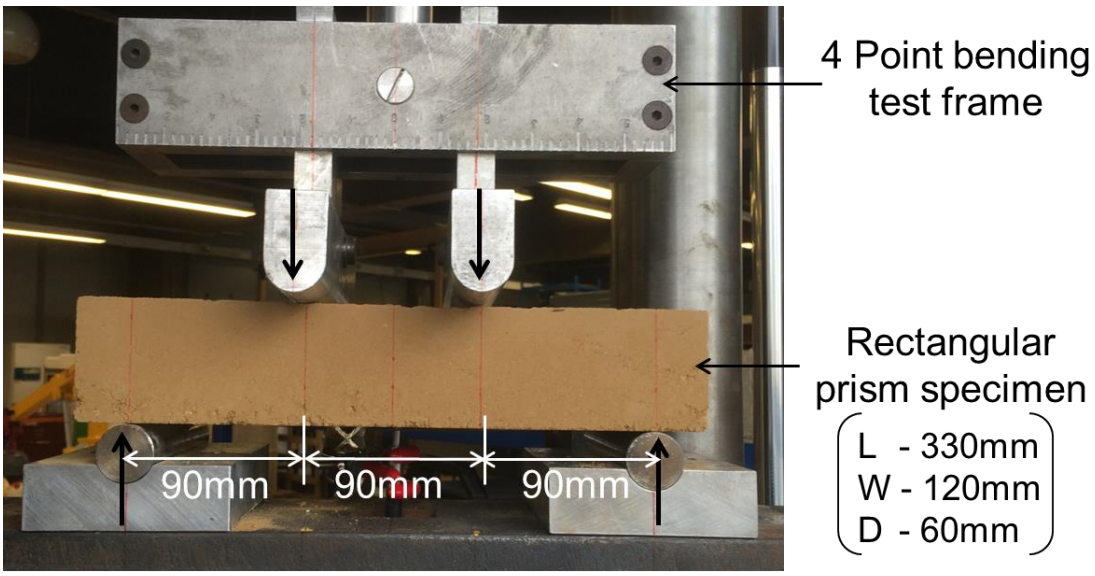

Figure 5-4 Specimen and apparatus for four point bending test

5.3.2. Result and discussion

The USRE beam specimen under flexural test failed in the mid 1/3rd span as shown in Figure 5-5, the failure is due to exceeding tensile stress at the bottom of the layer. Bending test on both CRA and Dagneux soil specimens were carried out, but only two beam specimens in CRA soil were tested. Dagneux beam specimens were tested for oven dry and ambient flexural strengths. Specimens stored in oven at 100-110° C for 48hr is taken as oven dry state, and the specimens stored in the climate chamber at 23° C and 50% RH is taken as ambient state. The moisture content of ambient state specimen was found to be around 1.6%, similar to that of the cylindrical specimens tested in compression test. The dry and ambient flexural strength of Dagneux beam specimen with respect to dry densities are plotted in Figure 5-6. It can be said that the flexural strength of the USRE specimen's increases with increase in dry density. The increasing tendency of ambient flexural strength with respect to dry density is not very clear due to scattered results. Some of the specimens exhibiting lower flexural strength might have incurred internal damage during the interface shear test, which might influence the flexural behaviour.

In Figure 5-7, the flexural strength of Dagneux USRE beam specimens with respect to moisture at test is presented. It can be seen that there is a decrease in flexural strength of the USRE specimen with increase in moisture content. The average flexural strength of dry specimens was found to be 0.38MPa, while that of ambient specimens were 0.15MPa; there is a decrease of 60% in strength.

Since the specimen in bending test failed due to tensile force, the flexural strength can be compared with the split tensile strength. For comparison only ambient state flexural strength are considered as the split tensile test specimen were tested at ambient condition.

From split tensile test, the average tensile strength of the CRA and Dagneux soil specimen was found to be 0.15MPa and 0.16MPa respectively; their respective dry densities were in the range of 1.82-1.86g/cc for CRA and 1.78-1.80g/cc for Dagneux. The average flexural strength of both CRA and Dagneux soil specimens were found to be 0.15MPa, at a much lower dry densities. Indeed the mechanical strength increases with increase in dry density, knowing this an increasing tendency of flexural strength with respect to dry density can be seen in Figure 5-6. Therefore the flexural strength of USRE seems to be higher than the tensile strength of USRE.

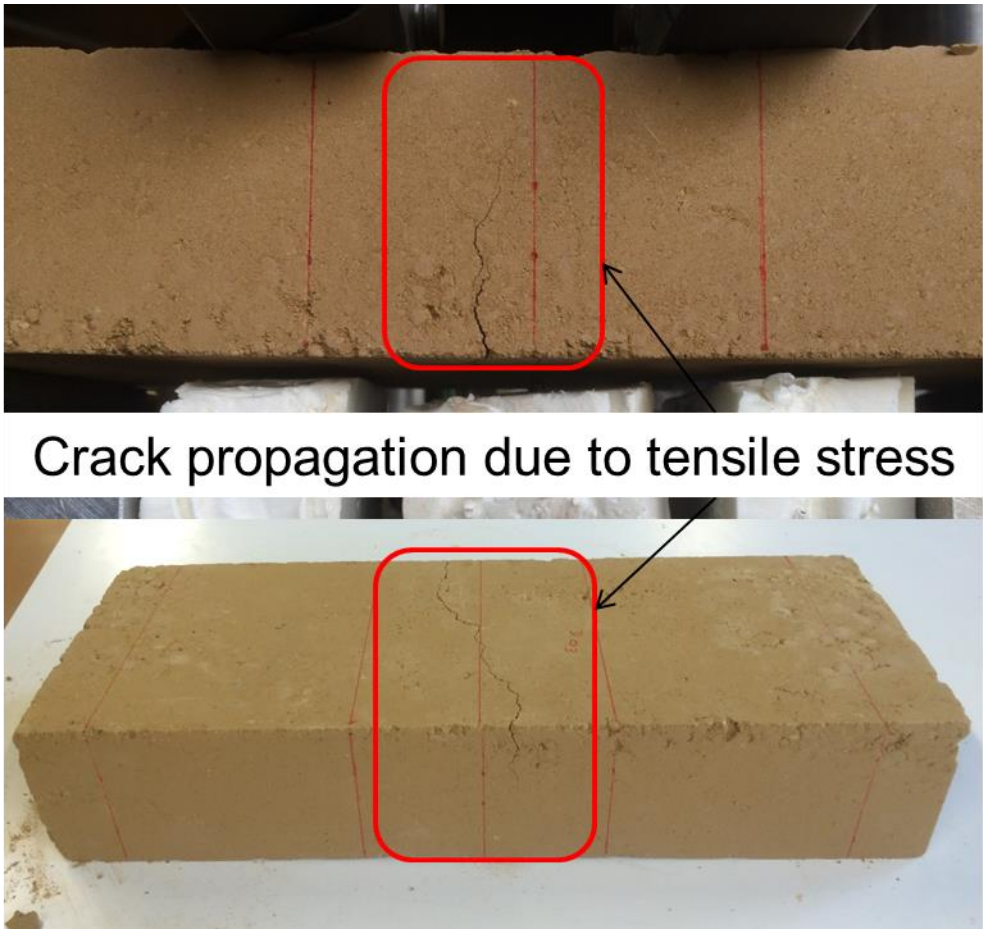

Figure 5-5 Failure of USRE beam specimens under 4 point bending test

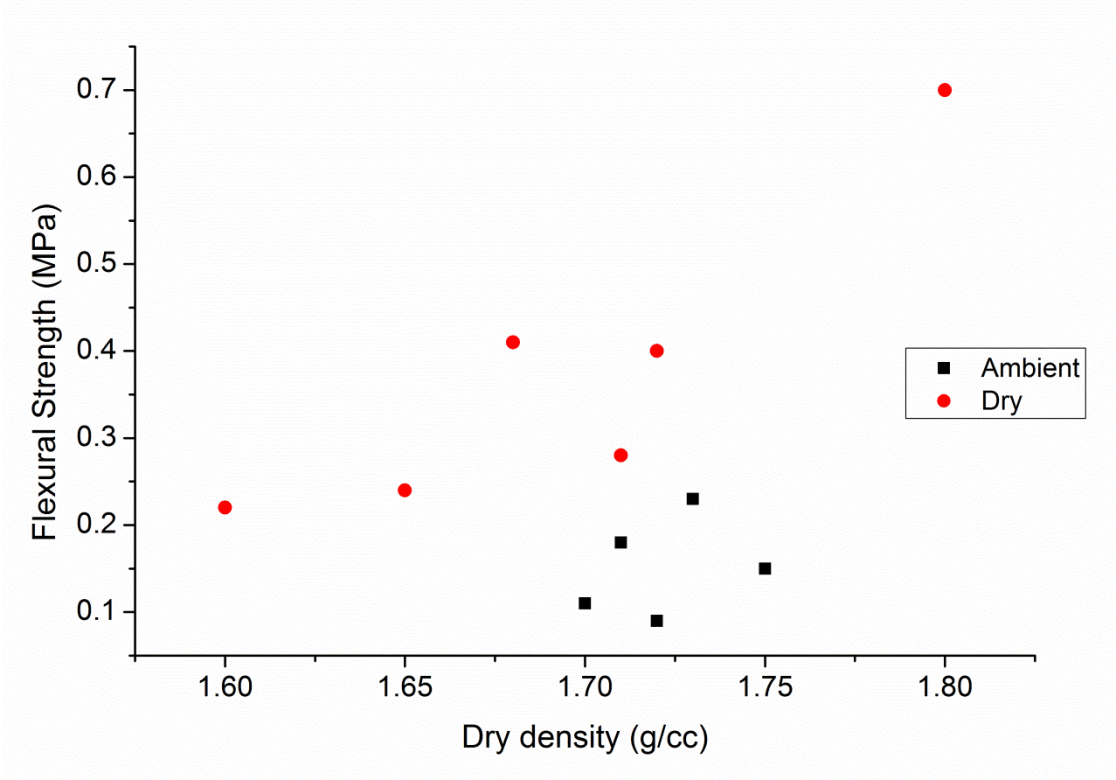

Figure 5-6 Flexural strength of Dagneux soil specimens with respect to dry density

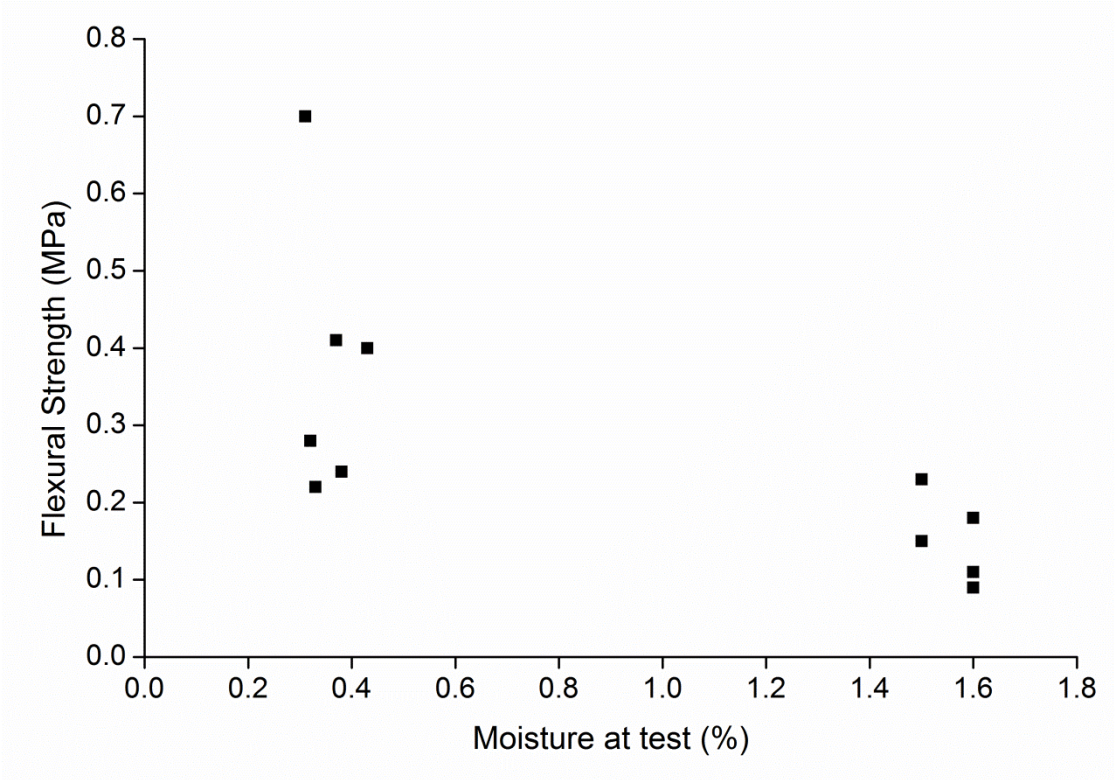

Figure 5-7 Flexural strength of Dagneux soil specimens with respect to moisture at test

5.4. Compression test on rectangular prisms

The separated layers of rectangular prism specimens tested at 30° inclination for interface shear parameters are recovered and tested for their compressive strength. The rectangular prisms tested are also conditioned in similar conditions that of cylindrical specimens used for compression test. This experiment is carried out in comparison with the cylindrical specimen's compressive strength.

5.4.1. Experimental procedure

The recovered rectangular prism specimens of dimension 210mm in height, 120mm in length and 60mm in width are placed in between the two plates of the compression loading cell as shown in Figure 5-8. Care has been taken to select specimens without any visible damage. The specimen surfaces touching both plates are smooth and flat, hence no lime paste to level the surface is added. The top surface is brought in contact with the loading cell and the test is programmed to run at a rate of 10µm/s displacement controlled loading rate.

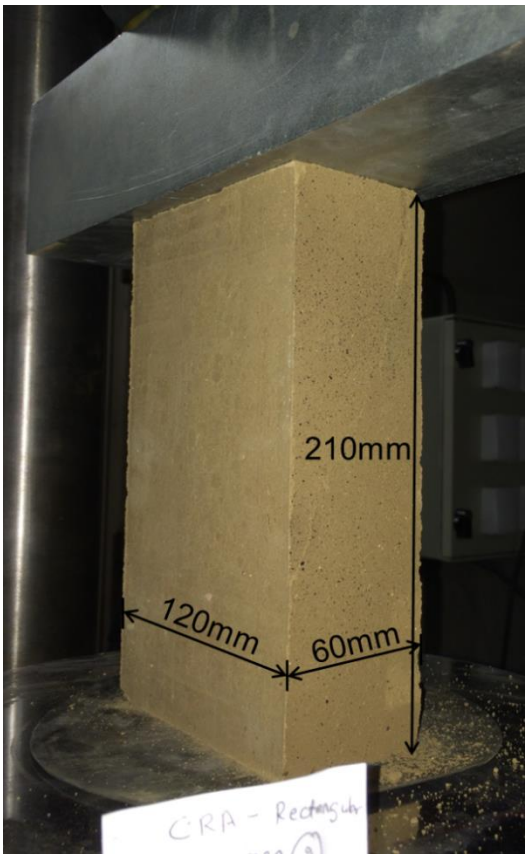

Figure 5-8 Compression test setup for rectangular prism specimens

5.4.2. Result and discussion

The compressive strength of the rectangular prism specimens of the CRA and Dagneux soil are presented in Figure 5-9. The compressive strength of CRA increases with

increase in dry density, whereas the compressive strength of Dagneux shows negligible variation, similar behaviour is observed in Dagneux cylindrical specimens for dry densities 1.8-1.86g/cc. The difference in behaviour of two soils might be due to the soil particle size distribution.

The density gradient of the cylindrical specimens is parallel to the compressive loading, whereas in rectangular prism they are perpendicular to loading as shown in Figure 5-10. The compressive strength of the cylindrical specimens is the mean compressive strength of the 5 layers, while the compressive strength of rectangular prism is of one layer and in the direction parallel to layer. The mechanical behaviour of rammed earth in the direction perpendicular to layer and parallel to layer was found to be similar from the study (Q.-B. Bui & Morel, 2009). The compressive strength of rectangular prism and cylindrical specimens of CRA and Dagneux are presented in Figure 5-11 and Figure 5-12. The dry densities of the CRA rectangular prisms and cylindrical specimens are not same (Figure 5-11). Assuming a linear variation of compressive strength with respect to dry density, decreasing tendency of compressive strength can be seen. Though the dry densities of the Dagneux rectangular prism and cylindrical specimens are in the same range of 1.78-1.86g/cc (Figure 5-12), rectangular prism specimen's exhibits low compressive strength. The low compressive strength of rectangular prism specimens for a given dry density can be seen in both CRA and Dagneux specimens, this might be due to the internal damage specimen had undergone during interface testing. It is difficult to conclude the behaviour of compressive strength due to scattered results obtained from the rectangular prisms. The compressive test on rectangular prism provides relevant material property, but considering some inaccurate results, the compression test on rectangular prism specimens recovered from interface test is not recommended.

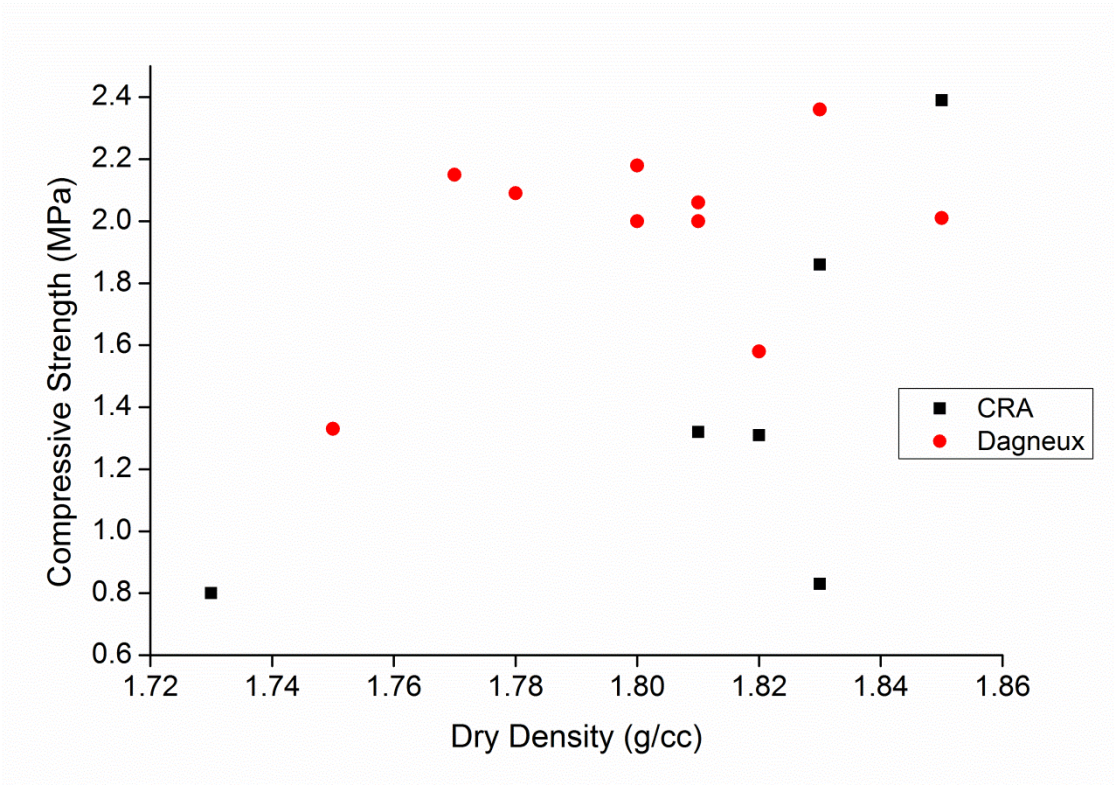

Figure 5-9 Compressive strength of rectangular prism specimens with respect to dry density

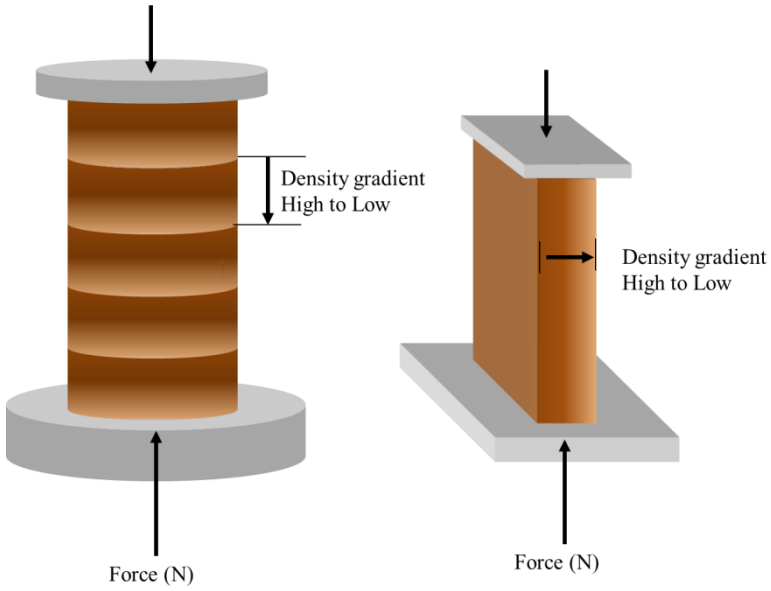

Figure 5-10 pictorial representation of cylindrical specimens and rectangular prism specimens under compression test with varying density, (a) compressive load perpendicular to layer on multi-layered cylindrical specimen, (b) compressive load parallel to layer on a single layer.

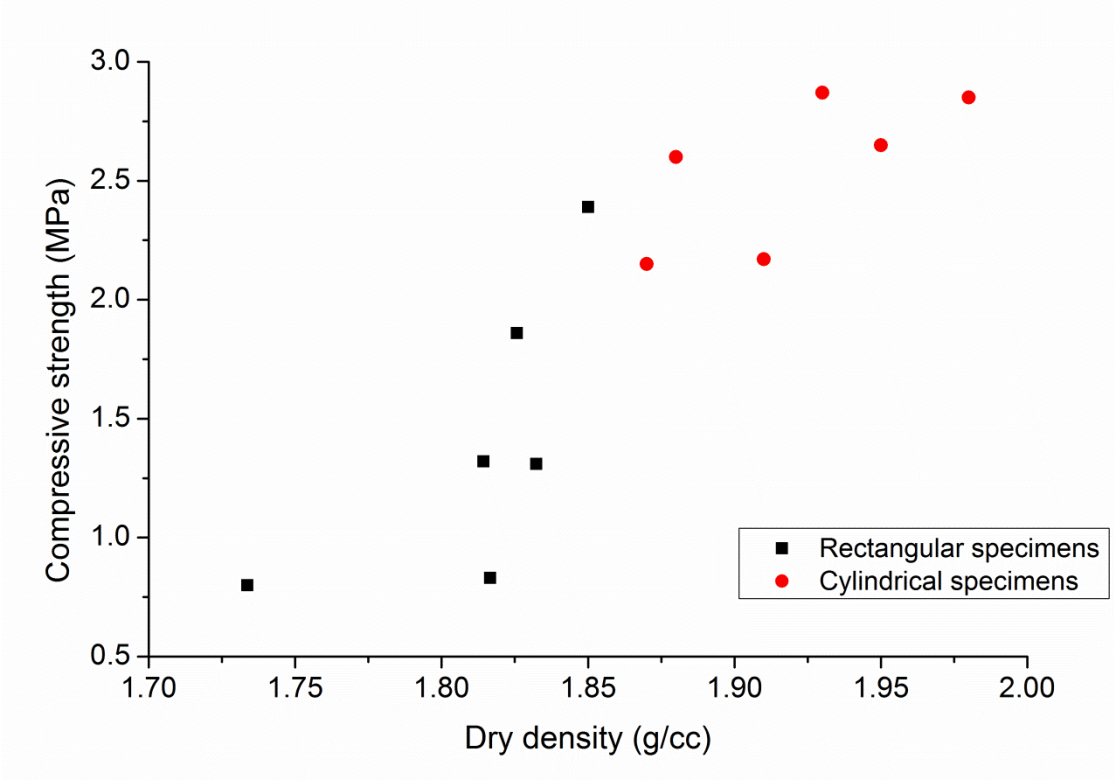

Figure 5-11 Compressive strength of CRA rectangular prism and cylindrical specimens

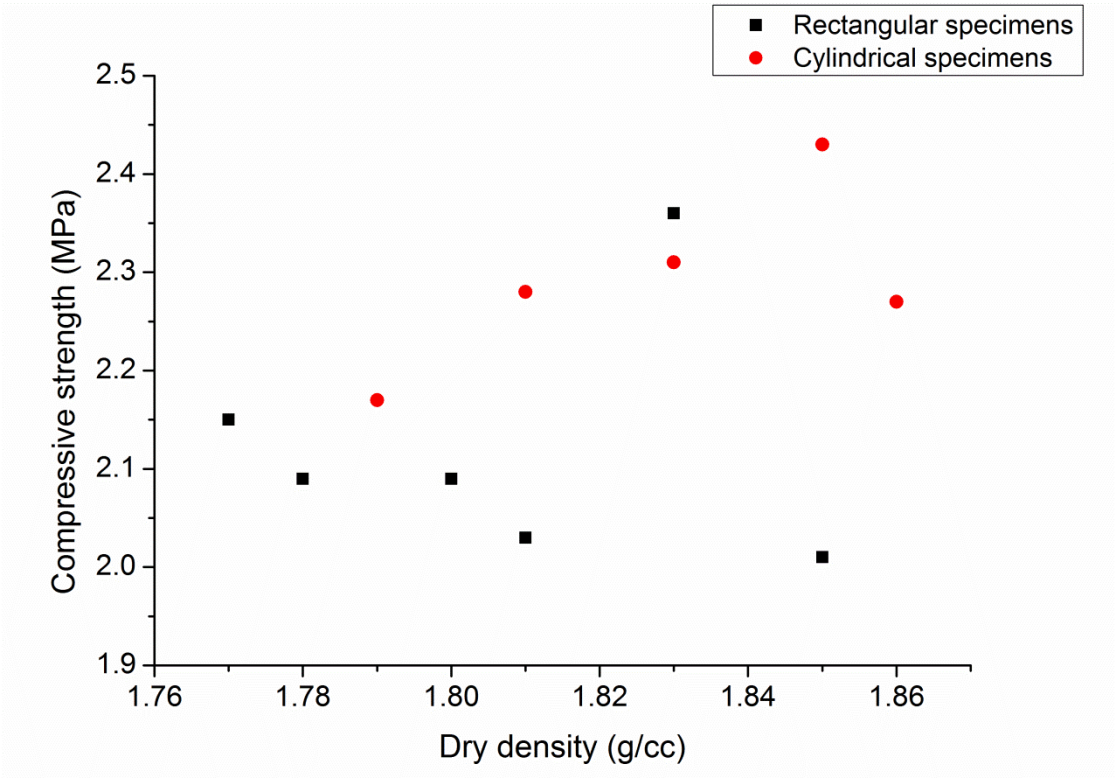

Figure 5-12 Compressive strength of Dagneux rectangular prism and cylindrical specimens

5.5. Conclusion

This chapter presents the split tensile test on USRE cylindrical specimens, flexural test and compressive test on rectangular prism specimens recovered from the interface test. The experimental results are summarised below.

- The tensile strength of the USRE specimens was found to be 0.15MPa and 0.16MPa for CRA and Dagneux soil respectively. Though the dry density of CRA soil specimens was significantly higher, the tensile strength was less than Dagneux. The tensile strength of CRA and Dagneux specimens were found to be around 7% of their respective compressive strength.
- The flexural strength of Dagneux beam specimens in dry and ambient state are studied, from the result it was found that the flexural strength of Dagneux beam specimen in ambient state is 60% less than that of dry flexural strength.
- The average flexural strength of Dagneux beam specimens for both CRA and Dagneux soil was found to be 0.15MPa.
- The compressive strength of rectangular prisms (recovered layers) was found to be 1.42MPa and 1.98MPa for CRA and Dagneux soil. Though the dry densities of CRA soil specimen were higher than the Dagneux, the compressive strength of Dagneux is found to be significantly high. Considering the scattered results of recovered rectangular prism specimens, the test is not recommendable.

6. Experimental procedure to study interface behaviour of Unstabilised Rammed Earth (USRE)

6.1. Introduction

The shear strength of a material should always be greater than the maximum shear load in design consideration of any structure. Therefore due to this fact it is necessary to assess the shear strength characteristics of USRE. Most natural soils exhibits shearing resistance due to cohesion and friction, these strength components are found to exhibit a wide range of relationship.

Rammed earth walls which are built in layers is assumed to behaves like a monolith structure (Cheah et al., 2012; Gomes et al., 2014; Miccoli, Oliveira, Silva, Müller, & Schueremans, 2014). The presence of layers in USRE exposes the fact that delamination of interfaces is a possible failure criteria under lateral loads (Daniela Ciancio & Gibbings, 2012), such as seismic loads. The manufacturing method indicates that, the interlocking mechanism of grains within the layer and in between the layers are different, hence the strength parameters are also different. The interface interlock mechanism also has an important contribution to the interface strength. The two contributing components of shear strength: (a) Friction, which is dependent on the internal friction between the soil grains and is proportional to the applied effective stress normal to the shear plane, and (b) Cohesion, which is influenced by the grain size, the state of packing of the material and moisture content, will differ for within the layers and in between the layers (Cheah et al., 2012; P. Jaquin, 2011).

Earlier works on rammed earth identified delamination of layers as a potential threat and lack of experimental investigation on interface strength parameters. At this moment, to our knowledge, there is no compact and handy testing procedure to investigate the interface behaviour of rammed earth under lateral loads. Therefore in this study, a novel experimental technique has been developed, which can be easily mounted on a conventional axial compression press to study interface shear strength parameters.

6.2. Literature review

In general practice, the experiments adopted to study shear parameters of earthen building materials are 'Tri-axial compression test', 'Shear box test', 'Diagonal compression test', 'Triplet test' and 'Push over test'. In this section, a brief literature review on the shear strength studies carried out on rammed earth specimens is discussed.

6.2.1. Push over test

In the study conducted by (Nabouch et al., 2016), the USRE walls of dimensions 1.5m×1.5m×0.25m and 1.5m×1.0m×0.25m was subjected to push over test as shown in Figure 6-1 (VH is the horizontal load, VE are the vertical preloads). During the experiment, at 85% of maximum load horizontal cracks were observed at the lower part of the wallet causing delamination of interface, and a quasi-diagonal cracks followed along the wall height. Author points out interface as the weak points in rammed earth walls with acceptable cohesion.

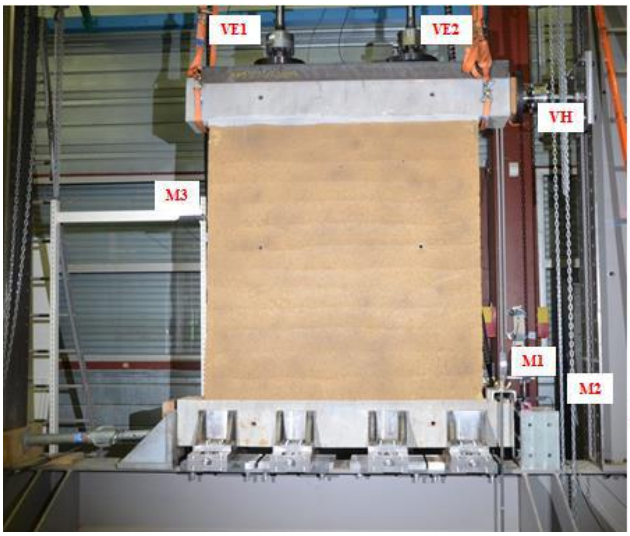

Figure 6-1 pictorial representation of push over test (source:(Nabouch et al., 2016)**)**

(Liu, Wang, & Wang, 2015) carried out push over experimental investigation on unstabilised rammed earth and fibre reinforced rammed earth wallet specimens. The dimensions of the wallets studied in this study were 2400mm×2100mm×600mm, there are no additional details with respect to specimen manufacturing water content, testing water content or density of the specimens given. This study evaluates the shear strength of the externally bonded fibre reinforced rammed earth and unreinforced rammed earth walls. This study shows that, there is an increase of 38% in resistance to lateral loads with proposed retrofitting system. From observation author points out at 50-60% of failure load the damage of rammed earth wallets were initiated by diagonal cracks associated with

peeling (delamination) of layers. Delamination of layers was witnessed in specimens with external fibre reinforcement and unreinforced rammed earth.

6.2.2. Diagonal compression test and other tests on wallets

(R.A Silva, Olliveira, Schueremans, Miranda, & Machado, 2014), conducted experimental study on unstabilised rammed earth wallets of dimensions 550mm × 550mm × 200mm. 11 specimens were tested in diagonal compression test as per ASTM standards, this study involved studying shear strength by testing new unstabilised rammed earth wallets and grouted unstabilised rammed earth wallets. Finally the reduction in strength due to grouting is evaluated with respect to shear strength and shear modulus of new unstabilised rammed earth wallets. The average shear strength of unstabilised rammed earth was found to be 0.15MPa and shear modulus of about 640MPa was reported for specimen with average dry density of 2.02g/cc. It was interesting to note that the failure mechanism of specimens, failure was initiated with a diagonal crack, but it also shows that there is significant layer delamination taken place.

From experimental investing carried out by (Miccoli, Müller, et al., 2014) on different earthen building materials, the shear strength of the unstabilised rammed earth wallets in diagonal compression test was reported as 0.71MPa along with the shear modulus of 2326MPa. In continuation (Miccoli, Oliveira, et al., 2014) extended their investigation to study compressive strength behaviour of USRE wallets along with shear behaviour. Author describes the damage (failure pattern) of USRE wallets under diagonal compression test occurred due to diagonal cracks running from top to bottom of the supports, passing through layer interface causing partial delamination of layers. Though the delamination of layers was partial, it shows that interface can behave as weakness. In addition, delamination of interface at the borders of the specimen was also noticed. This shows that, when material is sheared or tensioned due to seismic event, there is a potential risk of failure due to delamination of layer. In addition to experimental investigation, (Miccoli, Oliveira, et al., 2014) and (Rui A Silva, Oliveira, Miccoli, & Schueremans, 2014) carried out numerical analysis of USRE based on the parameters obtained through experimental investigation. In the numerical analysis macro and micro models were adopted, macro model considering homogenised approach and micro model considering stacked nature of rammed earth were designed. The micro modelling approach was designed by introducing the interface parameters based on Coulomb's friction criteria. The interface strength parameters were assumed due to lack of information; this is where author stresses the lack or non-availability of USRE interface strength parameters based on

experimental investigation. The macro and micro model simulated a good correlation with the experimental results. The micro model allows capturing the failure by delamination of interface between layers. Hence the need to study interface strength parameters of the USRE.

(P. A. Jaquin, Augarde, & Gerrard, 2006) carried out numerical simulations based on the experimental study conducted to observe the different failure mechanism of wallets by altering support and loading condition under compressive load. From experimental analysis it was observed that, some of the failure occurred due to delamination of layer interface. Hence authors thought it is important that the models capture in-plane failure through cracking and layer delamination. The finite element modelling carried out in this work incorporated the interface nature using Mohr coulomb's principle. The cohesion and angle of fiction for rammed earth wall and interface were assumed differently, the values of interface were lower than that of wall as a single unit. The assumed cohesion and angle of friction for interface varied from 15kPa to 60kPa and 20° to 37°, depending on the failure due to loading and boundary condition. From this analysis author points out the importance of incorporating interface parameters in the numerical model. From the comparison of the results obtained from tri-axial test and shear box test, author suggest the large scale shear box test as an alternative to achieve precision to calculate shear strength parameters of rammed earth interface.

6.2.3. Shear box test

(Corbin & Augarde, 2015) used the Direct Shear Test (DST) to evaluate the shear strength parameters of the rammed earth block specimens. Note that this study focuses on understanding the strength parameters within the layer, not the layer interface. In this study, the influence of cement stabilisation and wool reinforcement on shear strength parameters is presented. Rammed earth specimens with dimensions 60mm × 60mm × 20mm are prepared with combination of cement and wool. Unstabilised rammed earth specimens without wool reinforcement are also tested to study the influence of density and manufacturing water content on the shear strength. In this study, author shows there is an increase in shear strength with increase in cement content, on contrary there is decrease in shear strength with increase in wool presence. This study also shows a relation of shear parameters with respect to manufacturing water content as show in Figure 6-2 (source: (Corbin & Augarde, 2015)). The optimum moisture content (OMC) for the studied compaction energy is 11%. It is interesting to note that, the cohesion of unstabilised rammed earth decreases with increase in manufacturing water content in the dry side of

OMC, while contrary effect takes place in the wet-side of OMC. Similarly angle of internal friction increases with increase in water content in the dry side of OMC, and decreases with decrease in water content at the wet-side of OMC. Though this effect has not been explained, the inverse relation of cohesion and angle of internal friction is very interesting for further studies. In general the cohesion and angle of internal friction of unstabilised rammed earth specimens tested in shear box test (DST) were found to be varying in between 55kPa-80kPa and 23°-65° respectively.

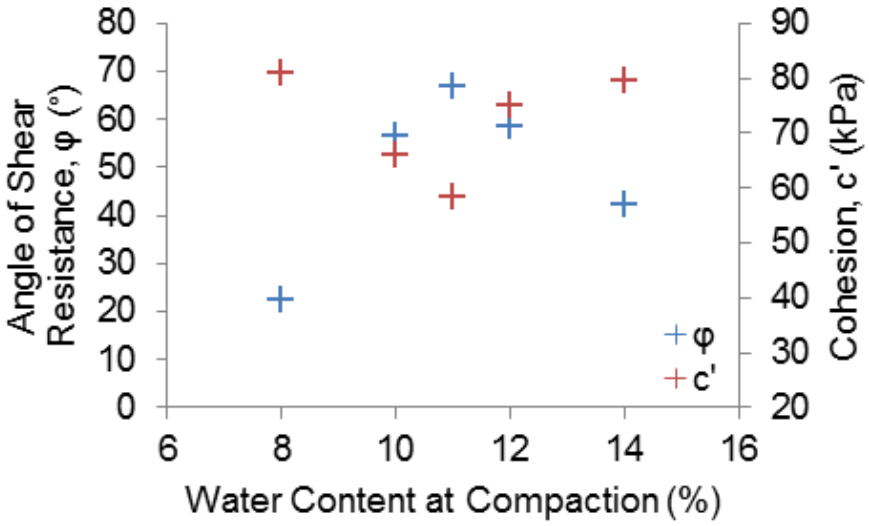

Figure 6-2 Relation of shear parameters (cohesion and angle of shear resistance) with respect to manufacturing water content presented in the study of (Corbin & Augarde, 2015)

6.2.4. Tri-axial and triplet test

(Araki et al., 2011) studied mechanical properties of the soil used for construction of rammed earth buildings in Japan. A part of this work included tri-axial compression test, which was adopted to study the shear strength parameters on the unstabilised rammed earth specimen manufactured with compaction energy of 2700kJ/m^3, to achieve an average dry density of 1.9g/cc. 5 numbers of 10 layered specimens with dimension 50mm in diameter and 100mm in height are subjected to tri-axial test for different confining stress. From this study, the cohesion and angle of internal friction was reported as 626kPa and 49 degrees respectively. It was also noted that, the average moisture content of the specimen at test was 1.6%.

(Gerard et al., 2015) carried out several experimental studies on the unstabilised rammed earth specimens, to derive unified failure criteria, in relation with the degree of saturation of the specimens. One of the experiments carried out in this experimental campaign is consolidated and undrained tri-axial test on saturated specimens. 4 numbers of homogeneous specimens with dimensions of 36mm in diameter and 72mm in height are

manufactured and subjected to tri-axial test at 4 different confining stresses. From the experimental result, the cohesion and angle of internal friction of the unstabilised rammed earth specimens were found to be 6.2kPa and 36.5° respectively. It has to be noted that the specimen were saturated, which is the reason for very low cohesion value. Interesting factor is the value of angle of internal friction (36.5°), which remains very close to the values derived from other studies.

(Cheah et al., 2012) in this study evaluated shear strength of cement stabilised rammed earth and fibre reinforced rammed earth using two methods namely, tri-axial test and triplet test. In this work cement stabilised rammed earth specimens reinforced with natural fibres (sisal and New Zealand flax) and without fibre reinforcements are studied. All the specimens manufactured for this study were three layered specimen with 70mm as layer thickness. Compaction energy of 1560kJ/m^3 was adopted to obtain dry densities of 2.04g/cc and 2.15g/cc for tri-axial and triplet test specimens respectively. The shear strength parameters of stabilised rammed earth specimens without fibre reinforcement discussed in (Cheah et al., 2012) are considered in this discussion.

In tri-axial test, 13 cylindrical specimens were manufactures, 4 numbers of specimens among them were without fibres. The cohesion and angle of internal friction for stabilised rammed earth without fibre reinforcement was found to be 724kPa and 48 degrees respectively from tri-axial test.

In triplet test, 28 numbers of rectangular prism specimens were tested for triplet test, 9 numbers of specimens among them were without fibre reinforcement. From triplet test, the cohesion and angle of internal friction of the interface was found to be 328kPa and 45 degrees respectively.

Author explains that, the variation of strength parameters from different tests is due to the change in failure plane. In tri-axial test, the specimens failed diagonally passing in-between layers, whereas in triplet test, the specimens failed due to delamination of interface, which is the weaker than rammed earth layers. Considering that diagonal failure of rammed earth structure to be more likely, author recommends using tri-axial test results for design consideration. Author considers triplet test shortfalls such as; requirement of custom formwork, weight of specimen, and experiment set up complication requires laboratories with more facilities.

6.2.5. Summary

- Diagonal compression test or push over test is widely accepted as a standard test procedure to study the shear strength of masonry or rammed earth wallets. In diagonal compression test only shear stress and shear modulus can be evaluated. But to completely understand the shear behaviour of rammed earth walls, one need to extract all the strength parameters such as cohesion, angle of internal friction, shear strength and shear modulus of the material.
- Considering the specimen thickness in small shear box, it is difficult to test the rammed earth prism specimens with multiple layers in shear box.
- The geotechnical test such as tri-axial test can be used to study the shear parameter of the rammed earth specimen. But, the specimen is relatively small and influence of layer interface is not exploited to maximum effect.
- The drawback of triplet test is its complication in setting up the experiment, which is time consuming and not economical.
- The summary of the shear strength investigations carried out on rammed earth by various researchers are given in Table 6-1.

Table 6-1 summary of shear test results on rammed earth from literature review

Author	Soil type	Test type	Dry density, g/cc	Moisture at test	Shear strength, MPa	Shear Modulus, MPa	Cohesion, kPa	Friction angle, °
(Liu et al., 2015)	USRE	Push over	-	-	73kN	-	-	-
(Nabouch et al., 2016)	USRE	Push over	-	3%	0.09-0.13	-	-	-
(R.A Silva et al., 2014)	USRE	DCT*	1.97-2.06	-	0.15	640	-	-
(Rui A Silva et al., 2014)	USRE	DCT*	2.19(bulk)	2-3%	0.7	1582	-	-
(Miccoli, Oliveira, et al., 2014)	USRE							
(P. A. Jaquin et al., 2006)	USRE	Assumed values for numerical analysis	-	2-3%	-	-	15-60	20°-37°
(Corbin & Augarde, 2015)	USRE	shear box	-	-	-	-	55-80	23°-65°
(Araki et al., 2011)	USRE	Tri-axial	1.99	1.45-1.65%	-	-	626	49°
(Gerard et al., 2015)	USRE	Tri-axial	2	-	-	-	6.2	36.5°
(Cheah et al., 2012)	CSRE	DCT*	-	-	0.73	-	-	-
		Tri-axial	2.04	2.4-3.5%	-	-	724	48°
		Triplet	2.15	2.4-3.5%	-	-	328	45°

Note: *DCT – Diagonal compression test

6.3. Objective

The preliminary objective of this study is to propose a new testing method for studying interface strength parameters of rammed earth wall. In order to study the interface failure parameters under lateral loads, the interface of the specimens should be subjected to inclined loading. To induce inclined loading, a pair of inclined metallic wedges are designed (Figure 6-3), which can be easily mounted on an axial compression loading frame. This is a compact and with-ease experimental procedure that can be carried out with limited space. To study how material undergoes deformation under lateral loads digital image correlation (DIC) method is adopted. The influence of interface surface condition on the shear strength is also studied.

6.4. Wedge design

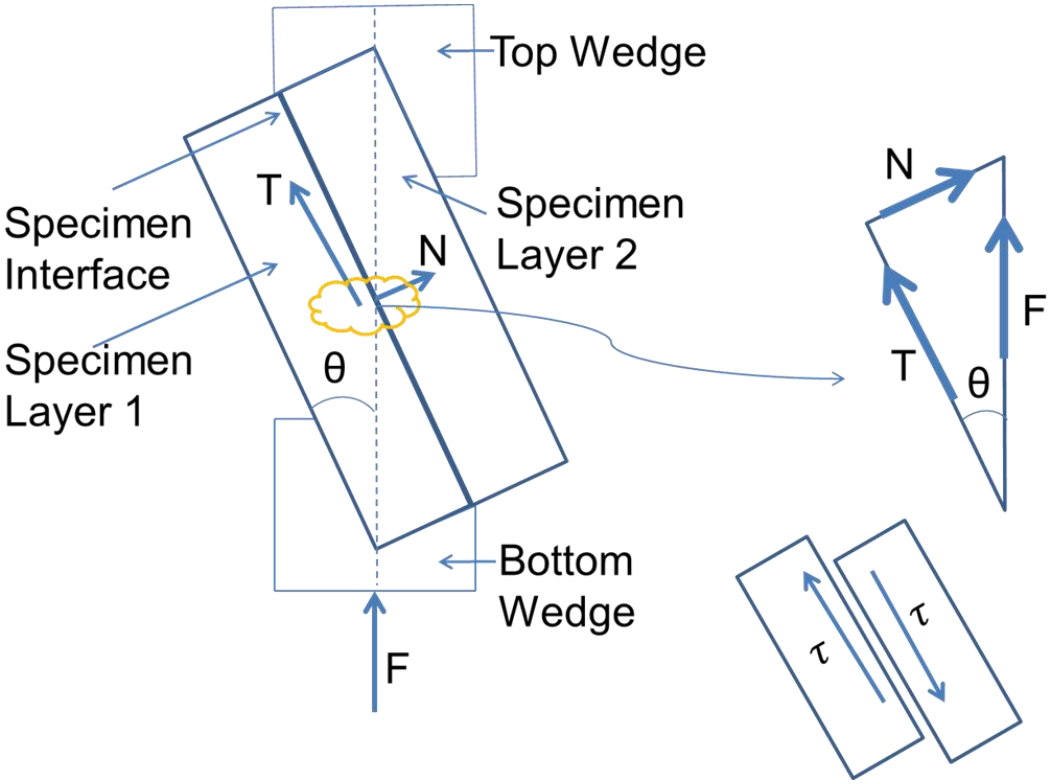

Figure 6-3 Resolution of force, where F = Axial force, T= Shear Force acting on the interface, N= Normal Force acting on the interface

The specimen has to be positioned at an angle such that, the axial force 'F' will induce shear force 'T' and normal force 'N' on the interface of the specimen as shown in Figure 6-3. Hence, pair of metallic wedge as shown in Figure 6-4 was designed. This test required two identical metallic wedges as shown in Figure 6-5, one for bottom support, which acts as a specimen holder and other on the top of the specimen, which is normally fixed to the press loading plate, such that, test specimen is symmetrical to the loading axis.

The metallic wedge support is designed considering the dimension of the loading frame, such that the wedge supports are easily mounted on the loading press. The width (W) and length (L1) of the specimen holder as shown in Figure 6-4 is fixed to 120mm and 60mm, which is equal to the specimen layer width and thickness respectively. Three pairs of metallic wedges which have different angle of inclinations (Θ) with respect to vertical axis are designed. Three different wedge angles help to induce different shear and normal force on the specimen interface. The wedge angle of inclinations (Θ) used in this study are 45°, 30° and 20°. As the angle of inclination changes, the length 'L2' (Figure 6-4) was adjusted with respect to base length of the wedge. The length L2 for 45°, 30° and 20° were 141.4mm, 115.5mm, and 106.4mm respectively. The engineering diagram of all the wedges is given in Annexure D.

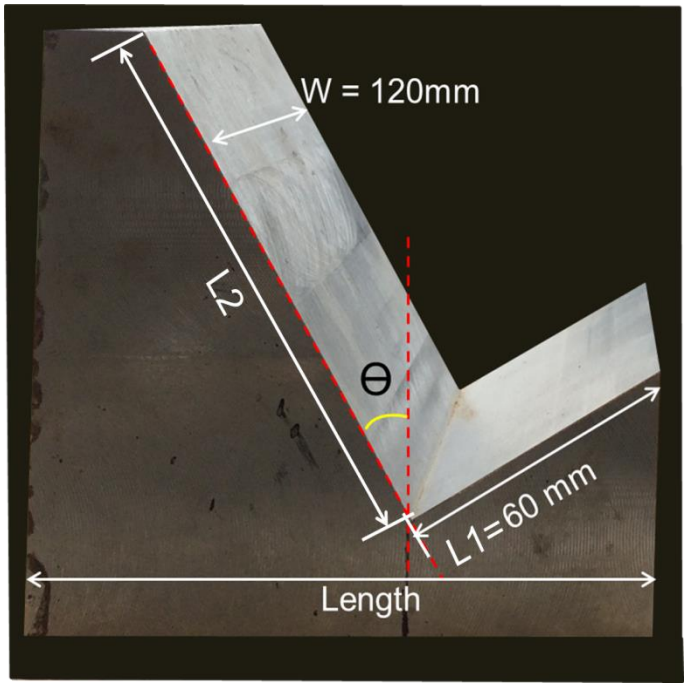

Figure 6-4 Metallic Wedge

It has to be noted that, when the angle of inclination of wedge changes, the height of the specimen should change to maintain vertical symmetry of the specimen with loading axis. Hence, the lengths of the specimens tested at different angle of inclination are not same. The dimensions of the specimens tested at 45°, 30° and 20° are presented in the Table 6-2.

Table 6-2 dimension of rectangular prism specimens used for interface test

Angle of inclination	Length, mm	Width, mm	Depth, mm
45°	120	120	120
30°	210	120	120
20°	330	120	120

Figure 6-5 Wedge setup to hold specimen in required inclination

6.5. Digital Image Correlation (DIC)

Digital image correlation (DIC) is a non-contact optical technique used to measure deformation, displacement and strain of the material undergone (Mccormick & Lord, 2010). DIC is widely accepted as an intelligent and cost effective method to study the material properties. Its application in civil engineering is spread from studying crack propagation in existing building to basic material properties in laboratory (Mccormick & Lord, 2010). Most importantly monitoring very sensitive structures such as power plants, bridges, dams, etc. has proven vital for their serviceable life. The major advantage of DIC is that, every minor detail in the area of interest (AOI) can be studied in detail.

The principle of DIC as explained by (Sutton, Wolters, Peters, Ranson, & McNeill, 1983), is that, the camera records the intensity of the light reflected by the specimen surface, as a set of numbers or grey levels. Each sensors converts the light intensity into a number, which are stored as set of arrays. The arrays of light intensity distribution stored in the first picture acts as the reference coordinate for mapping the deformation of the object. To calculate the deformation of the object, the set of arrays taken within the subset is assumed to undergo homogeneous deformation, therefore the chosen subset for analysis should be as small as possible. The deformations obtained through the digital image correlation are accurate in determining rigid body translation and rotations (Chu, Ranson, & Sutton, 1985).

6.6. Experimental protocol

In this test, wedge positioning, specimen positioning and camera positioning are most important parameters to be verified before loading the specimen. Therefore a set of protocol was defined and monitored before every test. In this segment, global test setup, positioning and checking the vertical alignment of the wedge, preparing specimen surface with speckle pattern and aligning & adjusting cameras are discussed. The test setup is shown in Figure 6-6

6.6.1. Test setup

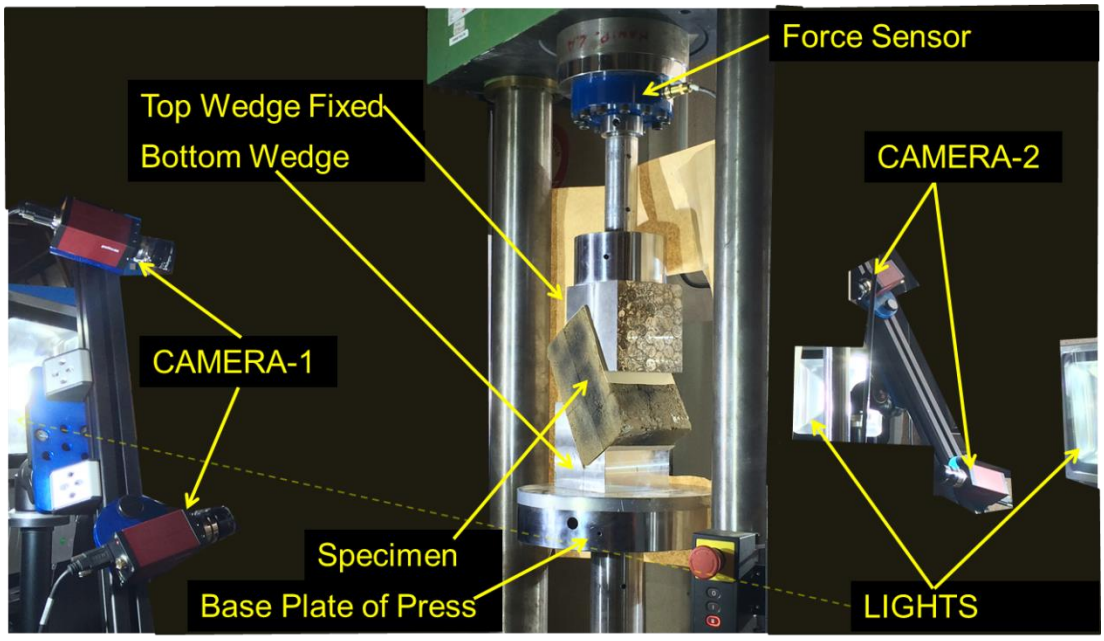

Figure 6-6 interface Test Setup

6.6.1.1. Positioning of wedges

As briefed earlier, in this study unstabilised rammed earth specimen interface are tested for 20°, 30° and 45° inclination with the vertical axis. Therefore there are three

different pairs of wedges, each pair has a bottom wedge which acts as support and top wedge which is glued to the top plate of the loading cell as shown in Figure 6-6. Top wedge is glued such that, the centroid of the loading plate and the point of intersection of specimen edges are in same axis. Similarly bottom is positioned on the bottom plate of the loading cell such that the diagonal opposite edge of specimen is intersecting with the vertical loading axis of the loading cell. To ensure that the vertical symmetry of the specimen and wedges are achieved a wooden box with similar dimension that of specimen are prepared and cross verified before beginning the test.

6.6.1.2.Positioning of cameras

Since positioning of cameras and light source takes more time, specimen positioning is carried out as a last step. In order to maintain the moisture and environmental homogeneity of specimen, specimens are taken out of climatic chamber just before the test. Hence, a wooden box similar to the dimension of specimen is used as the reference for positioning camera.

The cameras used in this study are supplied by the VIC-3D correlation solution. The cameras are high resolution monochrome with 29MP, with frame rate up to 110fps and exposure time 20µs-10s.

To make sure cameras are not disturbed while testing, all the cameras were mounted on a tripod, and were fixed to a bar on top of the tripod. Firstly, the camera holder bar is oriented to the same inclination as that of the specimen interface. Cameras inclination is positioned in the same angle as the interface testing inclination, so that the optical x-axis is parallel to the interface as shown in Figure 6-7, this will ease the transformation of displacement calculation in the post processing.

In this experiment, surface displacement on two opposite faces of the specimen are studied, hence pair of cameras on each face is positioned. Pair of cameras is positioned such that their optical centre is merging with the specimen interface centre as shown in Figure 6-8. The angle between the two optical views at the merging point should be in between 15-35°, for a better mapping as recommended by the manufacturer. Hence the cameras are positioned at a known distance ‘D’ from the specimen surface and for a given angle ‘L’ is calculated. Cameras are carefully rotated until the optical centre point is merging with the specimen interface centre and fixed, this is repeated to both the specimen faces.

Four high intensity light source, two on each face are positioned close to 45° of inclination to the specimen surface. Final adjustment of light is carried out during the calibration and test run of the cameras.

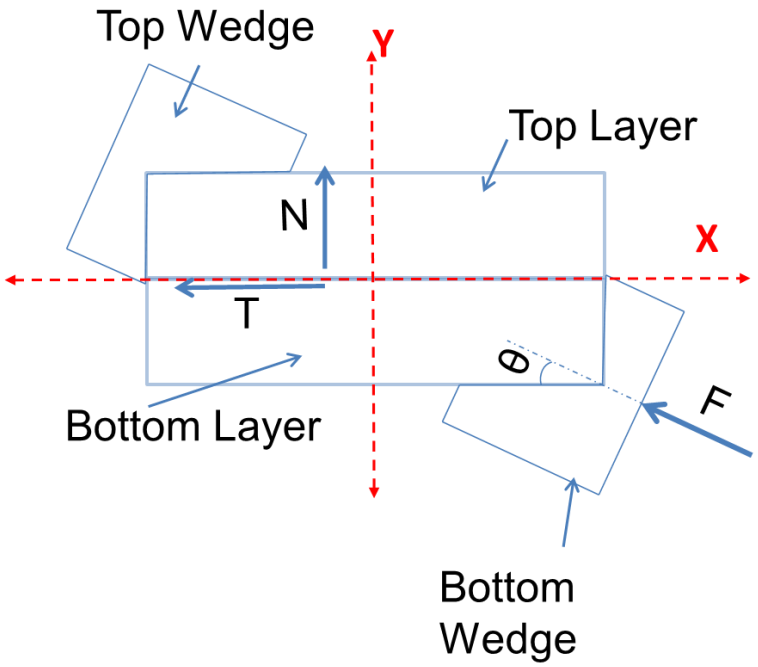

Figure 6-7 optical view of the specimen

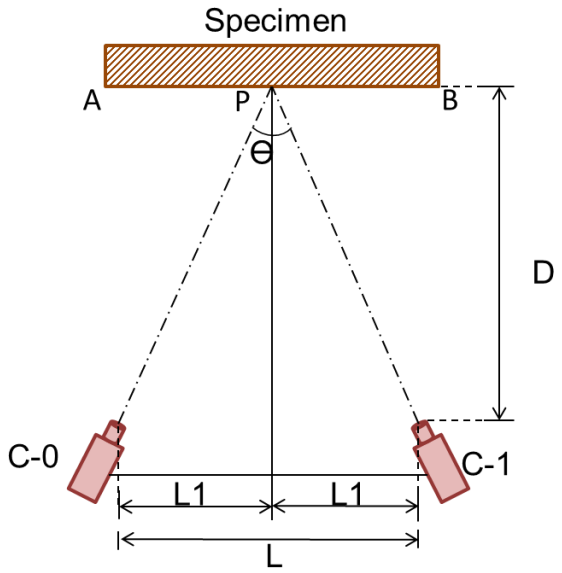

D – Camera lens distance from the specimen surface
L – Distance between the cameras
C-0 and C-1 are the cameras
A – Top edge of the specimen
B – Bottom edge of the specimen
P – Midpoint of the specimen

Figure 6-8 Orientation of cameras with specimen

6.6.1.3.Specimen Surface preparation and positioning

The top most surface of the rammed earth specimen will have surface undulation, which are created due to impression of rammer head. When specimen is positioned on the metallic wedge, these undulations will reduce the contact area between wedge and the specimen, which will have influence on loading of specimen. Hence the specimen surface undulations were smoothened using a knife and sand paper.

Next very important surface that has to be prepared is the one which is facing the cameras. Before painting speckle pattern on the surface, using a soft brush, any loose particle and dust on the specimen surface has to be removed. Using a black spray random speckle pattern (Figure 6-9) has to be painted on opposite surfaces of the specimen, which are facing the camera. Care has to be taken not to paint very dark spots, which will contribute to the error in correlation. Speckle pattern should be as fine as possible and random (Sutton et al., 1983), to ensure more subset within the area of interest (AOI), this will help in reading the images very accurately by the correlation software.

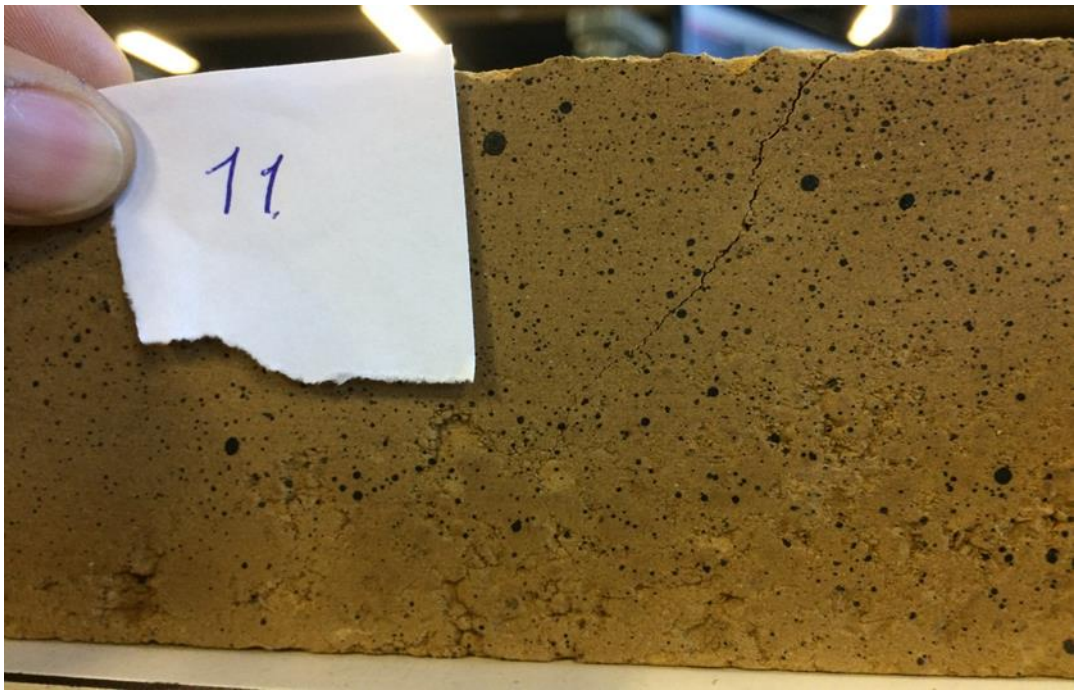

Figure 6-9 An example of speckle pattern

Immediately specimen weight is recorded with an accuracy of 0.01g, and its dimensions are measured to an accuracy of 1mm. Specimen is then mounted on the bottom metallic wedge and aligned with the top wedge. Before loading, with the help of L-angle vertical alignment is cross checked. The specimen positioning at different angle of inclinations are as shown in Figure 6-10.

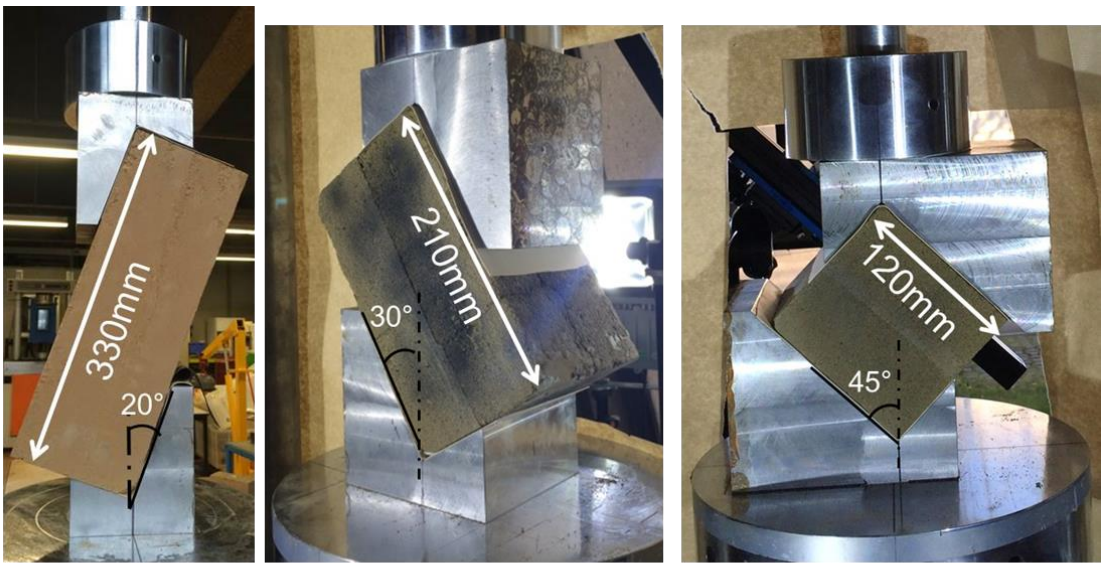

Figure 6-10 Specimens positioned at different angle of inclination

6.6.2. Camera calibration and test run

Calibration of camera sensors is one of the important steps; it serves as the basic criteria for reading error in pixels and position of the target. There are different types of calibration available, but in this case stereo calibration is adopted. Stereo calibration is used when there is good overlapping of images from both the cameras. There are different target speckle grids available to calibrate the sensor; the one used in this analysis is 12×9-5mm target grid as shown in Figure 6-11.

Chosen target speckle grid is positioned in front of the specimen surface and the digital brightness of the camera is adjusted using the computer tool for better reading of target speckle pattern. Images of target grid at different random orientation is captured (Figure 6-11), a minimum of 8-10 images per surface is taken. This is repeated to the opposite face as well.

The calibration images (target grid) are then opened in the VIC-3D software and verified for any error. VIC-3D has an inbuilt specification of the target grids, which identifies the offsets in x and y direction according to the grid dimension (Figure 6-12) to locate the target specimen. All the calibration images are processed for pixel error score, if the score is less than 0.02 (2%), it is considered to be acceptable. If the score is above 0.02, then there is a problem in reading the pixels, hence by adjusting the camera sensor and brightness, calibration process has to be redone. Calibration score should be as less as possible to minimise the error in correlation results.

After calibration images are processed and accepted. By readjusting the digital brightness of the camera sensors, a minimum of 10 images of specimen surface speckle patterns are captured without loading the specimen. The test run images are processed in the vic-3D correlation software to check for any large error in reading the specimen speckle pattern. If there is any error it has to be due to the intensity of light reflected, hence the required correction is carried out until the error is minimised to acceptable range.

When both calibration and test run is finished with satisfaction, the camera and specimen is ready for the loading. Attention was taken not to disturb the camera position or the specimen, until the test is finished.

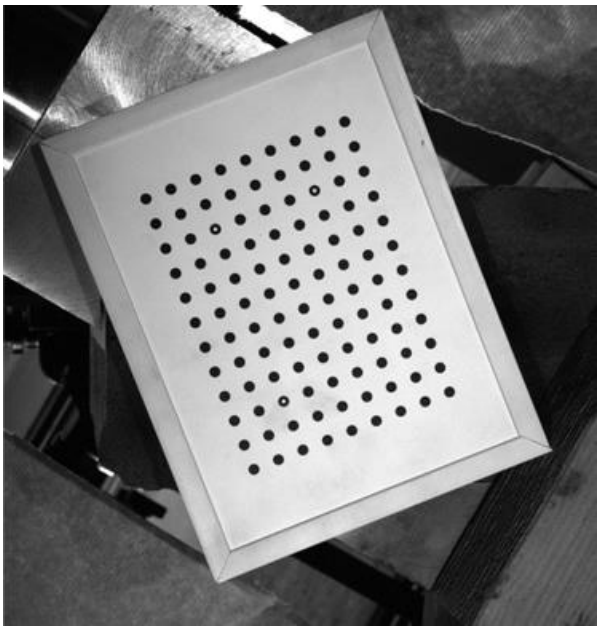

Figure 6-11 Image of a target speckle pattern (9cm × 12cm) taken during calibration

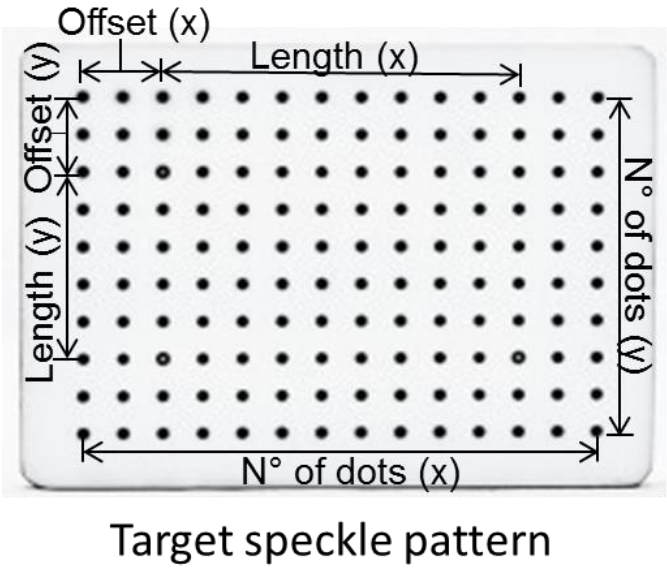

Figure 6-12 Target speckle pattern

6.6.3. Loading program

The test was programmed to run in loading press displacement control mode @ a rate of 5µm/s throughout the test. In this test, loading was programmed to be a simple axial compressive load applied to the wedges, which then resolves to compressive force into shear and normal force on the specimen as shown in Figure 6-13. The one disadvantage in this test is that the normal force is not controlled (fixed) as done in the direct shear test..

The failure load is then resolved to obtain the failure shear and normal load. The failure stress (τ and σ_n) is then calculated by dividing the failure load (T and N) with the area of interface (A_s) as shown in Figure 6-13.

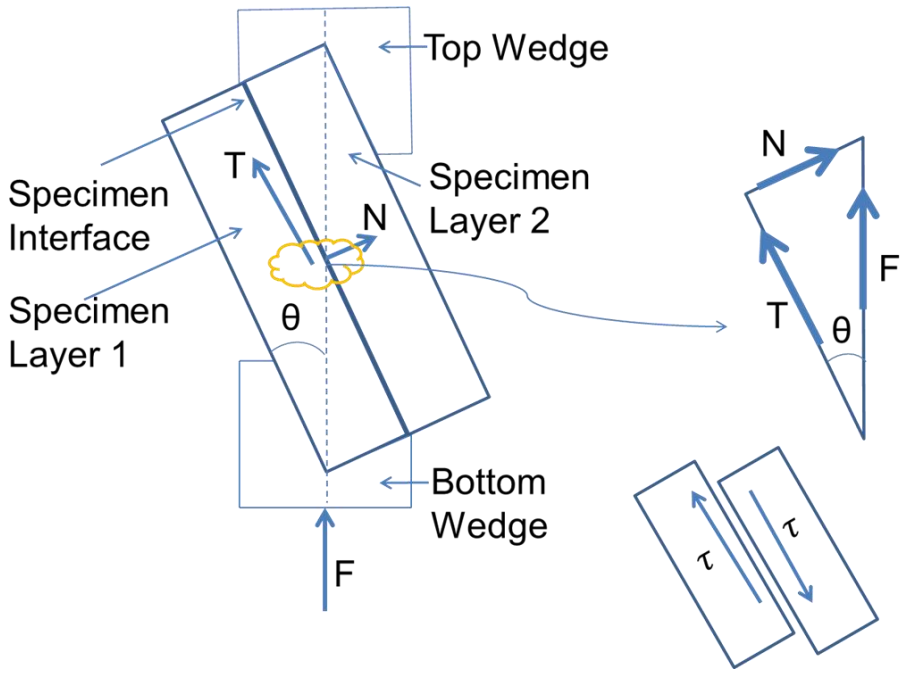

Figure 6-13 Resolution of force

$T = F \cos\theta$, and $N = F \sin\theta$, then $\frac{T}{N} = \tan\theta$;

$\tau = \frac{T}{A} = \frac{F \cos\theta}{A}$, and $\sigma_n = \frac{N}{A} = \frac{F \sin\theta}{A}$

Where; Θ is the angle of inclination; T is the shear force in 'N'; N is the normal force in 'N'; τ is the shear stress in MPa; σ_n is the normal stress in MPa; A is the area of contact surface (area of interface) in mm^2.

6.7. Results and discussion

Calculated failure shear stress (τ_f) is plotted against normal stress (σ_{nf}), from which coulomb's failure envelope for the interface is obtained. From coulomb's envelope, shear strength parameters of the interface such as cohesion (C) and angle of internal friction (Ø) for the interface is also obtained. Further, some light on how to increase the interface strength is discussed. Moisture content and dry density of the material at test has significant impact on the strength of the material, hence, shear strength variation with respect to moisture and density is also discussed. Finally, shear modulus calculated from the help of DIC is presented and discussed in this segment.

6.7.1. Coulomb's Failure Envelope

6.7.1.1.Cras Sur Reyzousse (CRA)

Out of four specimens manufactured for 30° and 45° inclinations, only three of them yielded results. One in each category had manufacturing defect and failed before testing. Only one specimen was tested successfully for 20° inclination. The resolved failure shear stress is plotted against normal stress as shown in Figure 6-14. In Figure 6-14, all the test specimens failure stresses are plotted. Interface test result of CRA soil specimens are given in Table 6-3. Though the materials were stored in the similar climatic condition until weight equilibrium is achieved, moisture at test for different inclination was found to vary by 0.3% which is not very significant and hence neglected.

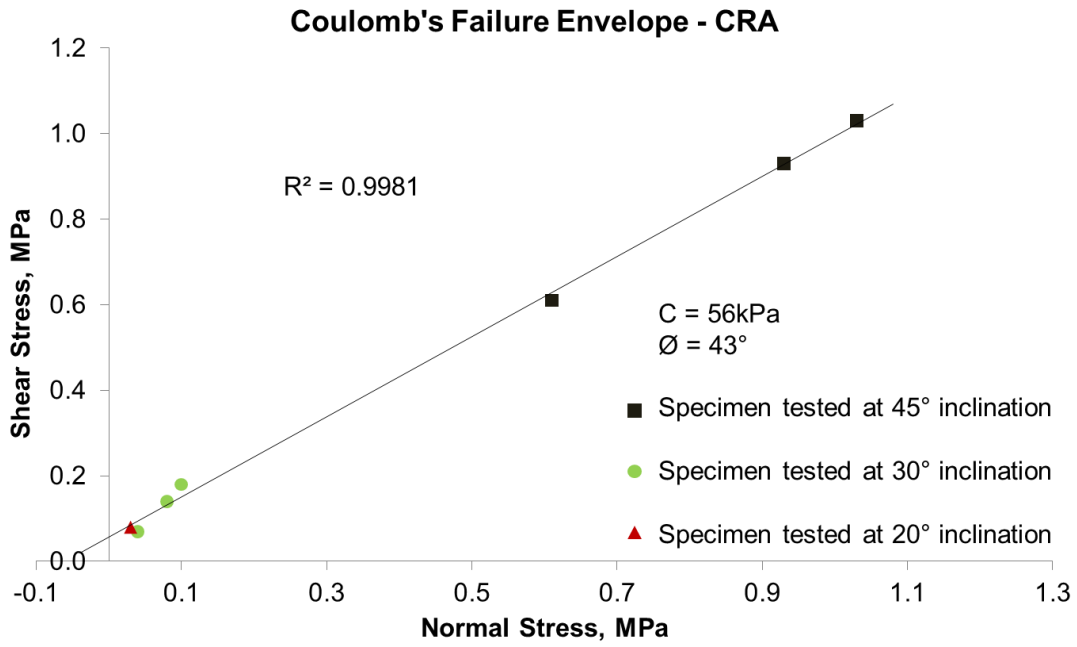

Figure 6-14 Coulomb's Failure Envelope CRA (all specimens) (moisture at test = 1.3-1.7%)

From the coulomb's failure criteria the shear strength parameters, i.,e Cohesion (C) and angle of internal friction (Ø) was found to be 56kPa and 43° respectively.

Table 6-3 Summary of CRA specimens, Failure Load, Dry density and Moistture at test

Angle of inclination	Dry Density, [g/cc]	Moisture at test, %	Tangential Strength, MPa	Normal Strength, MPa
20°	1.70	1.67	0.08	0.03
30°	1.81	1.41	0.07	0.04
	1.90	1.41	0.14	0.08
	1.92	1.36	0.18	0.1
45°	1.95	1.64	1.03	1.03
	1.94	1.62	0.61	0.61
	1.94	1.69	0.93	0.93

6.7.1.2.Dagneux

Similar to CRA soil, Dagneux soil specimens are also tested for interface shear strength. Nine specimens at 45° inclination, 10 specimens at 30° inclination and 3 specimens at 20° inclination were tested. Specimens at 45° inclination and 30° inclination are tested at different moisture state. The summary of shear test result on interface of Dagneux soil at ambient environment is given in Table 6-4.

The Coulombs failure envelope of Dagneux specimens is presented in Figure 6-15, the cohesion and angle of friction at ambient condition was found to be 118kPa and 37° respectively. Some of the specimens in 30° inclination exhibits low strength; this might be due to variation in moisture at test.

Table 6-4 summary of Dagneux interface test results

Angle of Inclination	Moisture at test, %	Dry Density, g/cc	Avg. Dry Density, g/cc	Tangential Stress, MPa	Normal Stress, MPa
45°	1.47	1.77	1.84	0.50	0.50
	2.27	1.87		0.41	0.41
	2.25	1.81		0.36	0.36
	2.2	1.92		0.23	0.23
30°	1.97	1.84	1.80	0.18	0.10
	2.06	1.84		0.13	0.07
	2.02	1.82		0.11	0.06
	1.57	1.72		0.32	0.18
	1.01	1.77		0.39	0.22
20°	1.45	1.7	1.72	0.20	0.07
	1.43	1.69		0.17	0.06
	1.41	1.77		0.17	0.06

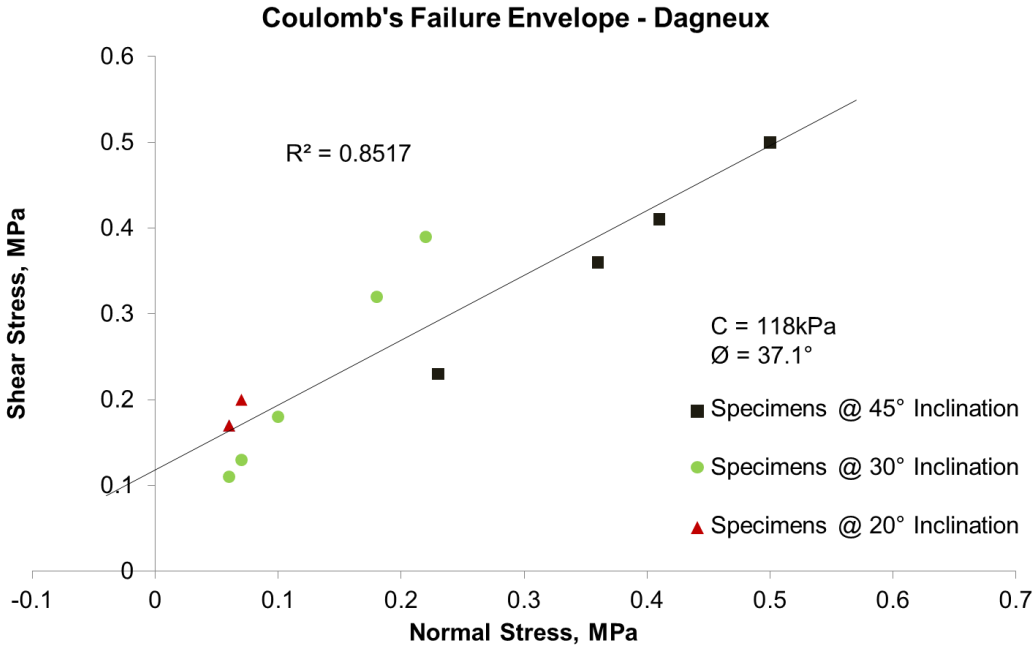

Figure 6-15 Coulomb's failure criteria of Dagneux specimens

6.7.2. Interface interlock mechanism

The cohesion of the interface can be improved by providing interlock between layers. After compacting the first layer, on surface of the interface a rough surface indentation of 1-2mm deep is made using a knife and some of the specimens were compacted without surface indentation. This enables to study the strength parameters of interface with and without interface surface indentation.

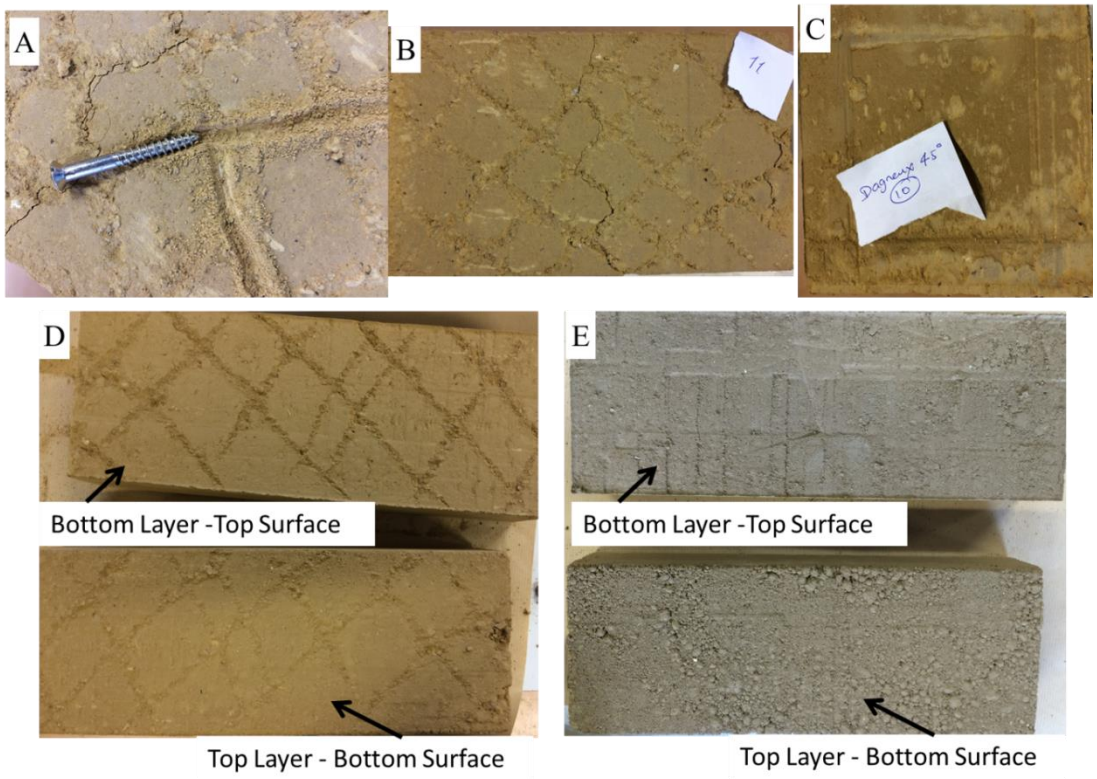

Figure 6-16 Interface surface indentation: (A) Surface indentation marked to a depth of 1-2mm, (B) An example pattern of Indentation marked, (C) Specimen interface surface without indentation, (D) Specimen Interface surface (top and bottom) with indentation, (E) Specimen interface without indentation (top and bottom)

In this study, the influence of interface interlock on the strength parameters of layer interface is studied only for Dagneux soil, interface surface indentation (as shown in Figure 6-16) was marked during specimen fabrication. 6 specimens at 30° angle of inclination and 5 specimens at 45° angle of inclinations were manufactured with interface indentation (interlock). 2 specimens each at 30° and 45° angle of inclinations were tested without indentation (smooth surface).

For specimens without and with interface indentation, failure shear stress is plotted against failure normal stress as shown in Figure 6-17 and Figure 6-18. By plotting best fit linear interpolation for all the points, cohesion(C) and angle of internal friction (Ø) is calculated. The angle of internal friction (Ø) does not vary much, whereas cohesion force of 72.6kPa for interface without surface indentation and 126kPa for interface with

indentation once again proves that, there is a drastic increase in bond strength of the interface. In Figure 6-17, 2 specimens each at 30° and 45° angle of inclination are presented; there are no specimens tested without interface surface indentation at 20° angle of inclination. In Figure 6-18, all the specimens with surface indentation tested at 20°, 30° and 45° angle of inclination are presented. For all the specimens presented in Figure 6-17 and Figure 6-18, moisture content at test was varying in between 0-2%.

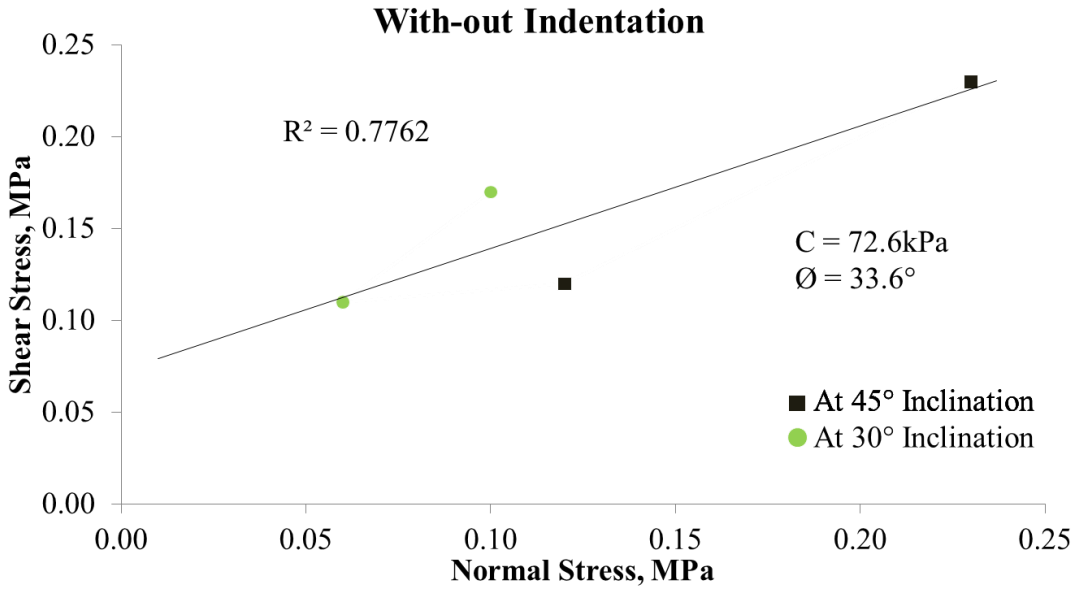

Figure 6-17 Specimens shear stress vs normal stress for interface surface without indentation

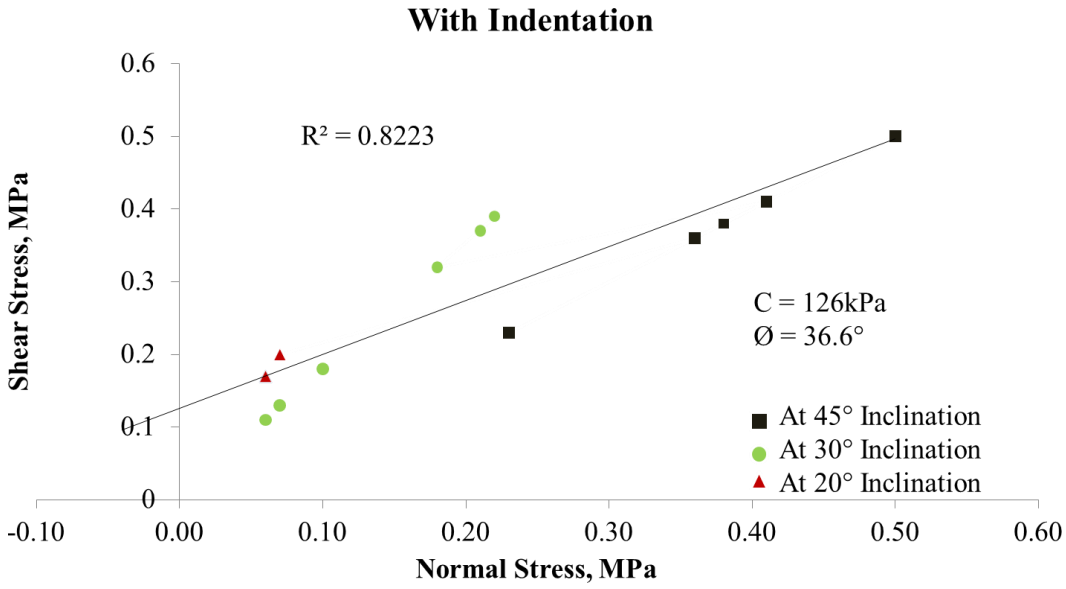

Figure 6-18 Specimens shear stress vs normal stress for interface surface with indentation

6.7.3. Moisture Impact

The moisture present in the voids of the material at service, which also called as the moisture content at test, its influence on the material strength is discussed in (Q. Bui et al., 2014; Champiré et al., 2016; P. A. Jaquin et al., 2009). From studies it can be seen that the moisture at service condition (i.e., during the life cycle of building) varies in between 0% to 5% (Chabriac, 2014; Soudani, Fabbri, Morel, Woloszyn, & Grillet, 2015). 0% moisture occurs when the material is oven dried at 100 °C-105 °C, and maximum moisture absorption is assumed, when the material is exposed to 97% RH at 23 °C.

In this study, Dagneux soil rectangular prism specimens are exposed to: oven dry state at 100 °C-105 °C to achieve 0% moisture at test, ambient state which is assumed to be 25 °C at 50% RH to achieve 1%-2% moisture at test, and finally the moist state which is assumed for the specimens with and above moisture of 3% at test. Moist state of the specimen is achieved by spraying water on all external surface of the specimen which was dried at ambient condition (25 °C and 50% RH).

Figure 6-19 shows the variation of shear strength of the rammed earth interface (with-indentation) with change in moisture state at test for specimens tested at 30° angle of inclination. Specimens at dry state generally have higher mechanical strength compared to the specimens at ambient state and moist state. In this case too, the shear strength of interface at dry state is higher compared to the moist state of the specimen.

For specimens tested at 30° inclination (Figure 6-19), the decrease in shear strength of interface was very evident. The shear strength at dry state was found to be 0.37MPa, which reduces by 62% (0.14MPa) at ambient state (2% moisture) and 76% (0.09MPa) at moist state (4.2% moisture). It can also be seen that the shear strength doesn’t vary much in between 0-2% moisture content. To understand the interface behaviour of the unstabilised rammed earth with change in moisture ingress, one has to obtain the precise moisture content near the interface.

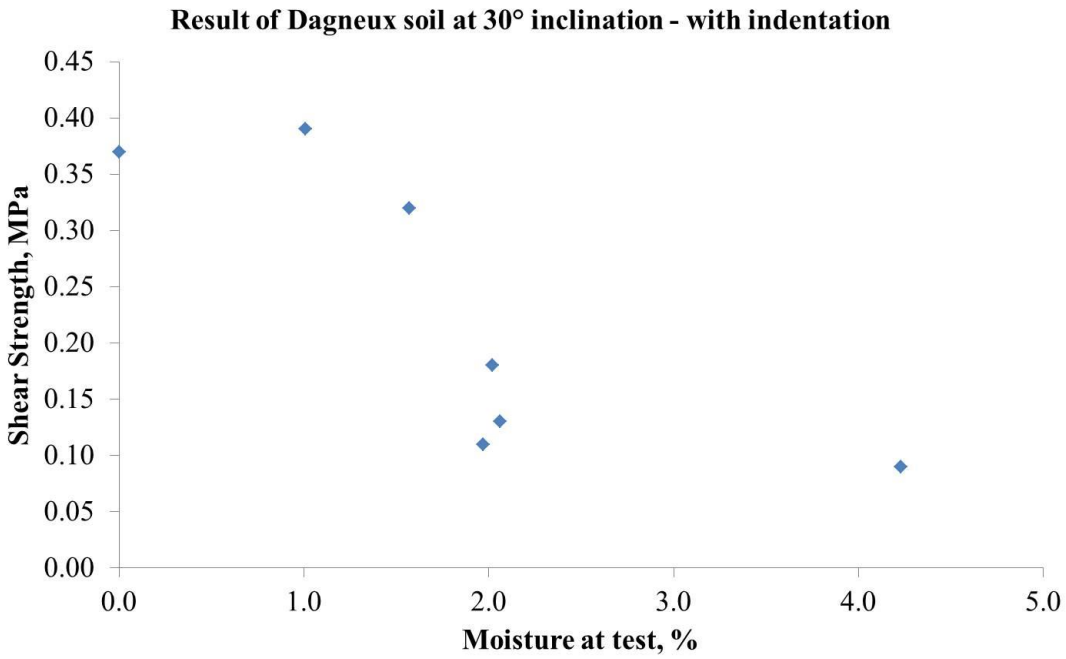

Figure 6-19 Variation of shear strength with moisture state at test – 30° inclination

6.8. Conclusion

The new experimental procedure to study shear strength parameters of USRE is tested on two soils. The cohesion and angle of internal friction for CRA and Dagneux soils at ambient condition were found to be 56.6kPa & 118kPa and 43° & 37° respectively. The cohesion value and angle of internal friction for USRE specimens reported by (Corbin & Augarde, 2015) from shear box test was in the range of 55-80kPa and 23-65° respectively. Similarly the interface cohesion values and angle of friction chosen (assumed) by (P. A. Jaquin et al., 2006) during correlating numerical simulation with experimental failure were in between 15-60kPa and 20-37° respectively, depending on the experiment. In the numerical model of (P. A. Jaquin et al., 2006), separate cohesion and angle of internal friction for interface and wall as a unit were chosen. The cohesion and angle of internal friction values found in this analysis is in close accordance with the earlier studies. But the cohesion and angle of internal friction values reported from the tri-axial test (Araki et al., 2011; Cheah et al., 2012) were very high in the order of 600-700kPa and 45-49° respectively. The cohesion and angle of internal friction values from tri-axial test is obtained for within the layer. Hence as suggested by (P. A. Jaquin et al., 2006; Miccoli, Oliveira, et al., 2014), the cohesion and angle of internal friction for both interface and within the layer has to be incorporated in the design principles.

By providing the interface interlock (rough surface), the variation of interface strength parameters were observed. The cohesion value of specimens with indentation was found to be 126kPa while without indentation was 72.6kPa. The change in angle of internal friction for different surface condition was negligible. It was also noticed that the interface strength of USRE specimens decreases with increase in moisture content.

From this analysis, it can be said that the new experimental procedure to study the interface strength parameters of rammed earth interface is in agreement with the results from earlier studies. The advantage of this experimental procedure is that, all the interface strength parameters can be studied in one experiment. This method is compact and conveniently adaptable to any laboratory, and also the size of the specimens is negotiated.

7. Experimental investigation to study compressive and flexural strength of Laterite building stones (LBS)

7.1. Introduction

The LBS which are abundantly available in tropical countries are porous building materials, which have moisture retention capacity within the material. The moisture presence within the material contributes to the complexity of its mechanical behaviour, too much of moisture within the material leads to reduction in strength. Yet the affinity of water molecules brings a well-known quality for interior comfort, both acoustic, hygric and thermal (Cagnon, Aubert, Coutand, & Magniont, 2014; Maillard & Aubert, 2014; McGregor et al., 2016; Soudani et al., 2015).

The LBS possess a good compressive and flexural strength (A. K. Kasthurba et al., 2007; A K; Kasthurba, Reddy R, & Reddy D, 2015; A Lawane et al., 2011; Unnikrishnan et al., 2010). (A K; Kasthurba et al., 2015) studied compressive strength of laterite stones by subjecting specimens in unconfined compression test at dry state and saturated state. (A. K. Kasthurba et al., 2007; Unnikrishnan et al., 2010) studied the compressive strength only at saturated state, while (Abdou Lawane et al., 2011) studied compressive strength at dry, natural and saturated state. The specimens used for compression test in the earlier works does not respect the aspect ratio of 2 or more, and also no correction factor was introduced to compressive strength reported. The flexural strength of laterite stones at dry and saturated state is reported by (A K; Kasthurba et al., 2015), but does not mention which type of test is carried out, whereas (Abdou Lawane et al., 2011) carried out three point bending test on saturated laterite stone specimens. From earlier works, it was noticed that the dry, natural and moist strength of laterite stones is important, but most of the work reports dry and saturated strength of laterite. Since LBS are porous in nature, it is also important to study influence of moisture ingress on the mechanical strength. More over hygroscopic parameters of LBS should also be studied to evaluate indoor comfort. Therefore an experimental procedure to study material response to moisture buffering condition and its influence on mechanical parameters is studied in this work. Mechanical and hygrothermal parameters are also critical in promoting laterite stone as a sustainable alternative, and lack of scientific data is hindering potential use of LBS. In this work, the LBS from Burkina-Faso is tested and analysed for its response to moisture buffering by studying sorption and desorption, dynamic moisture buffering, and mechanical characteristics such as flexural strength, compressive strength and modulus of elasticity.

7.2. Materials and methods

7.2.1. Description of the tested material

The quarry of studied LBS is situated in Toussiana, located at 10°50’ N, 4°37’W in the province of Houet, West of Burkina Faso, geographical map is show in Figure 7-1. Use of locally available LBS proves economical due to its low cost benefit and better thermal comfort, in surrounding locality the LBS are mainly used for building houses, churches, schools, etc. Lateritic stone blocks of dimension 240×120×120mm transported from the quarry are tested for its properties, the dry density of the material was found to be 1.85g/cm^3 with 23% porosity and the thermal conductivity at 23°C and 50% RH was found to be 0.96W/(m.K) from ‘FP2C’ hot wire apparatus manufactured by NEOTIM. The dry density of the other alternative building materials such as CEB, unstabilised rammed earth and bulk density of adobe, reported from earlier studies are in between 1.5-2.2g/cm^3 (J. Morel et al., 2007; Muntohar, 2011), 1.8-2.2g/cm^3 (Q. Bui et al., 2014; T.-T. Bui et al., 2014; Hall & Djerbib, 2004; Maniatidis & Walker, 2008) and 1.3-2.2 g/cm^3 (Adorni et al., 2013; Jean Emmanuel Aubert, Marcom, Oliva, & Segui, 2015; Oti, Kinuthia, & Bai, 2009; Silveira et al., 2013) respectively depending on the manufacturing water content and compaction energy adopted while manufacturing. Building houses with locally available materials, such as adobe, CEB, rammed earth, stone are proven to be economical by decreasing processing and transportation cost and at the same time they are also proven to be eco-friendly by reducing embodied energy (J.-C. Morel et al., 2001). LBS are abundantly available in tropical countries, where low cost and sustainable construction is the key for development. LBS with similar basic properties as of adobe, CEB, rammed earth, stone, can be looked as a potential alternative building material which provides economical and eco-friendly solution.

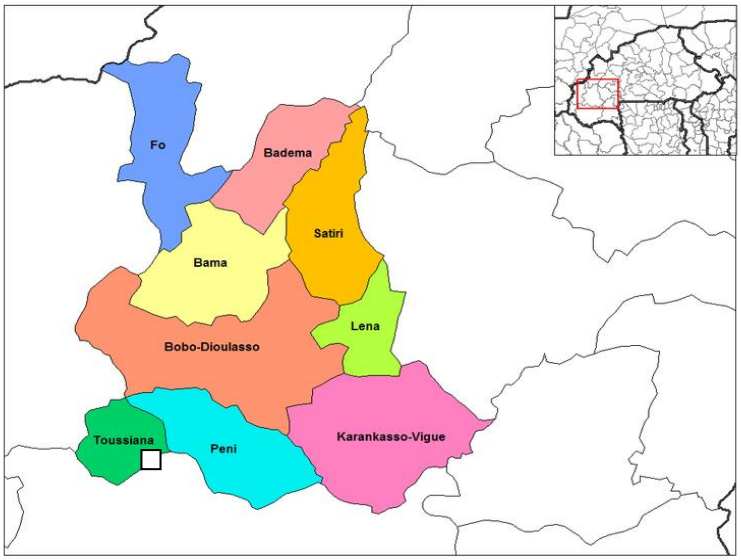

Figure 7-1: Location of Toussiana in the province of Houet in Burkina- Faso

7.3. Procedure and sample conditioning for the hydric tests

7.3.1. Sorption isotherms

The sorption isotherms were measured to describe the hygroscopic behaviour of the material. The sorption isotherms indicate the moisture content adsorbed by the material to reach equilibrium with the vapour pressure of the surrounding environment. Sorption and desorption isotherms were measured according to the ISO standard (ISO-24353, 2008). Airtight containers were used with saturated salt solutions to set imposed relative humidity (RH) levels. All samples were previously oven dried at 105°C to constant mass (varying in between 25g to 50g) before placing them successively in RH levels of 23, 43, 59, 75, 85 and 97%. The airtight containers were placed in a conditioning room at 20°C and 60% RH. Scales with a precision of 0.01 g were used to record the mass variation of the samples. The mass was recorded until the variation was less than 0.02 g between two measurements. Before starting the desorption curve the samples were humidified at 97% RH until stabilization and then placed in different RH levels. A repetition of three samples per RH was realized to minimize variance of the results due to random error.

7.3.2. Dynamic vapour sorption-desorption test

The moisture buffering test was used to investigate the dynamics of moisture adsorption when the material is exposed to a change in vapour pressure from the surrounding environment. With a high buffering capacity, the material may have a positive influence to stabilize fluctuations in the internal environment of dwellings. Such behaviour is commonly allocated to hygroscopic porous building materials such as raw earth and also bio-based materials. The moisture buffering test consists of exposing a known surface of

the sample to fluctuating RH levels under isothermal conditions. Small samples of 120 mm x 60 mm with a thickness of 60mm were sealed with aluminium tape on all faces, only the top face was left exposed. The procedure of the Nordtest was followed (Rode et al., 2005), the samples were exposed during 8h to a RH of 75% then during 16h to RH of 33% at 23°C. The moisture buffering value (MBV) practical (1) could be calculated from stable cycles.

$$MBV_{practical} = \frac{\Delta m}{A.\Delta RH} \qquad \text{Equation 1}$$

Depending on the nature of the material stable cycles are reached more or less rapidly, those occur when the variation between initial and final mass in between cycles does not vary by more than 5%. In this case the stabilization occurred rapidly after 4 to 5 cycles. The samples were preconditioned at 50 %RH and 23 °C.

7.4. Procedure and experimental protocols of the mechanical tests

7.4.1. Sample conditioning

Lateritic stones are cut into seven small beams of dimension 240mm×60mm×60mm (L×b×d). Two of these beams designated as N1 and N2 were stored at 25°C and 50% relative humidity in a climate controlled chamber until the moisture equilibrium is attained. The average moisture content of N1 and N2 during the test was found to be around 2%. Two other beams designated as D1 and D2 were stored at 100-105°C for obtaining oven dry state. The remaining two designated as W1 and W2 were moisten by spraying known quantity of water and wrapped air tight before storing in the climatic chamber at 25°C. The moisture content of W1 and W2 during the test was found to be around 4%.

From the specimens tested for the flexural strength, largest rectangular shaped part is recovered and dressed to fulfil the aspect ratio; such that dimension of the test specimen is 120mm×60mm×60mm (h×l×b). Samples tested for compressive strength are stored and conditioned in similar conditions as described for flexural beam specimens.

7.4.2. Three point bending test

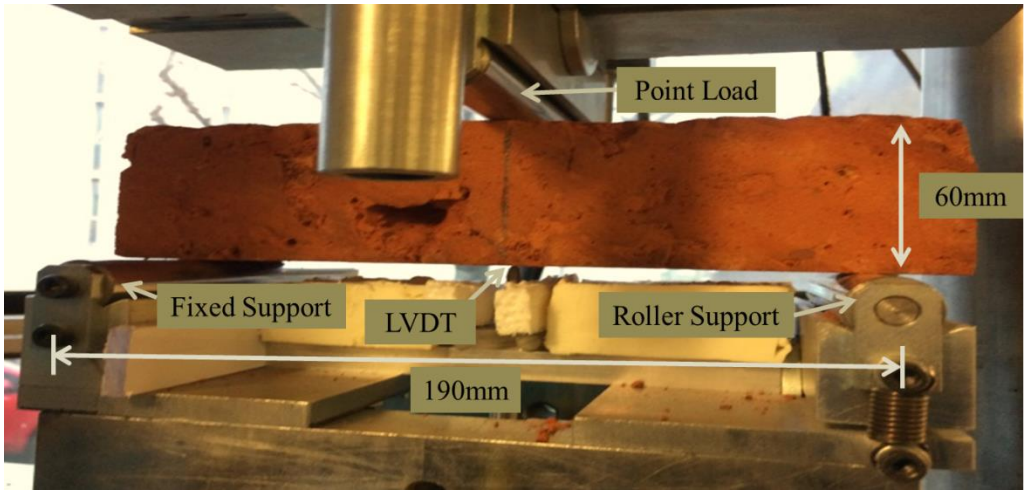

Figure 7-2 : Three Point Bending Test set up

Customized three point loading system is positioned on the uniaxial compressive testing frame. The base frame of the three point loading system has two adjustable supports (roller support at one end and hinge at the other end). Lateritic specimen of length 240mm is positioned on the supports with span of 190mm. Figure 7-2 shows the three point bending test setup for lateritic beam specimens. Beam displacement is measured using LVDT, which is placed below the point load where the maximum deflection occurs due to bending. Specimens in bending test are programmed to load at 5µm/s displacement controlled rate. Due to limited quantity of Lateritic stone blocks, flexural test are planned for three moisture content. Lime paste was used to prepare an even and smooth surface at LVDT point of contact.

7.4.3. Unconfined Compressive Test

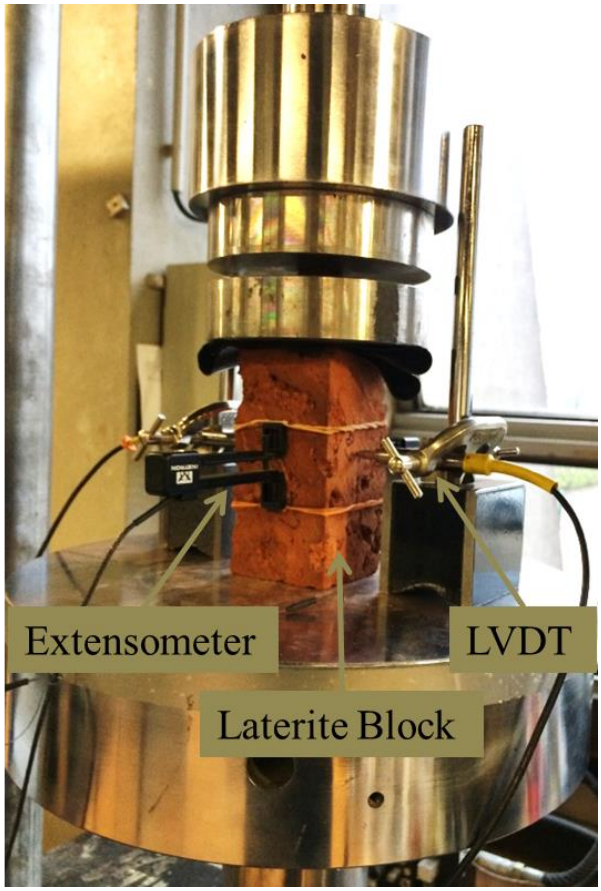

Figure 7-3 Compression Test Setup

In this study, it was decided to carry out unconfined compression test on the LBS because it gives the most accurate strength of the material [28,38,39]. The unconfined compression test setup of LBS specimen is shown in Figure 7-3. The compression test was programmed such that, the LBS specimens are subjected to repetitive cyclic loading at a loading cell controlled displacement rate of 5µm/s. The axial strain and lateral displacement of the specimen is measured using 22.5mm long extensometer and ±2.56mm long LVDT respectively. Considering potential heterogeneity of material, two extensometers are mounted on the opposite face of the specimen. Data from both the extensometers are analysed for any discrepancy. If the strains measured by both the extensometers are in accordance with each other, the average strain of two extensometer is taken as axial strain material as undergone. To avoid platen effect, extensometers are position at the 1/3rd height of the specimen. On the other two opposite faces, LVDT's are positioned at mid height of the specimen to measure the lateral displacement. Due to uneven surface, measurements of the LVDT's are not precise, hence the data of the lateral displacements are not presented in this analysis.

The elastic behaviour of the LBS is studied similar to USRE, by subjecting the specimens to cyclic loading at 5 pre-defined loads. To establish pre-defined loads, a laterite specimen with similar dimension was subjected to simple compressive test without cyclic loading at a controlled displacement rate of 20µm/s. The compressive strength at the failure of the material under compression was found to be 1.5MPa. Considering 1.5MPa as the material failure compressive stress, pre-defined loads at 20% (0.3MPa/1.08kN), 30% (0.45MPa/1.62kN), 50% (0.75MPa/2.72kN) and 70% (1.05MPa/3.78kN) of the failure compressive stress were chosen for cycles 2 to 5. While the first pre-defined load 0.1MPa (0.36kN) was restricted to the lowest possible stress the loading press can unload and reload without losing contact with the specimen.

For each pre-defined load (0.36kN, 1.08kN, 1.62kN, 2.72kN and 3.78kN), three repetitions of loading and unloading were followed before scaling up to the next pre-defined load. Only during the first cycle, the specimen was unloaded to 0kN this is to ensure that the LBS at very low stress completely regain strain undergone. From second pre-defined load (cycle 2), specimens were loaded until the defined maximum load for each cycle and unloaded until 0.36kN, this was repeated for each cycle. At the end of third repetition for cycle 5, test was programmed such that the specimen is loaded until failure.

7.5. Hydric characterization

7.5.1. Sorption-desorption isotherms

The experimental results of the measured mass variation are shown in Figure 7-4 as the moisture equilibrium points for the adsorption and the desorption curve. The difference between adsorption and desorption curves is the hysteresis loop. The International Union of Pure and Applied Chemistry (IUPAC) describe four types of hysteresis loops H1, H2, H3 and H4. The hysteresis loop observed for the lateritic stones is of H3 type. In Rouquerol et al. (Rouquerol, Rouquerol, & Sing, 1999) the H3 type hysteresis loop is described as resulting from aggregates of platy particles or adsorbents containing slit-shaped pores.

The error bars represented in Figure 7-4 represents the variation within at least 3 samples measured per RH. It is common to have greater uncertainty at higher humidity levels as seen in this case.

In Figure 7-4, the sorption isotherm of the Lateritic samples is compared with a soil used as unstabilised rammed earth (St Antoine) and a Stabilized Rammed Earth (SRE). The data

for the SRE sample was taken from Hall and Allinson (2009), the desorption data was ignored as only a very small hysteresis could be observed. The 433 mix corresponds to a SRE mix containing 4 volumes of gravels, 3 volumes of sand and 3 volumes of silty clay. The sorption isotherms of the lateritic material show strong adsorption capacity compared with the rammed earth materials, see Figure 7-4.

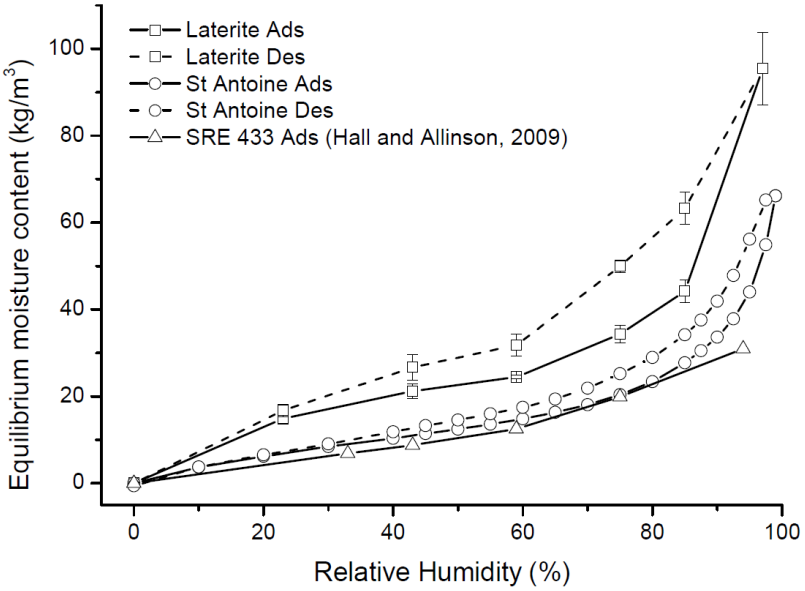

Figure 7-4 : Adsorption (Ads) and Desorption (Des) isotherms (SRE: Stabilized Rammed Earth, 433 samples from Hall and Allinson, 2009 (Hall & Allinson, 2009)**)**

7.5.2. Moisture Buffering Value Test

Figure 7-5, shows the results of the moisture buffering test. Data points are the average of the results of three samples. The error bar is a simple representation of the standard deviation within the results of the three samples. The results are compared with unstabilised earth (St Antoine) used for a rammed earth building and the SRE sample from Allinson et Hall (Allinson & Hall, 2012). The lateritic sample has a very high adsorption compared to the earth samples.

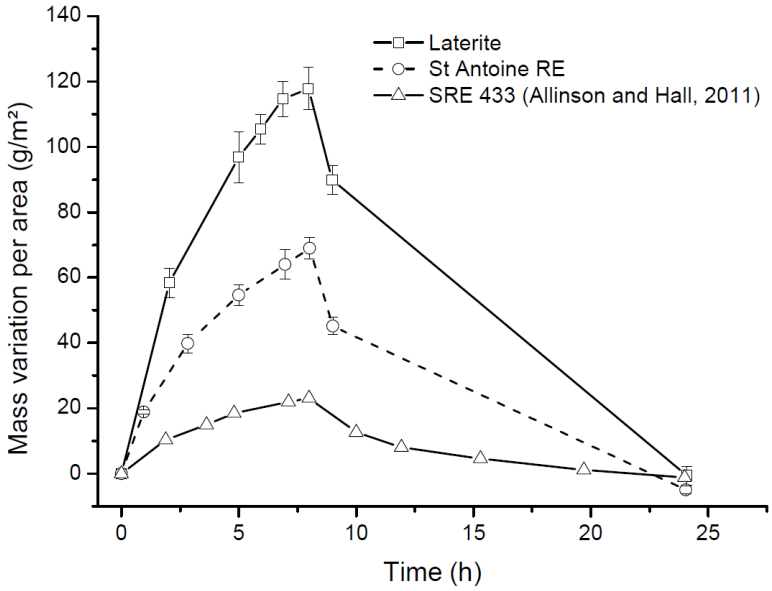

Figure 7-5: Moisture buffering test

From the experimental curve the $MBV_{practical}$ can be calculated according to equation 1. From the data of the three samples the maximum value after 8h of adsorption varies between 111 and 124 g/m². Therefore the MBV varies between 2.65 and 2.95 g/(m².%RH). In the classification proposed in (Rode et al., 2005) the lateritic building stones would therefore classify as excellent buffering materials.

7.6. Mechanical characterization

7.6.1. Three point bending test

As briefed earlier, in the flexural testing, beam deflection is measured by the LVDT positioned right below the load point. Point load is measured in Newton [N], and the deflection is measured in mm. From theory of bending, the equations to calculate flexural stress in MPa and Strain are given below.

$$\sigma_{xx} = \frac{3\,P\,L}{2\,b\,d^2} \qquad \text{Equation 2}$$

$$\varepsilon_{xx} = \frac{6\,d\,\delta}{L^2} \qquad \text{Equation 3}$$

With σ_{xx} : the flexural stress or modulus of rupture in [MPa], P : point load in [N], L : length of the beam span (in mm), b : breadth of the beam (in mm), d: depth of the beam (in mm), ε_{xx} : longitudinal strain (in mm/mm), δ : deflection of the beam under point load (in mm).

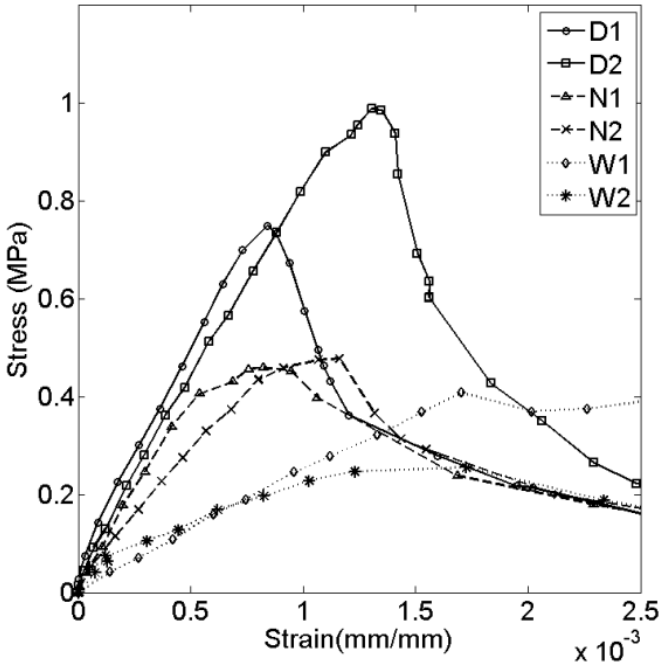

Figure 7-6: Flexural stress- strain of lateritic specimens

From the load and deflection data obtained during the test, the flexural stress-strain characteristics of the lateritic stone beams in 3 points bending test is plotted as shown in Figure 7-6. 'N' representing series exposed to ambient atmosphere with internal moisture of 2%, 'D' representing series with dry state specimens and 'W' representing specimen with average moisture content of 4% during the test. As predictable, specimen with low moisture content exhibits higher flexural strength characteristics. The average flexural strength of the lateritic specimens at ambient condition is found to be 0.49MPa. There is a tendency of decrease in flexural strength of the material with increase in moisture content as shown in Figure 7-7. The average flexural strength of the lateritic specimen at 4% moisture content is 40% of the dry state flexural strength. The average flexural modulus of the laterite in ambient condition is calculated to be 650MPa; the flexural modulus of the material is calculated by plotting the best fit linear secant tangent up to rupture of the material. Results of flexural properties of laterite stone beam are presented in Table 7-1.

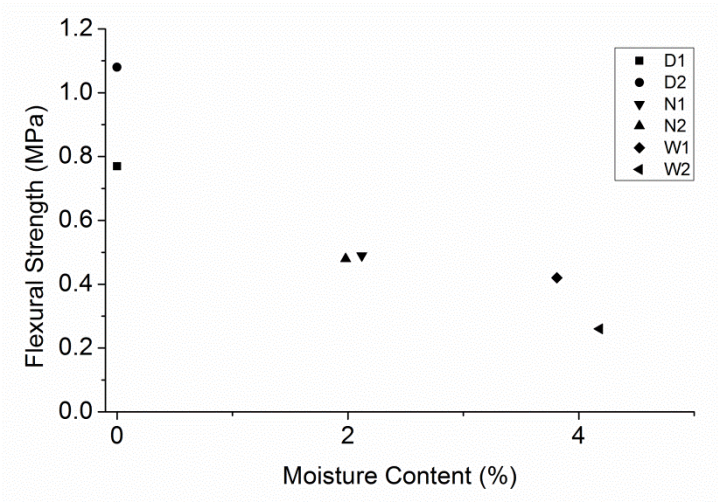

Figure 7-7 : Variation of Flexural Strength with change in Moisture at test

Table 7-1 - Flexural Property of Laterite Stone Beam

Flexural test	Storage	Water Content [%]	Loading rate [µm/s]	Max Load [N]	Flexural Strength, MPa	Flexural Modulus, MPa
D1	100°C	0	5µm/s	573.5	0.77	880
D2		0		750	1.08	780
average	-	-	-	-	0.93	830
N1	25°C, 50% RH	2.1%	5µm/s	333	0.49	800
N2		2.0%		362	0.48	510
average	-	2.0%	-	-	0.49	650
W1	25°C	3.8%	5µm/s	310	0.47	230
W2		4.2%		189	0.26	190
average	-	4.0%	-	-	0.37	210

7.6.2. Compressive Strength

The compressive stress strain characteristics of the laterite specimen tested in unconfined compression test are shown in Figure 7-8. The compression test was carried out on 6 specimens, 2 specimens each in 'N', 'D' & 'W' series. The average compressive strength of the laterite stone specimen exposed to ambient environment is found to be 2.4MPa, and its secant modulus at peak is 2470MPa. The summary of compressive test results is given in Table **7-2**. Similar to earthen construction materials, compressive strength of the laterite stone decreases with increase in moisture content as shown in Figure 7-9. The average compressive strength of the laterite stone specimen with 4% moisture content is found to be 55% of its dry compressive strength.

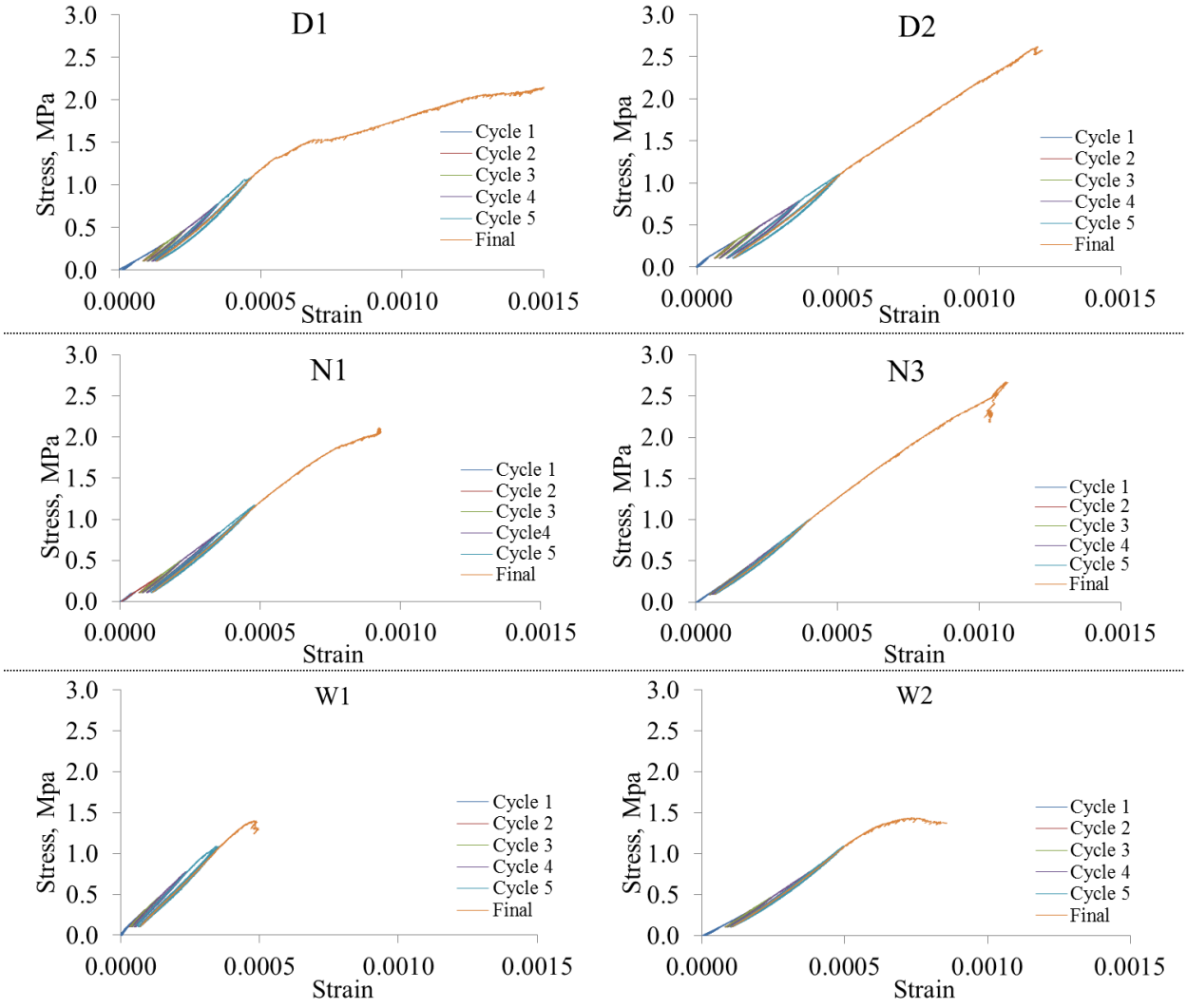

Figure 7-8- Stress-Strain Graph of Compression Test

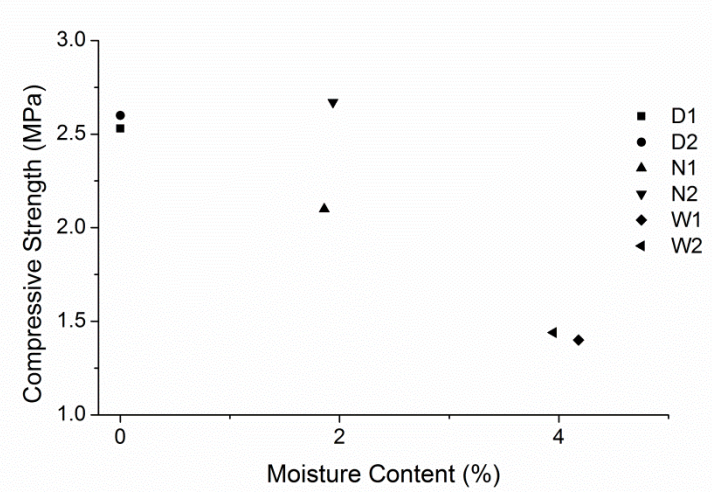

Figure 7-9: Variation of Compressive Strength with Moisture

Table 7-2- Results of Compression Test

Compression Test	Storage	Water Content	Compressive Strength, MPa	Secant Modulus (Peak), MPa
D1	100 °C	0	2.5	2220
D2			2.6	2150
average	-	0	2.6	2190
N1	25 °C & 50% RH	1.9%	2.1	2460
N2		1.9%	2.7	2490
average	-	1.9%	2.4	2470
W1	25 °C	4.2%	1.4	2970
W2		4.0%	1.4	2160
average	-	4.1%	1.4	2560

7.6.3. Young's modulus

Cyclic loading is very helpful in understanding the elastic behaviour of the material, in this analysis to calculate the elastic modulus (secant), best fit linear line is drawn to each cycles (including 3 repetitions) as shown in Figure 7-10, where all the cycles are shown. The secant modulus of the first cycle is called as the initial secant modulus, which is low compared to cycles (2-5), this may be attributed to the closer of micro cracks in the material. Figure 7-11 shows the secant modulus of samples at various stages during loading. The variation of the secant modulus between cycles 2-5 is less and exhibits linearity. The average cyclic (2-5) secant modulus of dry (D) and ambient (N) condition varies in between 2600MPa to 2800MPa (Figure 7-12). In Figure 7-12, initial secant modulus, average of secant modulus of cycles 2, 3, 4 and 5 and secant modulus at peak are plotted against the variation of moisture. The behaviour of moist samples doesn't provide convincing information. The variation between initial secant modulus and secant modulus at peak is seen to be negligible (less than 10%) for dry and ambient condition; this may suggest secant modulus at peak can be considered for analysis (given in Table 7-2). It should also be noted that the secant modulus at dry and ambient condition doesn't vary much, so the assumption of linear behaviour seems to be correct for this kind of material, if water content remains limited.

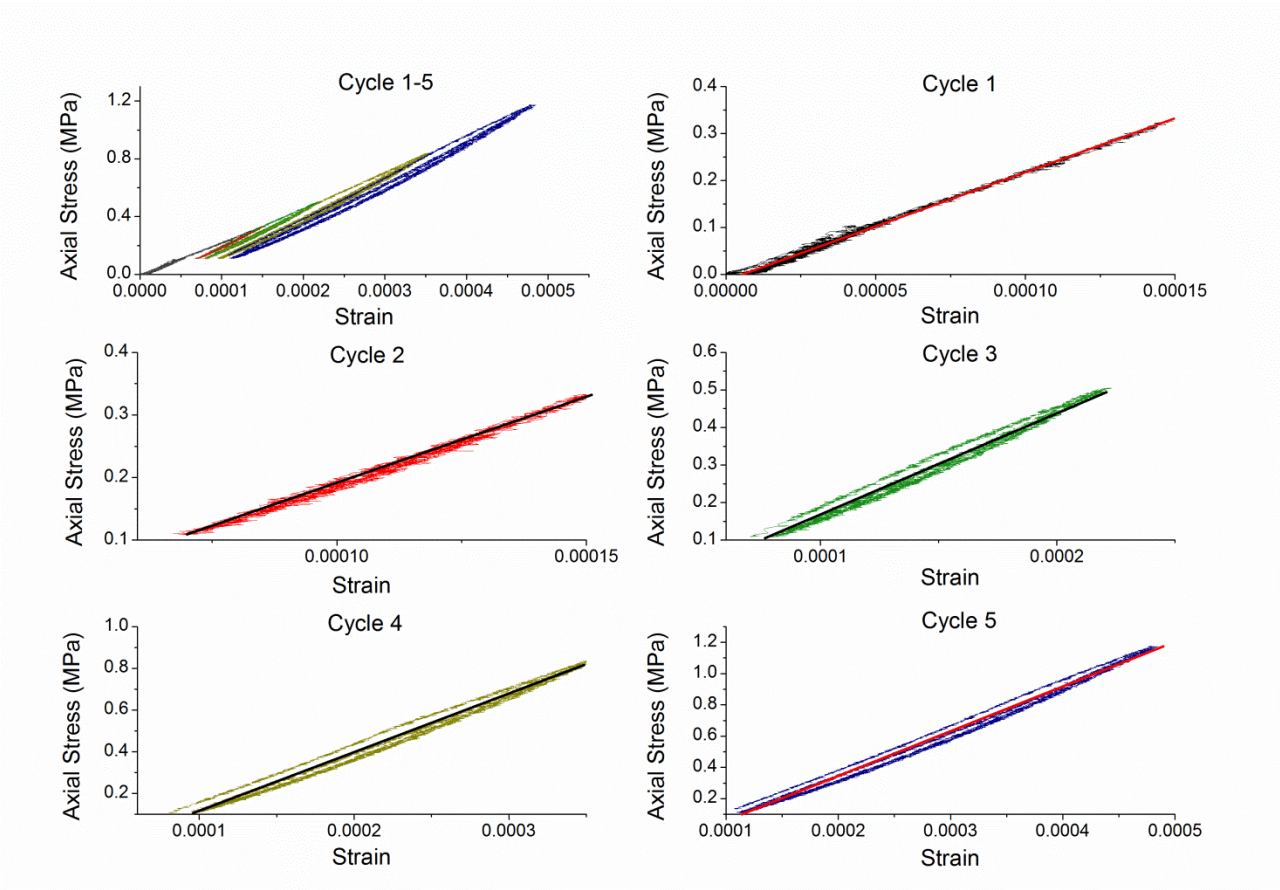

Figure 7-10 : An Example of Linear Elastic behaviour of Laterite Stone Specimen

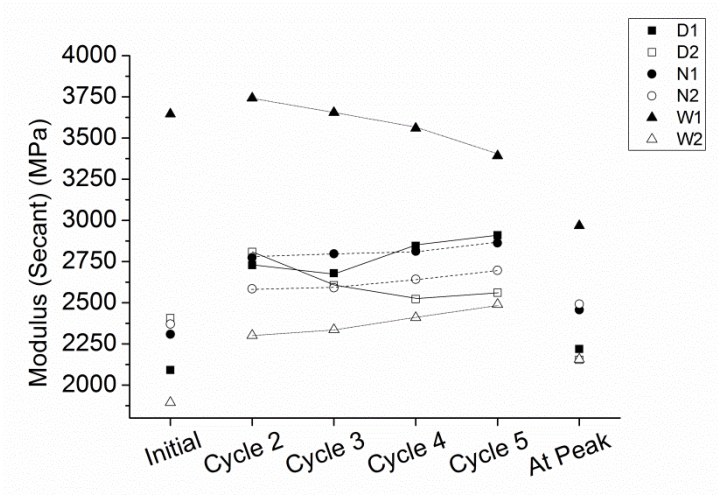

Figure 7-11: Variation of Modulus at each cycle

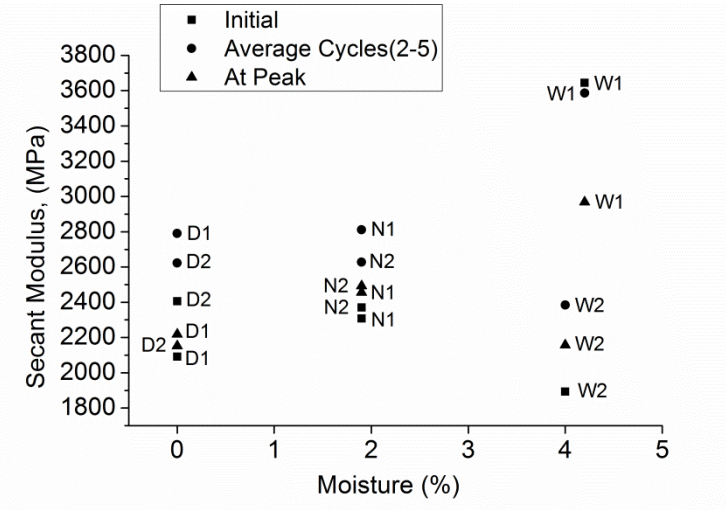

Figure 7-12: Change of secant modulus and average cyclic modulus with change in moisture

7.6.4. Irreversible strain

From cyclic loading it was observed that the material exhibits residual strain after reaching 1.08kN load (cycle2). In the first cycle, material completely regains its straining showing perfect elasticity. From second cycle, when material is loaded to 1.08kN and above, material does not regain its original shape upon unloading exhibiting irreversible straining. Though LBS exhibits hysteric loop during unloading and reloading, from Figure 7-10, it can be said the hysteric loop created is very small and negligible. The cyclic unloading and reloading is nearly linear, and for simplifying the analysis in this study linear variation is considered. To calculating elastic strain (ε_e) recovery and irreversible strain (ε_{ir}), the last known strain upon unloading of each cycle is linearly extended on to the x-axis as shown in Figure 7-13. The point of intersection on the x-axis is considered as the irreversible strain material has undergone for that respective cycle. The maximum strain material has undergone for each cycle at its maximum stress is taken as ε_t. The ratio of irreversible strain (ε_{ir}) to total strain (ε_t) of each cycle is taken as the percentage of irreversible strain material has undergone for a cycle. The percentage of irreversible strain LBS specimens has undergone is shown in Figure 7-14. Specimens D1 & W2 has wide spread of irreversible strain, it was observed these specimens have prolonged straining before failure, whereas the other specimen showed brittle failure nature. Though it is difficult to quantify the plasticity of the material, in general it can be said that material shows less than 20% of irreversible strain property. This information adds value to the assumption of linear behaviour. The maximum stress and strain values of the laterite test specimens are given in Table 7-3.

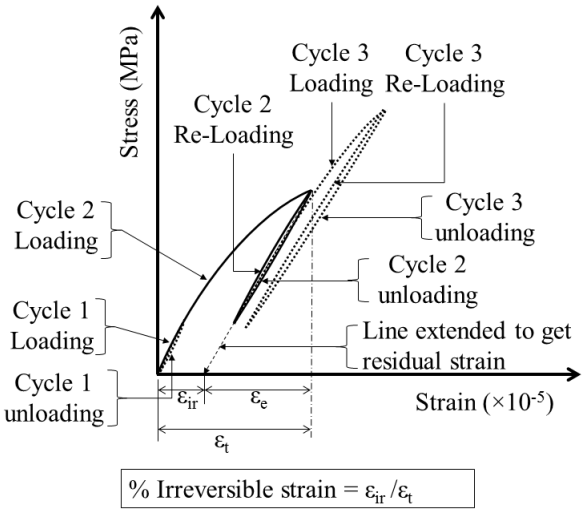

Figure 7-13: Graphical explanation for calculation of irreversible strain

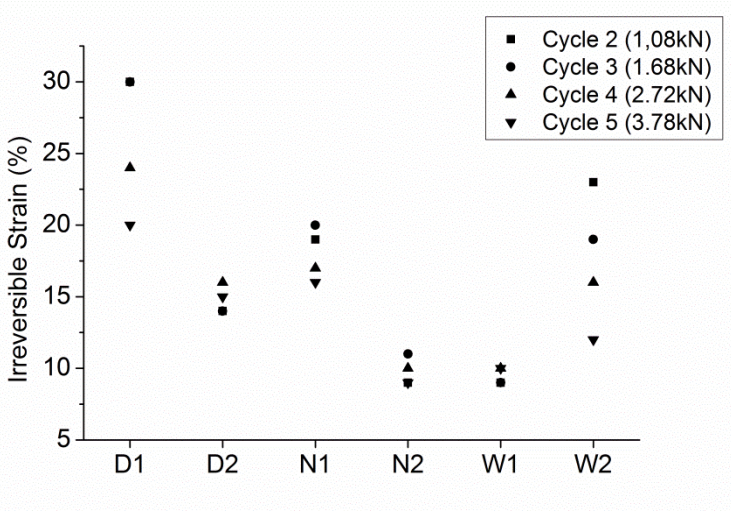

Figure 7-14: Percentage of Irreversible strain with respect to cycles (load)

Table 7-3: Failure Stress - Strain

Laterite Specimen	Moisture [%]	stress at failure σ(max), MPa	Strain at failure ε, [10^-5]
D1	0	2.5	160
D2	0	2.6	120
N1	1.9	2.1	90
N2	1.9	2.7	110
W1	4.2	1.4	50
W2	4.0	1.4	90

7.7. Discussion

The first remarks can be made on the highly hygroscopic characteristics of the material. Sorption isotherms exhibit a strong hysteresis and between 20 to 40 kg/m^3 water content in the middle range of relative humidities. In this study the laterite samples compared with rammed earth samples present higher hygroscopic water adsorption characteristics. The moisture buffering results show the same trend with a dynamic adsorption at least twice the values of the rammed earth samples and comparable to those obtained for unfired clay bricks (McGregor, Heath, Fodde, & Shea, 2014).

The corresponding calculated MBV is 2.8 g/m².%RH for 75%/33% RH cycles. MBVs over 2 g/m².%RH are considered as excellent moisture buffering materials. From these results it can be concluded that the material can have a positive impact on indoor air quality. Any exposed surface will act as a passive climate regulator. This potential has previously been described for other building materials (Padfield, 1998). It can however be discussed if such behaviour would also be effective in tropical climates where Laterite stones can usually be found. A study using simulation tools to access the influence of the building envelope on the interior climate in tropical climate conditions shows that the addition of hygroscopic materials lowers the interior RH peaks (Künzel, Holm, Zirkelbach, & Karagiozis, 2005).

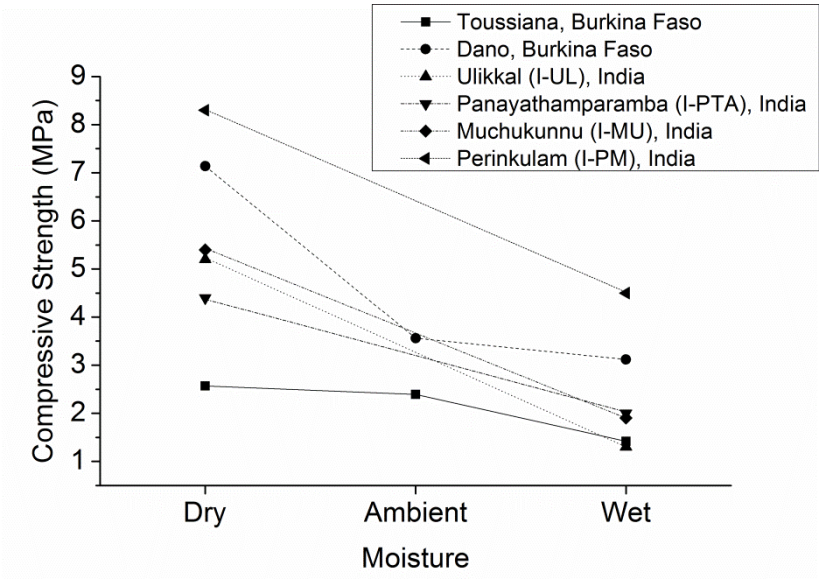

Figure 7-15: Variation of compressive strength of Laterite (different quarries) with moisture

Compressive strength of porous material varies with change in moisture condition. Experimental results show that, the compressive strength of LBS reduces with increase in the moisture content. In Figure 7-15, the compressive strength at different moisture state of laterite blocks from Dano, Burkina Faso (Abdou Lawane et al., 2011) and Malabar region, India (A K; Kasthurba et al., 2015) are presented along with the LBS (Toussiana) experimental results obtained from this study. Ulikkal (I-UL), Panayathamparamba (I-PTA), Muchukunnu (I-MU) and Perinkulam (I-PM) are different quarries of laterite blocks in Malabar region, India (A. K. Kasthurba et al., 2007; A K; Kasthurba et al., 2015). Wet compressive strength of laterite blocks from Malabar region in between 25%-54% of its dry compressive strength, the variation in compressive strength depends on the quarry and composition of rock (A. K. Kasthurba, Santhanam, & Achyuthan, 2008). The dry, ambient and saturated compressive strength of laterite blocks from Dano, Burkina Faso (Abdou Lawane et al., 2011) are shown in Figure 7-15, it has to be noted that, the aspect ratio (J. Morel et al., 2007) of the test specimens in this case were less than 2, hence compressive strength of laterite blocks from Dano, Burkina Faso might require coefficient of correction. The ambient compressive strength of laterite block (Dano) is 50% of its dry state, whereas the tested material from Toussiana losses only 7% of its dry compressive strength at ambient condition. In both cases, moisture at ambient condition is around 2%. Wet compressive strength of laterite blocks (Dano) is 45% of its dry compressive strength. In general, it can be said that the wet or saturated compressive strength of laterite stones is 40%-50% of its dry compressive strength.

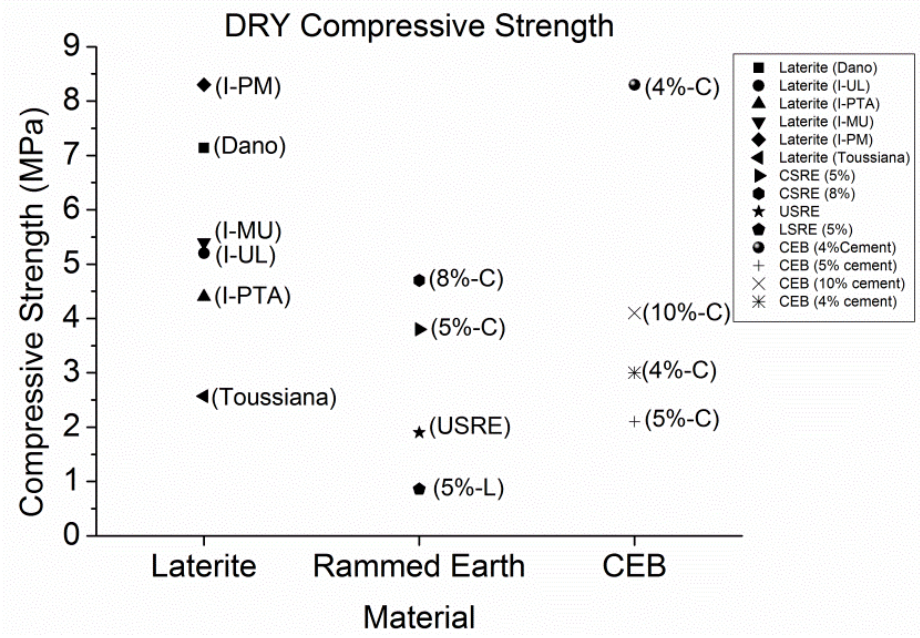

Figure 7-16: Comparison of compressive strength of Laterite, Rammed earth, CEB at dry state.

Compressive strength of a building material is one of the decisive factors in recommending its suitability as an alternative construction material. In this analysis for comparison, stabilised compressed earth block (CEB) (J. Morel et al., 2007; Reddy & Hubli, 2002; Reddy et al., 2007; P Walker & Stace, 1997), cement stabilised rammed earth (CSRE) (B. V. Venkatarama Reddy & Prasanna Kumar, 2011b), lime stabilised rammed earth (LSRE)(D. Ciancio, Beckett, & Carraro, 2014), and unstabilised rammed earth (USRE) (Q. Bui et al., 2014) are considered. The dry and wet compressive strength of the materials are considered and plotted as shown in Figure 7-16 & Figure 7-17. The dry compressive strength of the rammed earth varies between 1-5MPa, the compressive strength of the USRE being the lowest, with increase in the percentage of cement and lime content there is increase in strength. Similarly compressive strength of stabilized CEB varies between 2-8MPa, depending upon the percentage of cement and clay in the soil(Reddy et al., 2007). In the case of laterite, dry compressive strength varies from 2.5-8.3MPa depending on the quarry and its chemical and mineral composition, the material tested in this study exhibits 2.6MPa as the average dry compressive strength.

In general wet compressive strength of stabilised rammed earth and stabilised CEB losses 50% of its dry compressive strength, similar to the case of LBS. As shown in Figure 7-17, wet compressive strength of rammed earth is in between of 0.5-2.3MPa, and that of CEB is in between 1.2-3.2MPa. It is interesting to see that the wet compressive strength of

laterite also varies in the range of 1.4-3.2MPa; the material tested in this study has an average wet compressive strength of 1.4MPa.

This shows that the dry & wet compressive strength of LBS is similar to stabilized earth materials. According to (Maignien, 1966) the induration process of laterite soils involves the crystallisation of iron oxide minerals cementing the aggregates over a more or less long period of time. A further physico-chemical study of the nature of this induration may allow its comparison and potentially replicate the process to the stabilisation of earth materials. Compared to the stabilisation of earth materials the natural induration of laterite soils has no environmental impact yet the use of laterite stones involves extraction and transport from the quarry to the building site and therefore increasing its environmental impact compared to unfired earth. It is interesting to note that the mechanical characteristic of laterite varies with quarry, region, and nature of deposits. The variation of strength with quarries might be attributed to change in the chemical and mineral composition during induration process. To understand how laterite stone gains its strength, a detail mineral and chemical analysis has to be carried out.

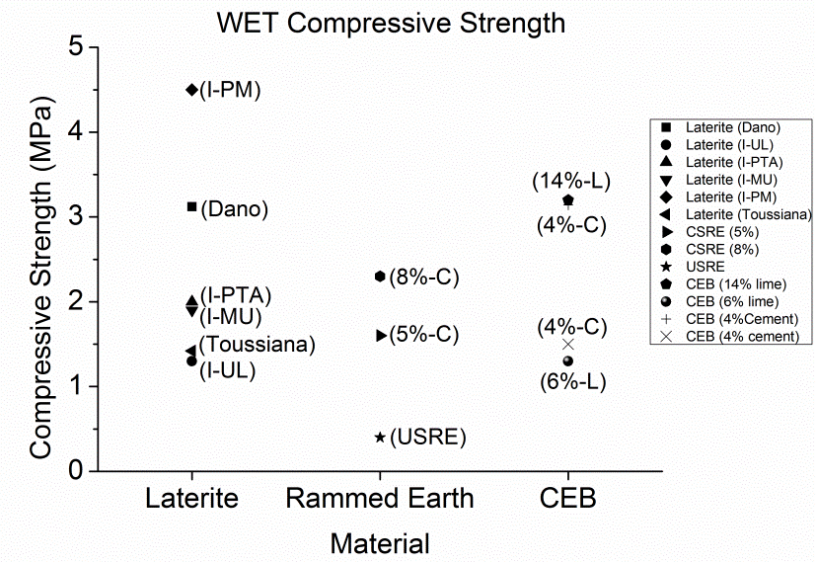

Figure 7-17: Comparison of compressive strength of Laterite, Rammed earth, & CEB at saturated / wet state.

The experimental procedure adopted in this study effectively utilises the specimens to study flexural and compressive strength properties of LBS along with the hygro-thermal properties. By inducing loading and unloading cycles, the material elastic properties can be also extracted along with compressive strength. From compressive stress strain characteristics the damage and irreversible strain material has undergone can also be

analysed, thanks to cyclic loading and unloading. It is also recommended to study the tensile and shear strength of LBS.

7.8. Conclusion

The experimental investigations on LBS from Toussiana, Burkina Faso are performed to study its hygroscopic and mechanical parameters. From sorption isotherm hysteresis and dynamic adsorption tests, laterite exhibits strong hygroscopic characteristics with MBV of 2.8 g/(m².%R.H). From three point bending and unconfined compression test at different moisture state, it was observed that the flexural strength and compressive strength of the LBS decreases with increase in moisture content. The flexural and compressive strength of the LBS at ambient conditions was found to be 0.55MPa and 2.4MPa respectively. Though the strength decreasing tendency is found with moisture, there is need for more experimental investigation to propose correlation of strength with moisture variation. From compressive stress strain analysis, the average secant modulus of the specimens at ambient condition was found to be 2470MPa and the irreversible strain was found to be 20% of maximum strain. It was also seen that that the mechanical properties of LBS varies with quarry and region, hence it is highly recommended to study mechanical properties of laterite from each quarry. Further studies on chemical and mineral analysis of laterite would provide comprehensive analysis of LBS.

8. General Conclusion

This experimental work focuses on building an experimental procedure to study the mechanical characteristics of unstabilised rammed earth (USRE) and laterite building stones (LBS). The procedure involves specimen manufacturing, conditioning, testing under compression, tension, shear and flexure. This complete experimental investigation is necessary to understand USRE and LBS material characteristics. The summary of the recommended experimental procedure is briefed below.

8.1. Specimen preparation and conditioning

USRE: Replicating in-situ USRE wall properties is important, the parameters that influence in-situ parameters are dynamic compaction (ramming), manufacturing water content, layer thickness and width. In laboratory, Proctor method of manufacturing specimens has close resemblance to in-situ practice, therefore cylindrical specimens with three different compaction energies are manufactured using Proctor method. Two locally available soils (CRA and Dagneux) are used in this investigation, CRA exhibited shrinkage cracks which is consistent with the in situ material which also exhibits shrinkage cracks.

LBS: LBS are mechanically cut into small beams for flexural test and recovered rectangular prisms are prepared for compression test.

Conditioning: The specimens in the laboratory should be stored in a climatic room, where the temperature and relative humidity is constantly monitored in order to ensure that all the specimens tested will have similar properties during the test. In this work both USRE and LBS specimens were stored in a climate controlled room at 25° C and 50% RH. For laterite the sorption-desorption curve and moisture buffering value are also analysed to obtain their moisture ingress property.

8.2. Compressive test

The compressive strength of earthen material is one of the most important parameters, to be used for design. In this program the compression test for both USRE and LBS are programmed such that, the compressive stress strain characteristics of both the materials are studied along with the compressive strength.

The compressive stress stain characteristics of USRE and LBS are studied by subjecting the specimens under cyclic loading and unloading, this will also enable to study the materials non-elastic behaviour. The local strain of the material is analysed with the

help of extensometers that are mounted on the specimen surface. The cyclic loading and unloading at 10%, 20%, 35% and 50% of failure compressive stress are adopted for USRE. In case of laterite the repetitive cyclic loading and unloading are carried out at <10%, 20%, 30%, 50% and 70% of failure compressive stress. The parameters studied in cyclic loading and unloading cycles can be used in numerical modelling considering the elasto-plastic behaviour.

For CRA specimens, the analysis of stiffness parameters is difficult due to presence of shrinkage cracks. Therefore in presence of cracks the strain measurements using extensometers are inconsistent or non-repetitive. Even though there are shrinkage cracks, the compressive strength of CRA specimens is found to be more reliable, as the compressive strength of the specimen is a mean or global measurement of the specimen.

From initial tangent modulus and cyclic modulus, the damage of material was observed in case of Dagneux, whereas for LBS the degradation of stiffness remained constant during cyclic loading. From cyclic loading and unloading LBS exhibits less than 20% irreversible strain, and the variation of initial tangent modulus and secant modulus of LBS is negligible. The cyclic loading and unloading of the USRE and LBS will help in extracting important stiffness parameters, hence it is highly recommended to test such material with cyclic loading. With the help of LVDT's the coefficient of Poisson was measured to be in between 0.2 – 0.25 for USRE (both soils).

The USRE cylindrical specimens manufactured at different compaction energies will have different dry densities. The influence of compaction energy and dry densities was also studied in this work. It was found that the compressive strength of CRA and Dagneux from normal Proctor energy to modified Proctor energy increased by 40% and 112% respectively. Hence due importance should be given to compaction energy while manufacturing USRE soil specimens and its influence on mechanical parameters should be studied.

In case of LBS, the compressive strength variation with respect to moisture content in the material is studied. The compressive strength of the LBS was found to be decreasing with increase in the moisture content, the wet (4% moisture) compressive strength of the LBS was found to be 55% of its dry compressive strength.

8.3. Interface strength

The shear behaviour of USRE which acts as a monolithic structure is critical especially under lateral loads. From shear test on small walls (wallets), it was observed that the failure of wall can take place due to delamination of layer interface (Cheah et al., 2012; P. A. Jaquin et al., 2006; Miccoli, Oliveira, et al., 2014; R.A Silva et al., 2014). Research work by (Q.-B. Bui & Morel, 2009; P. A. Jaquin et al., 2006; Rui A Silva et al., 2014) identifies the lack of experimental investigation on USRE interface strength parameters and its necessity in numerical modelling.

This study presents a novel experimental approach to study the USRE interface strength parameters using metallic wedges that can support specimens in an axial compression press. The metallic wedges are designed such that, they support the rectangular prism specimens at an inclination to the vertical loading axis, there by inducing normal and tangential load on the layer interface of the specimen. Metallic wedges at three different inclinations (20°, 30° and 45°) with respect to vertical axis is designed and used in this study. The failure normal and tangential stress at these three inclinations will help to plot the Coulomb's failure criteria and obtain interface strength parameters. From this experimental investigation the interface strength parameters such as cohesion and angle of friction of CRA were found to be 57kPa and 43°, and for Dagneux it was 144kPa and 32°.

It was also noticed that interface strength parameters can be enhanced by changing the interface surface texture. The rough indentation on the interface surface increases the cohesion twice that of smooth surface, while change in angle of friction is negligible. To validate the influence of interface surface texture on the interface strength parameters, more experimental investigation is needed.

The advantage of this procedure is:

- It can be easily mounted on an axial compression press, hence reducing the cost incurred.
- It can be designed for more angle of inclinations, which helps to interpret coulomb's failure criteria.
- The size of the specimens is drastically reduced in comparison to wallets tested under diagonal compression test.
- Since it consumes less space and device is portable, it can be used in any laboratory with basic facilities.

- Use of DIC helps in observing material behaviour and study interface failure mechanism.

8.4. Tensile test

Tensile strength of the USRE cylindrical specimens are studied from split tensile test. The cylindrical specimens are manufactured in manual Proctor method, and stored in the climate chamber similar to that of compressive test specimens. It is recommended to test specimens with dry densities similar to compressive test, and also have same moisture at test (conditioning), this will help to correlate the tensile strength in terms of compressive strength.

8.5. Flexural test

USRE: The rectangular prism specimens (single layer) recovered from the USRE interface test was subjected to four point bending test. The test was carried out at two different moisture contents namely oven dry state and ambient state (25° C &50% RH). The flexural strength of the specimen with respect to dry density and moisture at test are analysed. The flexural strength of USRE at different dry densities has to be studied, so that the in design consideration knowing compressive strength at a given dry density can lead a way to relate flexural strength as well.

LBS: Mechanically cut small laterite beam specimens are subjected to three point bending test to study their flexural properties. The flexural strength and flexural modulus of LBS at three different moisture contents are studied. Similar to the compressive behaviour of LBS the flexural strength of the LBS was reducing with increase in moisture at test. Since LBS is a porous building material, it is important to study the flexural and compressive strength of LBS at different moisture contents.

For earthen building material study of compressive, tensile, shear and flexural strength is important, and all the parameter should be comparable, that is possible only if the dry density and moisture at test is similar. To obtain similar dry densities, manufacturing procedure of specimens is critical and at the same time replicating in-situ characteristics is also important. Replicating USRE in-situ methodology in manufacturing laboratory specimens is difficult, but specimen's manufactured using Proctor method can have closer resemblance to the in-situ condition given its dynamic ramming process and layered structure. Though Proctor method is not suitable for soil specimens with shrinkage cracks as they interfere in the analysis of stiffness parameters, its reliability in measuring compressive strength seems to be accurate. Proctor test needs further investigation to prove

its accuracy in resembling in-situ characteristics. Comparing results of Proctor specimens with wallets and full scale walls will help to build confidence, but at present Proctor method is one of the best methods to manufacture USRE specimens. To obtain similar moisture at test, specimen conditioning becomes important, and monitoring the temperature and relative humidity is highly recommended.

Reference

Adorni, E., Coïsson, E., & Ferretti, D. (2013). In situ characterization of archaeological adobe bricks. *Construction and Building Materials*, *40*, 1–9. http://doi.org/10.1016/j.conbuildmat.2012.11.004

Alley, P. (1948). Rammed Earth construction. New Zealand Eng 1948. *New Zealand Engineering*, *3*(6), 548.

Allinson, D., & Hall, M. (2012). Humidity buffering using stabilised rammed earth materials. *Proceedings of the ICE - Construction Materials*, 1–10. http://doi.org/10.1680/coma.11.00023

Araki, H., Koseki, J., & Sato, T. (2011). MECHANICAL PROPERTIES OF GEO-MATERIALS USED FOR CONSTRUCTING EARTHEN WALLS IN JAPAN. *Builletin of ERS, Institute of Industrial Science, University of Tokyo*, (44), 101–112.

ASTM-D-2216-98. (1998). *Standard Test Method for Laboratory Determination of Water (Moisture) Content of Soil and Rock by Mass*. *ASTM International*. West Conshohocken, PA,.

ASTM C496/ C496M. (2004). *Standard Test Method for Splitting Tensile Strength of Cylindrical Concrete*. *ASTM International*. West Conshohocken, PA,.

ASTM D1557-12. (2012). *Standard Test Methods for Laboratory Compaction Characteristics of Soil Using Modified effort*. *ASTM International*. West Conshohocken, PA,.

ASTM D5298-03. (2003). *Standard Test Method for Measurement of Soil Potential (Suction) Using Filter Paper* (Vol. 11).

ASTM D698-12e2. (2012). *Standard Test Methods for Laboratory Compaction Characteristics of Soil Using Standard Effort*. *ASTM International*. West Conshohocken, PA,.

ASTM D 1635. (2000). *Standard Test Method for Flexural Strength of Soil-Cement Using Simple Beam with*. *ASTM International*. West Conshohocken, PA,: ASTM International.

Aubert, J. E., Fabbri, a., Morel, J. C., & Maillard, P. (2013). An earth block with a compressive strength higher than 45MPa! *Construction and Building Materials*, *47*,

366–369. http://doi.org/10.1016/j.conbuildmat.2013.05.068

Aubert, J. E., Maillard, P., Morel, J. C., & Al Rafii, M. (2015). Towards a simple compressive strength test for earth bricks ? *Materials and Structures*, *49*(APRIL), 1641–1654. http://doi.org/10.13140/RG.2.1.4641.4242

Aubert, J. E., Marcom, A., Oliva, P., & Segui, P. (2015). Chequered earth construction in south-western France. *Journal of Cultural Heritage*, *16*(3), 293–298. http://doi.org/10.1016/j.culher.2014.07.002

Beckett, C. (2011). *The role of material structure in compacted earthen building materials: Implications for design and construction*. Durham university.

Beckett, C., & Ciancio, D. (2014). Effect of compaction water content on the strength of cement-stabilized rammed earth materials. *Canadian Geotechnical Journal*, *51*(5), 583–590. http://doi.org/10.1139/cgj-2013-0339

Bicalho, K. V, Correia, A. G., Ferreira, S. R., Fleureau, J.-M., & Marinho, F. A. M. (2007). Filter paper method of soil suction measurement. *Proceedings of 13th Panamerican Conference on Soil Mechanics and Geotechnical Engineering, Isla Margarita, Venezuela*, 215–219. Retrieved from http://repositorium.sdum.uminho.pt/handle/1822/12305

Bolton, M. (2001). *Manual for The Constuction of A Simple Building Using The Rammed Earth Technique*. MIDRAND: CSIR.

Bruno, A. W., Gallipoli, D., Perlot, C., Mendes, J., & Salmon, N. (n.d.). MECHANICAL PROPERTIES OF UNSTABILIZED EARTH COMPRESSED AT HIGH PRESSURES. In *Proceedings 1st International Conference on Bio-based Building Materials*. Clemont-Ferrand, France.

Bruno, A. W., Gallipoli, D., Salmon, N., Bruno, A. W., Gallipoli, D., & Mendes, J. (2015). Briques de terre crue : procédure de compactage haute pression et influence sur les propriétés mécaniques. In *33èmes Rencontres de l'AUGC, ISABTP/UPP, Anglet*. http://doi.org/hal-01167676

BS 1377-2. (1990). *Soils for Civil Engineering Purposes - PArt 2: Classification tests*. *British Standard*.

Bui, Q.-B., Morel, J.-C., Hans, S., & Meunier, N. (2008). Compression behaviour of non-

industrial materials in civil engineering by three scale experiments: the case of rammed earth. *Materials and Structures*, *42*(8), 1101–1116. http://doi.org/10.1617/s11527-008-9446-y

Bui, Q.-B., & Morel, J. J. C. (2009). Assessing the anisotropy of rammed earth. *Construction and Building Materials*, *23*(9), 3005–3011. http://doi.org/10.1016/j.conbuildmat.2009.04.011

Bui, Q. B., Morel, J. C., Reddy, B. V. V., Ghayad, W., Venkatarama Reddy, B. V., & Ghayad, W. (2009). Durability of rammed earth walls exposed for 20 years to natural weathering. *Building and Environment*, *44*(5), 912–919. http://doi.org/10.1016/j.buildenv.2008.07.001

Bui, Q., Morel, J., Hans, S., & Walker, P. (2014). Effect of moisture content on the mechanical characteristics of rammed earth. *Construction and Building Materials*, *54*, 163–169.

Bui, T.-T., Bui, Q.-B., Limam, a., & Maximilien, S. (2014). Failure of rammed earth walls: From observations to quantifications. *Construction and Building Materials*, *51*, 295–302. http://doi.org/10.1016/j.conbuildmat.2013.10.053

Bulut, R. (1996). *A re-evaluation of the filter paper method of measuring soil suction*. Texas Tech University.

Cabeza, L. F., Barreneche, C., Miró, L., Morera, J. M., Bartolí, E., & Inés Fernández, a. (2013). Low carbon and low embodied energy materials in buildings: A review. *Renewable and Sustainable Energy Reviews*, *23*, 536–542. http://doi.org/10.1016/j.rser.2013.03.017

Cagnon, H., Aubert, J. E., Coutand, M., & Magniont, C. (2014). Hygrothermal properties of earth bricks. *Energy and Buildings*, *80*, 208–217. http://doi.org/10.1016/j.enbuild.2014.05.024

Chabriac, P.-A. (2014). *MESURE DU COMPORTEMENT HYGROTHERMIQUE DU PISE*. L'UNIVERSITÉ DE LYON.

Chabriac, P.-A., Fabbri, A., Morel, J.-C., Laurent, J.-P., & Blanc-Gonnet, J. (2014). A Procedure to Measure the in-Situ Hygrothermal Behavior of Earth Walls. *Materials*, *7*, 3002–3020. http://doi.org/10.3390/ma7043002

Champiré, F., Fabbri, A., Morel, J., Wong, H., & McGregor, F. (2016). Impact of relative humidity on the mechanical behavior of compacted earth as a building material. *Construction and Building Materials*, *110*(in revision), 70–78. http://doi.org/10.1016/j.conbuildmat.2016.01.027

Cheah, J. S. J., Walker, P., Heath, A., & Morgan, T. K. K. B. (2012). Evaluating shear test methods for stabilised rammed earth. *Proceedings of Institution of Civil Engineers, Constructions Materials*, *165*, 325–334. http://doi.org/10.1680/coma.10.00061

Chu, T. C., Ranson, W. F., & Sutton, M. A. (1985). Applications of digital-image-correlation techniques to experimental mechanics. *Experimental Mechanics*, *25*(3), 232–244. http://doi.org/10.1007/BF02325092

Ciancio, D., & Augarde, C. (2013). Capacity of unreinforced rammed earth walls subject to lateral wind force: elastic analysis versus ultimate strength analysis. *Materials and Structures*, *46*(9), 1569–1585. http://doi.org/10.1617/s11527-012-9998-8

Ciancio, D., Beckett, C. T. S., & Carraro, J. A. H. (2014). Optimum lime content identification for lime-stabilised rammed earth. *Construction and Building Materials*, *53*, 59–65. http://doi.org/10.1016/j.conbuildmat.2013.11.077

Ciancio, D., & Gibbings, J. (2012). Experimental investigation on the compressive strength of cored and molded cement-stabilized rammed earth samples. *Construction and Building Materials*, *28*(1), 294–304. http://doi.org/10.1016/j.conbuildmat.2011.08.070

Ciancio, D., & Jaquin, P. (2011). An Overview of Some Current Recommendations on the Suitability of Soils for Rammed Earth. *Proceedings of International Workshop on Rammed Earth Materials and Sustainable Structures & Hakka Tulou Forum 2011: Structures of Sustainability*, 2–7.

Ciancio, D., Jaquin, P., & Walker, P. (2013). Advances on the assessment of soil suitability for rammed earth. *Construction and Building Materials*, *42*, 40–47. http://doi.org/10.1016/j.conbuildmat.2012.12.049

Corbin, A., & Augarde, C. (2015). INVESTIGATION INTO THE SHEAR BEHAVIOUR OF RAMMED EARTH USING SHEAR BOX TESTS. In *First International Conference On Bio-based Building Materials* (pp. 93–98). Clemont-Ferrand, France.

Deboucha, S., & Hashim, R. (2011). A review on bricks and stabilized compressed earth

blocks. *Scientific Research and Essays*, *6*(3), 499–506. http://doi.org/10.5897/SRE09.356

Delgado, M. J., & Guerrero, I. (2007). The selection of soils for unstabilised earth building: A normative review. *Construction and Building Materials*, *21*, 237–251. http://doi.org/10.1016/j.conbuildmat.2005.08.006

Gallipoli, D., Bruno, A., Perlot, C., & Salmon, N. (2014). Raw earth construction: Is there a role for unsaturated soil mechanics? In *Unsaturated Soils: Research & Applications* (pp. 55–62). CRC Press. http://doi.org/10.1201/b17034-8

Gerard, P., Mahdad, M., Robert McCormack, A., & François, B. (2015). A unified failure criterion for unstabilized rammed earth materials upon varying relative humidity conditions. *Construction and Building Materials*, *95*(2015), 437–447. http://doi.org/10.1016/j.conbuildmat.2015.07.100

Gomes, M. I., Gonçalves, T. D., & Faria, P. (2014). Unstabilized Rammed Earth: Characterization of Material Collected from Old Constructions in South Portugal and Comparison to Normative Requirements. *International Journal of Architectural Heritage*, *8*(2), 185–212. http://doi.org/10.1080/15583058.2012.683133

Hall, M., & Allinson, D. (2009). Assessing the effects of soil grading on the moisture content-dependent thermal conductivity of stabilised rammed earth materials. *Applied Thermal Engineering*, *29*(4), 740–747.

Hall, M., & Djerbib, Y. (2004). Rammed earth sample production: context, recommendations and consistency. *Construction and Building Materials*, *18*, 281–286. http://doi.org/10.1016/j.conbuildmat.2003.11.001

Harris, D. (1999). A quantitative approach to assessment of the environmental impact of building materials. *Building and Environment*, *34*, 751–800.

Houben, H., & Guillaud, H. (1994). *Earth Construction: A Comprehensive Guide*. Intermediate Technology Publication, London.

Illampas, R., Ioannou, I., & Charmpis, D. C. (2014). Adobe bricks under compression: Experimental investigation and derivation of stress-strain equation. *Construction and Building Materials*, *53*, 83–90. http://doi.org/10.1016/j.conbuildmat.2013.11.103

Ionescu, C., Baracu, T., Vlad, G.-E., Necula, H., & Badea, A. (2015). The historical

evolution of the energy efficient buildings. *Renewable and Sustainable Energy Reviews*, *49*(2015), 243–253. http://doi.org/10.1016/j.rser.2015.04.062

ISO-24353. (2008). Hygrothermal performance of building materials and products-Determination of moisture adsorption/desorption properties in response to humidity variation. Geneva, Switzerland: International Organization for Standardization.

Jaquin, P. (2011). A History of Rammed Earth in Asia. In *Proceedings of International Workshop on Rammed Earth Materials and Sustainable Structures & Hakka Tulou Forum 2011: Structures of Sustainability*.

Jaquin, P. A. (2008). *Analysis of Historic Rammed Earth construction*. Durham University.

Jaquin, P. A., Augarde, C. E., Gallipoli, D., & Toll, D. G. (2009). The strength of unstabilised rammed earth materials. *Géotechnique*, *59*(5), 487–490. http://doi.org/10.1680/geot.2007.00129

Jaquin, P. A., Augarde, C. E., & Gerrard, C. M. (2006). Analysis of Historic Rammed Earth construction. In *Structural Analysis of Historical Constructions* (pp. 1–8).

Jayasinghe, C., & Kamaladasa, N. (2007). Compressive strength characteristics of cement stabilized rammed earth walls. *Construction and Building Materials*, *21*(11), 1971–1976. http://doi.org/10.1016/j.conbuildmat.2006.05.049

Jayasinghe, C., & Mallawaarachchi, R. S. (2009). Flexural strength of compressed stabilized earth masonry materials. *Materials & Design*, *30*(9), 3859–3868. http://doi.org/10.1016/j.matdes.2009.01.029

John, G., Clements-Croome, D., & Jeronimidis, G. (2005). Sustainable building solutions: a review of lessons from the natural world. *Building and Environment*, *40*(3), 319–328. http://doi.org/10.1016/j.buildenv.2004.05.011

Kasthurba, A. K., Reddy R, K., & Reddy D, V. (2015). Use of Laterite as a Sustainable Building Material in Developing Countries. *International Journal of Earth Sciences and Engineering*, *7*(MAY), 1251–1258.

Kasthurba, A. K., Santhanam, M., & Achyuthan, H. (2007). Investigation of laterite stones for building purpose from Malabar region, Kerala, SW India - Part 1: Field Studies and Profile Characterisation. *Construction and Building Materials*, *21*, 73–82. http://doi.org/10.1016/j.conbuildmat.2006.12.003

Kasthurba, A. K., Santhanam, M., & Achyuthan, H. (2008). Investigation of laterite stones for building purpose from Malabar region, Kerala, SW India - Chemical analysis and microstructure studies. *Construction and Building Materials*, *22*, 2400–2408. http://doi.org/10.1016/j.conbuildmat.2006.12.003

Kouakou, C. H., & Morel, J. C. (2009). Strength and elasto-plastic properties of non-industrial building materials manufactured with clay as a natural binder. *Applied Clay Science*, *44*(1–2), 27–34. http://doi.org/10.1016/j.clay.2008.12.019

Künzel, H. ., Holm, A., Zirkelbach, D., & Karagiozis, A. N. (2005). Simulation of indoor temperature and humidity conditions including hygrothermal interactions with the building envelope. *Solar Energy*, *78*, 554–561. http://doi.org/10.1016/j.solener.2004.03.002

Lawane, A., Pantet, A., Vinai, R., & Hugues, J. (2011). Etude géologique et géomécanique des latérites de Dano (Burkina Faso) pour une utilisation dans l ' habitat. In *XXIXe Recontres Universitaires de Genie Civil* (pp. 206–215).

Lawane, A., Vinai, R., Pantet, A., & Thomassin, J. (2011). Characterisation of laterite stone as building material in Burkina Faso : state of the art of the on-going research and its perspectives. In *Journées Scientifiques du 2iE* (pp. 2–5). ouagadougou.

Liu, K., Wang, M., & Wang, Y. (2015). Seismic retrofitting of rural rammed earth buildings using externally bonded fibers. *Construction and Building Materials*, *100*(2015), 91–101. http://doi.org/10.1016/j.conbuildmat.2015.09.048

M. D. Gidigasu. (1976). *Laterite Soil Engineering, Pedogenesis and Engineering Principles*. Elsevier Scientific Publishing Company.

Maignien, R. (1966). Review of research on laterites. *Natural Resources Research, IV*, 1–136.

Maillard, P., & Aubert, J. E. (2014). Effects of the anisotropy of extruded earth bricks on their hygrothermal properties. *Construction and Building Materials*, *63*(2014), 56–61. http://doi.org/10.1016/j.conbuildmat.2014.04.001

Maniatidis, V., & Walker, P. (2003). A review of rammed earth construction. *University of Bath*, (May). Retrieved from http://staff.bath.ac.uk/abspw/rammedearth/review.pdf

Maniatidis, V., & Walker, P. (2008). Structural capacity of rammed earth in compression.

Journal of Materials in Civil Engineering, *20*(3, March), 230–239. http://doi.org/10.1061/(ASCE)0899-1561(2008)20:3(230)

Mccormick, N., & Lord, J. (2010). Digital Image Correlation. *Materials Today*, *13*(12), 52–54. http://doi.org/10.1016/S1369-7021(10)70235-2

McGregor, F., Heath, A., Fodde, E., & Shea, A. (2014). Conditions affecting the moisture buffering measurement performed on compressed earth blocks. *Building and Environmenti*, *75*, 11–18.

McGregor, F., Heath, A., Maskell, D., Fabbri, A., Morel, J.-C., Maskel, D., … Morel, J.-C. (2016). A review on the buffering capacity of earth building materials. *Proceedings of the Institution of Civil Engineers - Construction Materials*, *0*(0), 1–11. http://doi.org/10.1680/jcoma.15.00035

McHenry, P. G. (1984). *Adobe and Rammed Earth Building: Design and Construction*. A Wiley- Interscience Publication, New York, USA.

Mesbah, A., Morel, J. C., & Olivier, M. (1999). Comportement des sols fins argileux pendant un essai de compactage statique: détermination des paramètres pertinents. *Materials and Structures*, *32*(9), 687–694.

Miccoli, L., Müller, U., & Fontana, P. (2014). Mechanical behaviour of earthen materials: A comparison between earth block masonry, rammed earth and cob. *Construction and Building Materials*, *61*, 327–339. http://doi.org/10.1016/j.conbuildmat.2014.03.009

Miccoli, L., Oliveira, D. V., Silva, R. a., Müller, U., & Schueremans, L. (2014). Static behaviour of rammed earth : experimental testing and finite element modelling. *Materials and Structures*, (2015), 3443–3456. http://doi.org/10.1617/s11527-014-0411-7

Morel, J.-C., Mesbah, A., Oggero, M., & Walker, P. (2001). Building houses with local materials: Means to drastically reduce the environmental impact of construction. *Building and Environment*, *36*(10), 1119–1126. http://doi.org/10.1016/S0360-1323(00)00054-8

Morel, J., Pkla, A., & Walker, P. (2007). Compressive strength testing of compressed earth blocks. *CONSTRUCTION & BUILDING MATERIALS*, *21*, 303–309. http://doi.org/10.1016/j.conbuildmat.2005.08.021

Muntohar, A. S. (2011). Engineering characteristics of the compressed-stabilized earth brick. *Construction and Building Materials*, *25*(11), 4215–4220. http://doi.org/10.1016/j.conbuildmat.2011.04.061

Nabouch, R., Bui, Q. B., Plé, O., Perrotin, P., Poinard, C., Goldin, T., & Plassiard, J. P. (2016). Seismic Assessment of Rammed Earth Walls Using Pushover Tests. *Procedia Engineering*, *145*(October 2016), 1185–1192. http://doi.org/10.1016/j.proeng.2016.04.153

Norton, J. (1986). *Building With Earth: A Handbook*. *Intermediate Technology Publications*. Intermediate Technology Publication, London. http://doi.org/10.1017/CBO9781107415324.004

Nowamooz, H., & Chazallon, C. (2011). Finite element modelling of a rammed earth wall. *Construction and Building Materials*, *25*(4), 2112–2121. http://doi.org/10.1016/j.conbuildmat.2010.11.021

Oti, J. E., Kinuthia, J. M., & Bai, J. (2009). Engineering properties of unfired clay masonry bricks. *Engineering Geology*, *107*(3–4), 130–139. http://doi.org/10.1016/j.enggeo.2009.05.002

Pacheco-Torgal, F., & Jalali, S. (2012). Earth construction: Lessons from the past for future eco-efficient construction. *Construction and Building Materials*, *29*(2012), 512–519. http://doi.org/10.1016/j.conbuildmat.2011.10.054

Padfield, T. (1998). *PhD Thesis : The role of absorbent building materials in moderating changes of relative humidity*. *Department of Structural Engineering and Materials, Lyngby, Technical University of Denmark*. The Technical University of Denmark.

Pan, H., Qing, Y., & Pei-yong, L. (2010). Direct and Indirect Measurement of Soil Suction in the Laboratory. *Electronic Journal of Geotechnical Engineering*, *15*(A).

Quoc-Bao, B. (2008). *Stabilite Des Structures En Pise : Durabilite, Caracteristiques Mecaniques*. *Institut National Des Sciences Appliquees De Lyon*. MEGA-Universite de Lyon.

Radanovic, J. (1996). *Design Criteria for Reinforced Stabilised Earth Structures*. University of Western Australia, Crawley, Australia.

Reddy, B. V. V. (2009). Sustainable materials for low carbon buildings. *International*

Journal of Low Carbon Technologies, *4*, 175–181.

Reddy, B. V. V., & Hubli, S. R. (2002). Properties of lime stabilised steam-cured blocks for masonry. *Materials and Structures*, *35*(June), 293–300. http://doi.org/10.1007/BF02482135

Reddy, B. V. V., & Kumar, P. P. (2009). Compressive Strength and Elastic Properties of Stabilised Rammed Earth and Masonry. *Masonry International*, *22*(1), 1–8.

Reddy, B. V. V., Lal, R., & Rao, K. N. (2007). Optimum Soil Grading for the Soil-Cement Blocks. *Journal of Materials in Civil Engineering*, *19*(2), 139–148.

Rendell, F., & Jauberthie, R. (2009). Performance of rammed earth structures in east Brittany. *11th International Conference on Non-Conventional Materials and Technologies, NOCMAT 2009*, (September), 6–9.

Rode, C., Peuhkuri, R. H., Mortensen, L. H., Hansen, K. K., Time, B., Gustavsen, A., … Arfvidsson, J. (2005). *Moisture buffering of building materials*.

Rouquerol, F., Rouquerol, J., & Sing, K. S. W. (1999). *Adsorption by Powders and Porous Solids: Principles, Methodology and Applications*. (A. Press, Ed.). Academic Press.

SAZS 724:2001. (n.d.). *Zimbabwe Standard. Rammed Earth Structures.* Harare.

Schrader, C. A. (1981). Rammed Earth Construction: A re-emerging Technology. In *6th Natural Passive Solar Conference*.

Silva, R. ., Olliveira, D. ., Schueremans, L., Miranda, T., & Machado, J. (2014). Shear behaviour of rammed earth walls repaired by means of grouting. In *9th International Masonry Conference* (pp. 1–12). Guimaraes: International Masonry Society.

Silva, R. A., Oliveira, D. V, Miccoli, L., & Schueremans, L. (2014). MODELLING OF RAMMED EARTH UNDER SHEAR LOADING. In *SAHC2014-9th International Conference on Structural Analysis of Historicak Constructions* (pp. 14–17).

Silveira, D., Varum, H., & Costa, A. (2013). Influence of the testing procedures in the mechanical characterization of adobe bricks. *Construction and Building Materials*, *40*, 719–728. http://doi.org/10.1016/j.conbuildmat.2012.11.058

Smith, J. C., & Augarde, C. (2014). Optimum water content tests for earthen construction materials. *Construction Materials*, *167*(April 2014 CM2), 114–123.

http://doi.org/10.1680/coma.12.00040

SOUDANI, L. (2016). *Modelling and experimental validation of the hygrothermal performances of earth as a building material*. Université de Lyon, ENTPE.

Soudani, L., Fabbri, A., Morel, J., Woloszyn, M., & Grillet, A. (2015). A coupled hygrothermal model for earthen materials. *Energy and Buildings*, (under revision).

Spence, R., & Mulligan, H. (1995). Sustainable development and the construction industry. *Habitat International*, *19*(3), 279–292. http://doi.org/10.1016/0197-3975(94)00071-9

Sutton, M., Wolters, W., Peters, W., Ranson, W., & McNeill, S. (1983). Determination of displacements using an improved digital correlation method. *Image and Vision Computing*, *1*(3), 133–139. http://doi.org/10.1016/0262-8856(83)90064-1

Tardy, Y., Kobilsek, B., & Paquet, H. (1991). Mineralogical composition and geographical distribution of african and brazilian periatlantic laterites. The influence of continental drift and tropical paleoclimates during the past 150 million years and implications for India and Australia. *Journal of African Earth Sciences*, *12*(1/2), 283–295. http://doi.org/10.1017/CBO9781107415324.004

Thormark, C. (2006). The effect of material choice on the total energy need and recycling potential of a building. *Building and Environment*, *41*(8), 1019–1026. http://doi.org/10.1016/j.buildenv.2005.04.026

Unnikrishnan, S., Narasimhan, M. C., & Venkataramana, K. (2010). Uniaxial Compressive Strength of Laterite Masonry Prisms – An Evaluation. In *International Conference on Earth science and Engineering - 2010* (pp. 115–128). International Journal of Earth Science and Engineering.

Venkatarama Reddy, B. V., Leuzinger, G., & Sreeram, V. S. (2014). Low embodied energy cement stabilised rammed earth building—A case study. *Energy and Buildings*, *68*, 541–546. http://doi.org/10.1016/j.enbuild.2013.09.051

Venkatarama Reddy, B. V. (2004). Sustainable building technologies. *Current Science*, *87*(7), 899–907.

Venkatarama Reddy, B. V., & Gupta, A. (2006). Strength and Elastic Properties of Stabilized Mud Block Masonry Using Cement-Soil Mortars. *Journal of Materials in Civil Engineering*, *18*(3), 472–476. http://doi.org/10.1061/(ASCE)0899-

1561(2006)18:3(472)

Venkatarama Reddy, B. V., & Gupta, A. (2008). Influence of sand grading on the characteristics of mortars and soil-cement block masonry. *Construction and Building Materials*, *22*(8), 1614–1623. http://doi.org/10.1016/j.conbuildmat.2007.06.014

Venkatarama Reddy, B. V., & Prasanna Kumar, P. (2011a). Cement stabilised rammed earth. Part A: compressive strength and stress–strain characteristics. *Materials and Structures*, *44*(3), 695–707. http://doi.org/10.1617/s11527-010-9659-8

Venkatarama Reddy, B. V., & Prasanna Kumar, P. (2011b). Cement stabilised rammed earth. Part B: compressive strength and stress–strain characteristics. *Materials and Structures*, *44*(3), 695–707. http://doi.org/10.1617/s11527-010-9659-8

Walker, P., Keable, R., Martin, J., & Maniatidis, V. (2005). *Rammed Earth Design and Construction Guidelines*. WATFORD: BRE Bookshop.

Walker, P., & Stace, T. (1997). Properties of some cement stabilised compressed earth blocks and mortars. *Materials and Structures/Materiaux et Constructions*, *30*(203), 545–551. http://doi.org/10.1007/BF02486398

Walker, P., & Standards Australia. (2002). *HB 195-2002, The Australian Earth Building Handbook. Waitakere City Council's Sustainable Home Guidelines*. Retrieved from http://www.waitakere.govt.nz/abtcit/ec/bldsus/pdf/materials/earthbuilding.pdf

9. Annexure

Annexure - A **Soil characteristics**

A.1. Particle size distribution

A.1.1 Sieve Analysis

The material retained above 80µm sieve from wet sieve method is dried in oven at 100-110°c for 48 hours, until the difference between two successive readings of dry mass is negligible with an accuracy of 0.01g. The dry mass is then allowed to pass through the sieves arranged in descending order from largest sieve size of 10mm to 75µm. After sieving process, material retained on each sieve is weighed with precision to 0.01g and percentage of material retained on each sieve is calculated.

A.1.2 Sedimentation Analysis

Sedimentation test is a process adopted to calculate the percentage of finer soil particles (<80µm) present in the soil. By assuming all fines to be spherical and adopting stokes principle, we can calculate the size of particles settling at different times suspended in a homogenous solution.

Fine particles passing through the 80µm sieve in wet sieving is dried in oven at 100-110°C until the weight of two successive reading of the dry fines are same. Using laboratory pestle and mortar the dry fine particles are grounded to fine powder, 80g of which is soaked in solution of 300cm^3 of distilled water and 60cm^3 of dispersing agent[5] for about 12-15 hours (overnight). The solution is then mechanically stirred for about 3 minutes before transferring it to a 2L graduated cylinder half filled with distilled water. Fil up the rest of 2L graduated cylinder with distilled water, and use another 2L graduated cylinder filled with distilled water and same quantity of dispersing agent for hydrometer reading correction. Shake graduated cylinder with the solution, such that the solution is uniformly suspended (distributed), immediately insert the clean hydrometer into solution and note down the hydrometer reading with respect to time intervals of 30”, 1’, 2’, 5’, 10’, at every doubled time interval until 240’. Hydrometer was not be disturbed for the first 4 reading (I.e., upto 5’ time interval), after the 5 reading hydrometer was removed from the solution and placed in the other graduated cylinder with distilled water and dispersing agent, care has been taken not to lose any material nor disturb the solution during removal or insertion of hydrometer henceforth. Necessary corrections are added to the hydrometer

[5] Dispersing agent is the solution of sodium hexametaphosphate

reading with respect to the reading obtained from the solution of distilled water and dispersing agent, soil specific gravity was assumed to be 2.65g/m^3.

From stokes theory we know the size of the particles settling in a solution at given time interval. By knowing variation of hydrometer readings (density) of the soil solution with respect to known time intervals, percentage of different sized fine particles present in the mix can be calculated.

Combining the total mass of the soil considered for grain size distribution as shown in Figure 2-2 is plotted in semi-log graph for both soils, percentage of gravel, sand, silt and clay are calculated from the graph. In Figure 2-2, the maximum and minimum proposed grain size distribution as per British standard (BS 1377-2, 1990) are also presented, both the soils chosen in this study does not fit in the guidelines proposed to soil used for civil engineering purpose. But there are many building constructed in and around the region with this soils, hence it is very important to understand the behaviour of the soil as naturally available.

A.2. Suction measurements

- The calibration chart of Whatman 42 filter paper carried out by (SOUDANI, 2016) to calculate the suction values are plotted in Figure 9-1.
- The Whatman 42 filter paper water content in relation with CRA and Dagneux soil water content are plotted in Figure 9-2.
- The variation of suction values calculated for CRA and Dagneux soil specimens using different Whatman 42 calibration curves are given in Figure 9-3 and Figure 9-4.

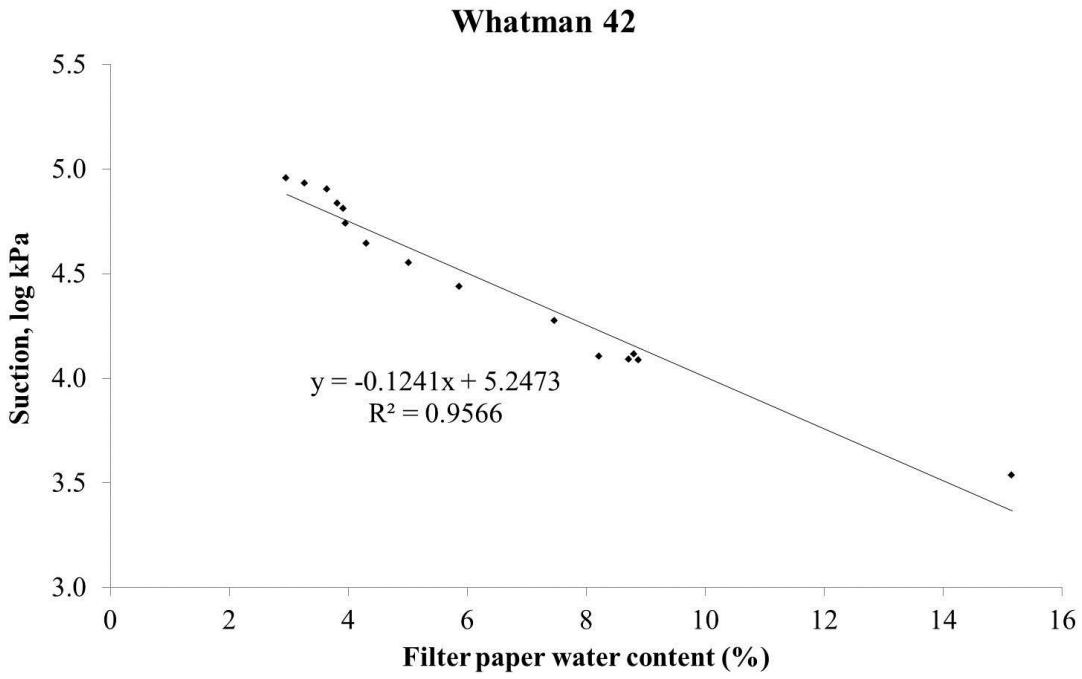

Figure 9-1 Whatman 42 calibration curve obtained in ENTPE, Lyon (source: (SOUDANI, 2016))

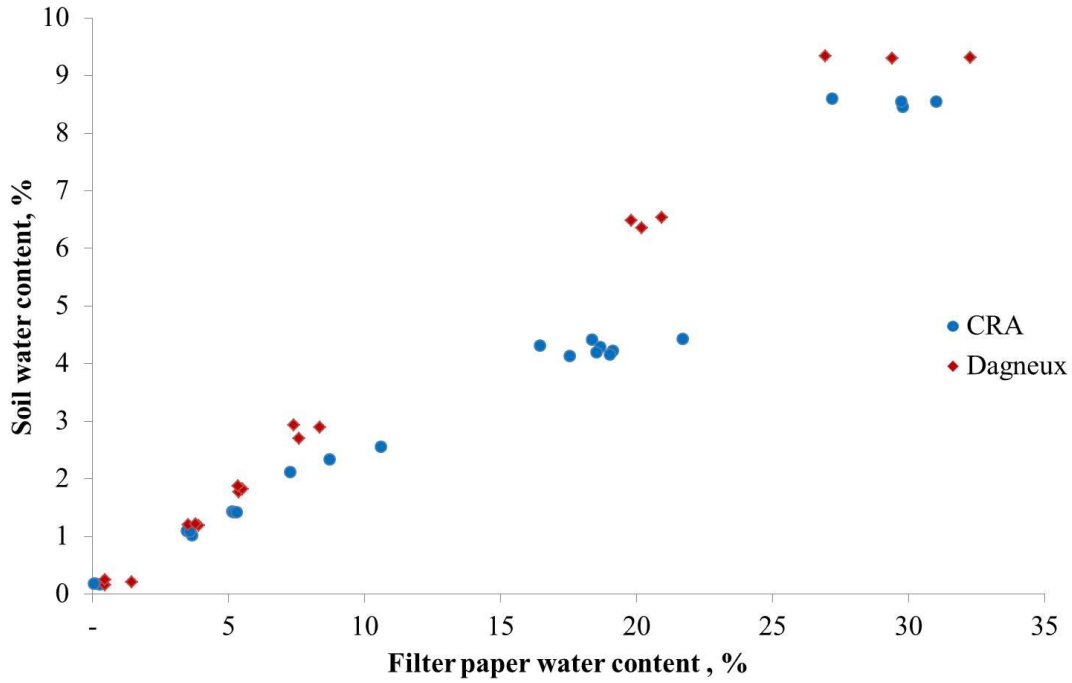

Figure 9-2 soil water content vs Whatman 42 filter paper water content

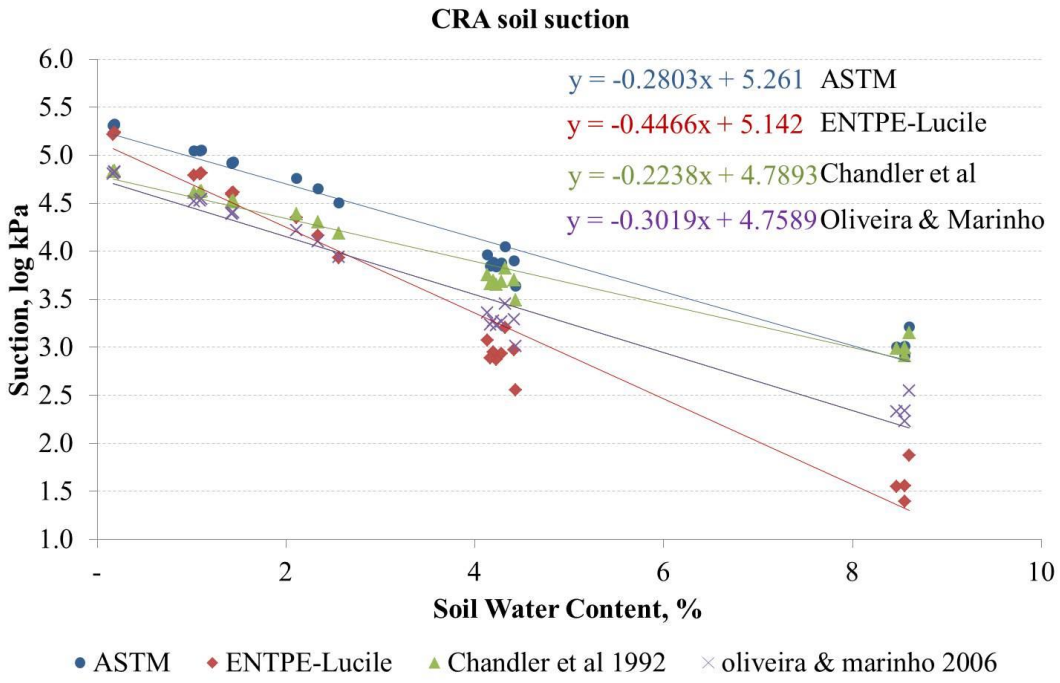

Figure 9-3 suction for CRA soil specimens

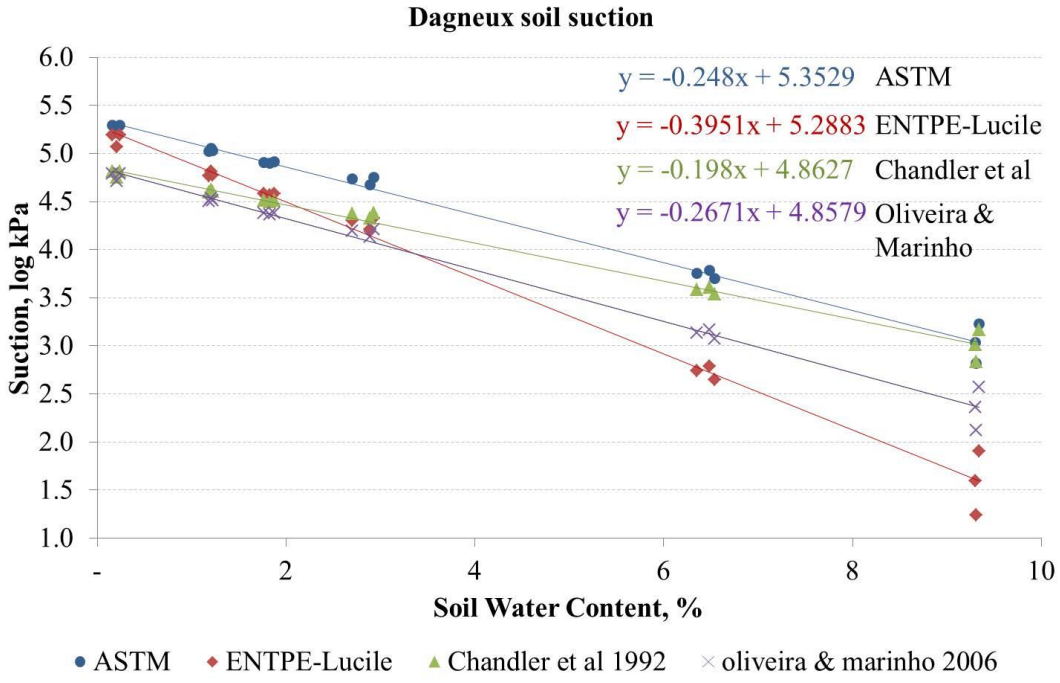

Figure 9-4 suction for Dagneux soil specimens

Annexure - B **Calculation of dry density using Archimedes principle**

The densities calculated are all dry densities; hence the extracted samples were oven dried at 100-110° C for 24hrs before coating with paraffin. Using volume displacement method, the volume of sample coated with paraffin is directly measured. Knowing the mass and density of paraffin (0.9g/cc), volume of the paraffin and sample can be deduced using Equation 9-1. Finally dry density of the sample can be easily calculated.

Equation 9-1

$$V_p = \frac{m_{s+p} - m_p}{\gamma_p}$$

$$V_s = V_{s+p} - V_p$$

$$\gamma_d = \frac{m_s}{V_s}$$

Where, m_s is the mass of dry sample, m_p is the mass of paraffin, m_{s+p} is the mass of sample coated with paraffin, V_s is the volume of the dry sample, V_p is the volume of paraffin, V_{s+p} is the volume of sample coated with paraffin, and γ_d is the dry density of the sample.

Annexure - C **Determining the expansion from the measurements provided by the LVDT**

In order to determine the deformation, we shall place the LVDT's at mid height of the specimen. The centre of the specimen is considered as the origin of the coordinate axis as shown. At first we assume that the shape of the specimen remain circular throughout the test, irrespective of the level of deformation as shown in figure.

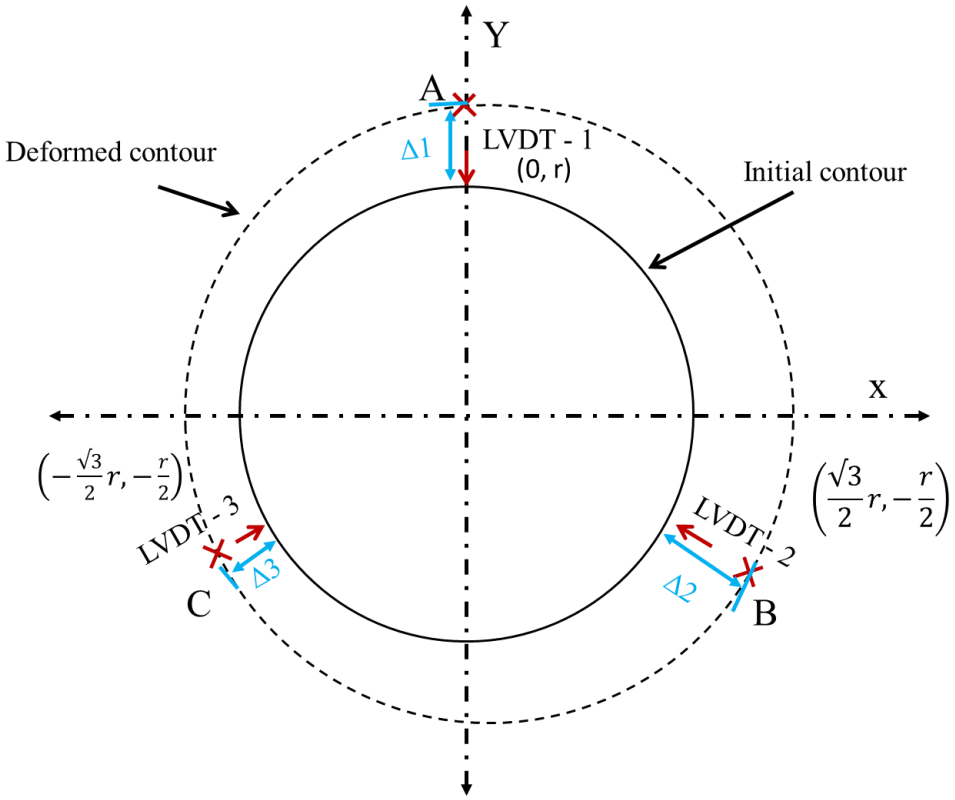

We will use the coordinates of the LVDT's point of contact with specimen, which we can easily define knowing the radius of the specimen. Know we will use the displacement measured by the LVDT's to profile new or deformed shape of specimen.

The initial coordinates of LVDT's considering radius as 'r' are:

For LVDT-1: (0, r)

For LVDT-2: $\left(\frac{\sqrt{3}}{2}r, -\frac{r}{2}\right)$

For LVDT-3: $\left(-\frac{\sqrt{3}}{2}r, -\frac{r}{2}\right)$

To derive the final shape of the deformed body, we denote the displacements obtained from the LVDTs as Δ1, Δ2, and Δ3 for LVDT-1, LVDT-2 and LVDT-3

respectively. From the displacements obtained we can now derive the new final coordinates of the deformed body, as:

For LVDT-1: $(0,\ r+\Delta 1\ )$ new point 'A'

For LVDT-2: $\left(\frac{\sqrt{3}}{2}(r+\Delta 2)\ , -\frac{1}{2}(r+\ \Delta 2)\right)$ new point 'B'

For LVDT-3: $\left(-\frac{\sqrt{3}}{2}(r+\Delta 3)\ , -\frac{1}{2}(r+\ \Delta 3)\right)$new point 'C'

For simplifying the following equations, we shall adopt the following notations for the coordinates 'A', 'B' and 'C':

A$(\alpha_1,\ \beta_1)$, B$(\alpha_2,\ \beta_2)$, and C$(\alpha_3,\ \beta_3)$

In order to derive the deformation of the specimen, we must find out the centre of the circle passing through points A, B and C.

The equation of line passing through A and B is

$$(\beta_2-\beta_1\ )x-\ (\alpha_2-\alpha_1\ )y+(\alpha_2\beta_1-\alpha_1\beta_2\ )=0$$

We can then determine the equation of the bisector of segment AB as following:

$$(\alpha_2-\alpha_1\ )x+\ (\beta_2-\beta_1\ )y+d=0$$

Considering the centre of the line segment [AB] which passes through the bisector. The coordinates of the centre are$\left(\frac{\alpha_1+\alpha_2}{2}, \frac{\beta_1+\beta_2}{2}\right)$, we get:

$$d\ =\ \frac{1}{2}\left({\alpha_1}^2-{\alpha_2}^2+{\beta_1}^2-{\beta_2}^2\right)$$

So, the equation of the bisector of the segment [AB] is:

$$2(\alpha_2-\alpha_1)x+2(\beta_2-\beta_1)y+\left({\alpha_1}^2-{\alpha_2}^2+{\beta_1}^2-{\beta_2}^2\right)=0$$

Similarly the equation for the bisector of the segment [AC]:

$$2(\alpha_3-\alpha_1)x+2(\beta_3-\beta_1)y+\left({\alpha_1}^2-{\alpha_3}^2+{\beta_1}^2-{\beta_3}^2\right)=0$$

So, from the intersection of two lines, we can easily deduce the coordinates for the new circle formed with respect to the new deformed shape of specimen, which is:

$$x_c = \frac{1}{2}\left[\frac{-(\beta_2-\beta_1)({\alpha_1}^2-{\alpha_3}^2+{\beta_1}^2-{\beta_3}^2)+(\beta_3-\beta_1)({\alpha_1}^2-{\alpha_2}^2+{\beta_1}^2-{\beta_2}^2)}{(\alpha_3-\alpha_1)(\beta_2-\beta_1)-(\alpha_2-\alpha_1)(\beta_3-\beta_1)}\right]$$

$$y_c = \frac{1}{2}\left[\frac{-(\alpha_3-\alpha_1)({\alpha_1}^2-{\alpha_2}^2+{\beta_1}^2-{\beta_2}^2)+(\alpha_2-\alpha_1)({\alpha_1}^2-{\alpha_3}^2+{\beta_1}^2-{\beta_3}^2)}{(\alpha_3-\alpha_1)(\beta_2-\beta_1)-(\alpha_2-\alpha_1)(\beta_3-\beta_1)}\right]$$

Hence the radial deformation of the specimen ‘Δr’ is

$$\Delta r = \left[\sqrt{((\beta_1}-y_c)^2+(\alpha_1-x_c)^2)\right]-r$$

Annexure - D **Drawings of Wedge design**

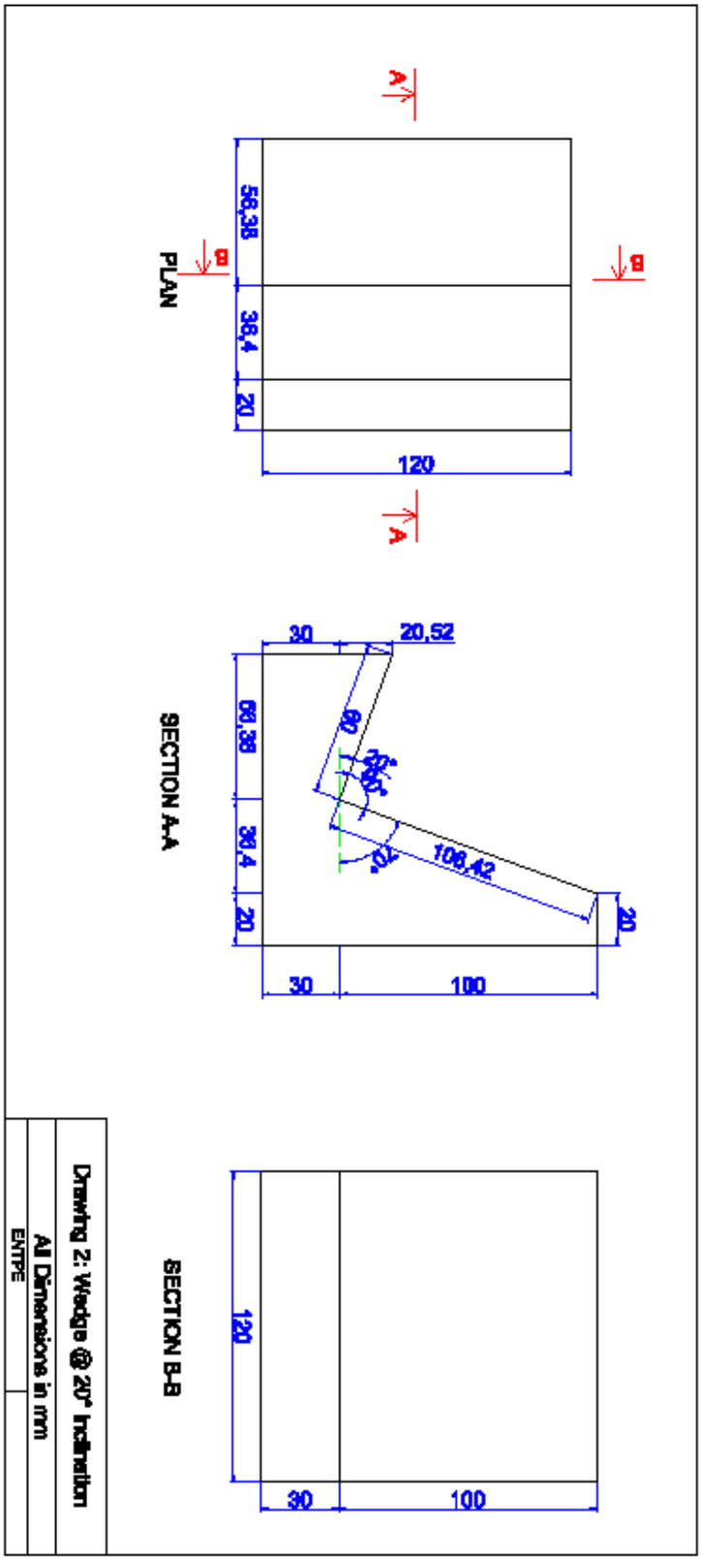

Figure 9-5 Wedge layout - 20° inclination

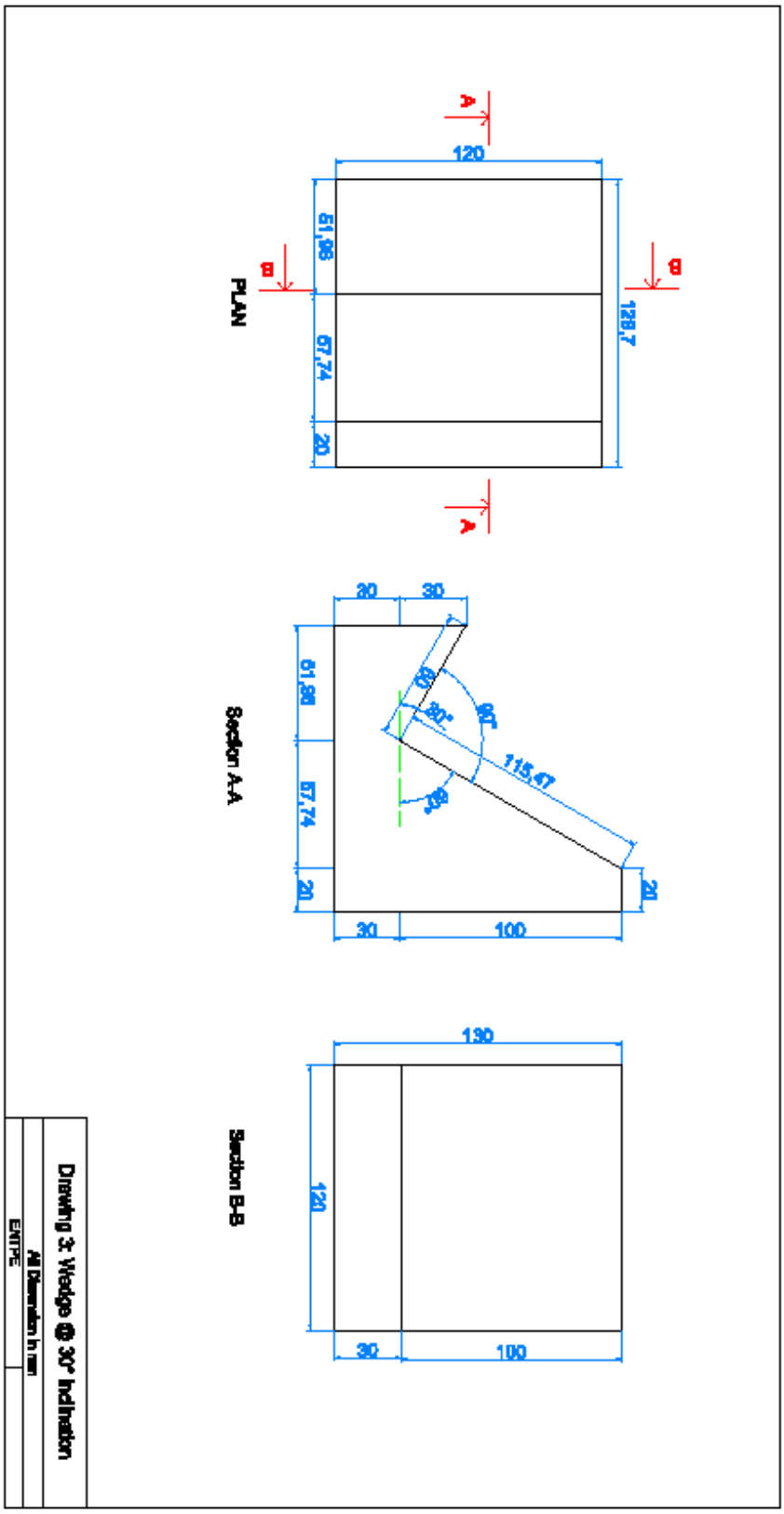

Figure 9-6 Wedge layout - 30° inclination

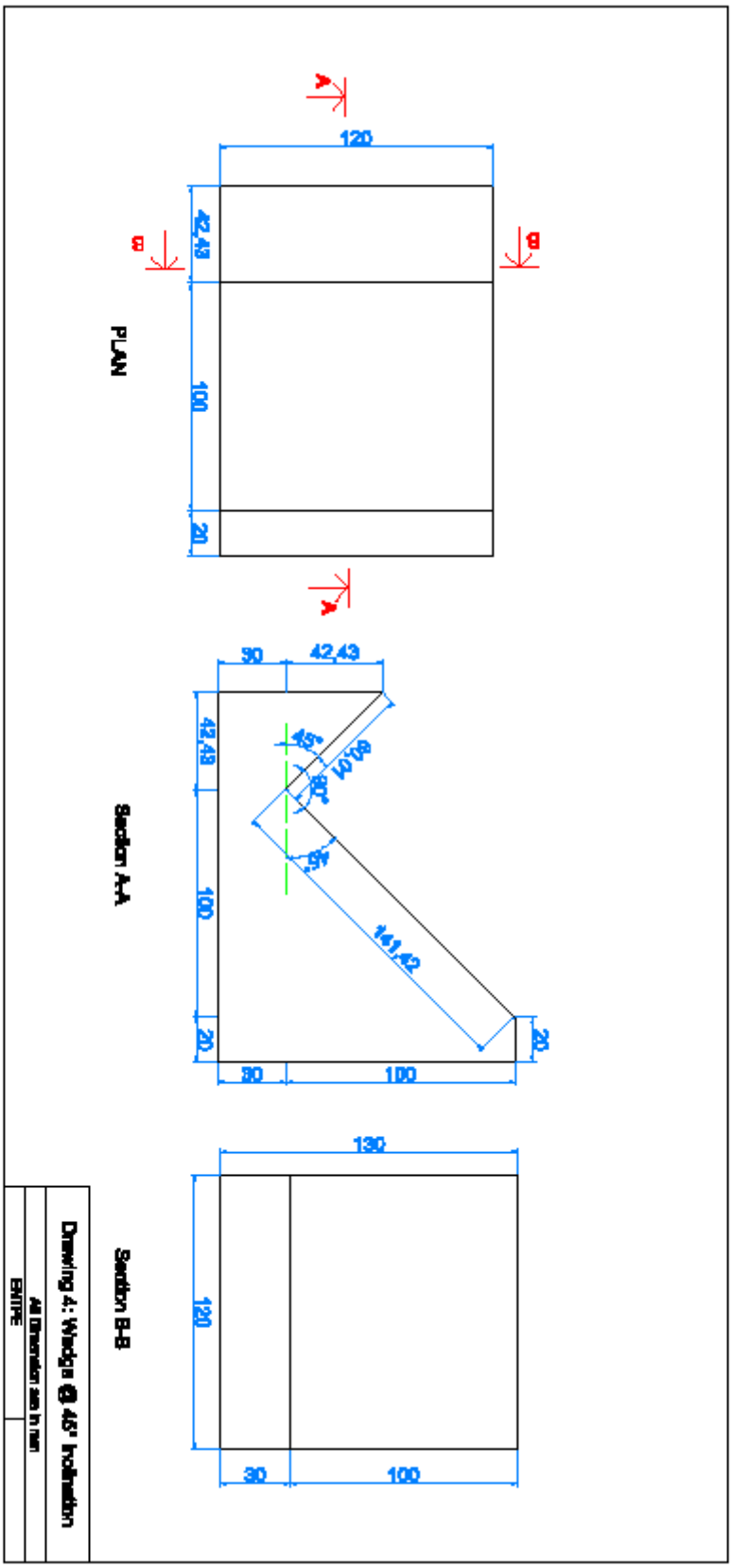

Figure 9-7 wedge layout - 45° inclination